

FLUID INCLUSION STRATIGRAPHY
A NEW METHOD FOR GEOTHERMAL RESERVOIR ASSESSMENT

By

Lorie M. Dilley

Submitted in Partial Fulfillment
of the Requirements for the

Doctorate of Philosophy in Geology

New Mexico Institute of Mining and Technology
Department of Earth and Environmental Science

Socorro, New Mexico

August 2009

ABSTRACT

The purpose of this research is to adapt Fluid Inclusion Stratigraphy (FIS), a new well logging method used in the petroleum industry, to geothermal fields. FIS conducts a bulk analysis of fluid inclusion gases in well cuttings to differentiate fluid types and horizons. Fluid types in geothermal fields are different than in petroleum fields. Instead of mixtures of water and hydrocarbons which occur in petroleum fields, geothermal fields have fluids that are mixtures of water and various gases. Geothermal gases typically include water vapor, carbon dioxide (CO₂), methane (CH₄), nitrogen (N₂), argon (Ar), and hydrogen sulfide. This research shows that geothermal fluid types such as plume fluids, condensate, meteoric fluids, and mixed fluids can be identified by relative amounts of these gases.

Ratios of N₂/Ar, and CO₂/CH₄, the presence or absence of water, and hydrogen sulfide, are used to identify the geothermal fluid types. The procedure for identifying and displaying the results of FIS analysis is automated with a computer program to assign fluid types based on inclusion gas geochemistry. Fluid types identified in wells using the FIS method show a stratigraphy across the Coso geothermal field that agrees with current knowledge of the field. Peaks in the gas concentrations correlate to fractures occurring in cores from the field. Location of large condensate zones are also indicated using the FIS method and correspond to those zones encountered during drilling. Present-day production zones correspond to areas the FIS method identifies as plume fluids.

ACKNOWLEDGMENTS

The author wishes to acknowledge the support received from various people during the course of this research. This project would not have been possible without Dave Norman who was the principal advisor on this project. He will be greatly missed. My sincere thanks to Joe Moore of the Energy & Geoscience Institute at the University of Utah for providing access to core samples and for his geothermal expertise. This research would not have been possible without the support of the Coso Company geologists including Brian Berard and Jess McCulloch. My thanks to the many scientists and industry people who asked questions and provided comments on this research during the conferences and paper presentations. These questions and comments helped to focus the research and develop answers. Thank you to Ron Churchill of the California Geological Survey and Bill Bourcier of Lawrence Livermore National Laboratory for their reviews. Thank you to Gail Wiggett, the project manager for the California Energy Commission (CEC) for slogging through the drafts of CEC report and providing important and timely comments on the research as it developed. I would also like to thank my colleagues at Hattenburg Dilley & Linnell who helped in too many ways to count. Lastly, I would like to thank my family especially Elisya, Sam, Chai, John and Theresa.

TABLE OF CONTENTS

	PAGE
ACKNOWLEDGMENTS	ii
TABLE OF CONTENTS.....	iii
LIST OF TABLES	vi
LIST OF FIGURES	vii
CHAPTER 1. INTRODUCTION.....	1
CHAPTER 2. BACKGROUND	4
2.0 Geothermal Systems.....	4
2.1. Fluid Inclusion Gas Analysis – Previous Work.....	10
2.2. Well Logging/Testing.....	16
2.3. Coso Geologic Setting.....	18
2.4. Coso Geothermal System	22
2.5. Beowawe Geology.....	26
CHAPTER 3. METHODS	28
3.0 Wells.....	28
3.1. Rock Cores.....	31
3.2. Sampling.....	32
3.3. Laboratory Analysis.....	32
CHAPTER 4. DATA	35
4.0 Data Quality.....	35

4.1.	Sampling Interval.....	42
4.2.	Displaying the Data	47
4.3.	Relation to Fractures.....	61
4.3.1.	Coso Wells.....	61
4.3.2.	Karaha Wells.....	63
4.3.3.	Steamboat Springs Well 87-29	65
4.4.	Beowawe.....	68
4.5.	Timing.....	71
4.6.	Temperature Logs.....	75
CHAPTER 5. DISCUSSION.....		79
5.0	Fluid Chemistry	79
5.1.	Fluid Source Log	88
5.2.	The CO ₂ /N ₂ vs. Total Gas Diagram.....	100
5.3.	Comparison to Temperature Logs	105
5.4.	Correlation with Rocks and Veins.....	116
5.5.	Timing of Fluid Inclusions	119
5.6.	Fluid Models.....	123
5.6.1.	East Flank	123
5.6.2.	Western Edge.....	126
5.6.3.	Middle of the Field	128
5.6.4.	Across the Field	130
5.6.5.	Reservoir Model	132
CHAPTER 6: CONCLUSIONS		135

REFERENCES139

APPENDIX A: FIT DATA SET FOR ENTIRE PROJECT (CD)144

APPENDIX B: EXCEL LOGGER FILES AND LOGGER FILE (CD).....145

APPENDIX C: FIS LOGS FOR THE COSO WELLS146

LIST OF TABLES

TABLE	PAGE
Table 1. Summary of Fluid Inclusion Gas Chemistry and Fluid Types.	16
Table 2. Initial Gas Data (ppm/v) from the fluid samples collected in 40 wells in Coso Field.....	25
Table 3. Coso Geothermal Field Well Names and Descriptions. Low temperature wells have temperatures of 212 to 428 ⁰ F (100 to 220 C), medium temperature wells have temperatures of 428 to 572 ⁰ F (220 to 300 C) and high temperature wells have temperatures > 572 ⁰ F (300 C). Well temperatures are not exact and change with time and well depth.	29
Table 4. Beowawe, Nevada, Geothermal Field Well Names and Descriptions.	30
Table 5. Sampling Interval of Rock Cores.....	31
Table 6: Common chemical species and their mass number	34
Table 7. FIT analytical precision determined on 124 replicate analyses for repeating measurement of individual species and repeating gas ratios.	40
Table 8. Comparison of standard errors (%) of NMT and FIT. The standard error is the precision in measuring gas standard's gas ratios. The standard error in NMT analyses in part reflects sample to sample variations in gas ratios.....	41
Table 9. Karaha Cores: Select chemical species and their occurrence in relation to the fracture.....	64
Table 10. Percent change between the original and the redrill well for H ₂ O and CO ₂	75
Table 11: Fluid type rules.	89

LIST OF FIGURES

FIGURE	PAGE
Figure 2.1. Typical geothermal system in silicic-volcanic environment. Temperature distribution is based on the system at Wairakei, New Zealand. (From: Henley & Ellis 1985).....	6
Figure 2.2. Fluid flow model in a geothermal system. Modified from Henley & Ellis (1985).	7
Figure 2.3. Map of California with location of Coso Geothermal Field. Top photograph modified from Southern California Earthquake Data Center indicating the Basin & Range and Mojave Block as well as location of major fault zones.....	19
Figure 2.4. Geologic Map of the Coso volcanic field indicating the three sets of faults in the region. Abbreviated locations: CP=Coso Peaks, LCF=Lower Cactus Flat, UCF=Upper Cactus Flat, SP=Silver Peaks, CHS=Coso Hot Springs, SM=Sugarloaf Mountain, VB= Volcanoe Butte, VP= Volcano Peak, AL=Airport Lake, and LL = Little Lake (From: Wohlez K. and Heiken G. 1992).....	21
Figure 2.5. North-south cross-sections of the reservoir prepared based on fluid inclusion studies in 1999/2000 in Adams et al. (2000). A) Maximum fluid-inclusion homogenization temperatures and B) maximum salinities of inclusion in weight percent NaCl equivalent. A on the cross-section is to the north and A' is to the south.	24
Figure 2.6. Cross-sectional model of the Beowawe geothermal system. Note the Rossi well cuts the Malpais fault at about 5500 feet and the zone of high permeability lies within the Valmy Formation (From: Layman, 1984).	27
Figure 3.1. Location of wells used in the study and surface features of Coso Field. CHS=Coso Hot Springs. Colors represent topography with pinks being high areas and grays and whites low areas.	30
Figure 4.1 FIT and NMT data for several ratios for samples from Coso Well 83-16. Although the absolute abundances differ, the patterns of high and low concentrations are similar.....	37
Figure 4.2. Plots of mass 28 against mass 14 and against mass 44. Blue: Well 33-7; Pink Well 38C-9; Yellow: Well 84-30; Light Blue: Well 58A-18	39
Figure 4.3. Graph of H ₂ O for 10 feet and 20 feet sampling.....	44

Figure 4.3 (continued). Graphs of N ₂ /Ar for 10 feet and 20 feet sampling.	45
Figure 4.3 (continued). Graphs of CO ₂ /CH ₄ for 10 feet and 20 feet sampling.....	46
Figure 4.4. Typical FIT mass spectra of fluid inclusions in drill chips from Well 58A-10 at 4350 ft.....	47
Figure 4.5. FIT's mudlog type graph presentation of mass spectra.....	48
Figure 4.6. FIS log with select mass spectra plotted versus depth for Well 38C-9 a major producing well.....	51
Figure 4.7. FIS log with select mass spectra plotted versus depth for Well 51B- 16, a high temperature, non-producing well.....	52
Figure 4.8. FIS mudlog with select mass spectra plotted versus depth for an injection well, Well 67-17.	53
Figure 4.9. FIS log with select mass spectra plotted versus depth for Well 84-30 (a non-producing well) located at the southern margin of the field.	54
Figure 4.10 (continued) FIS logs for Wells 46A-19RD and 73-19, which occur along the western side of the field.	56
Figure 4.11. FIS logs for Wells 67-17C and 52-20, located in the middle southern portion of the field.	57
Figure 4.11 (continued) FIS logs for Wells 68-20 and 68-20RD located in the middle southern portion of the field.	58
Figure 4.12. FIS logs for Wells 34-9RD2 and 38D-9 located on the east flank of the field.	59
Figure 4.12. (continued) FIS logs for Well 58A-10 located on the east flank of the field.....	60
Figure 4.13. Graphs of H ₂ O, CO ₂ /CH ₄ , and N ₂ /Ar for a calcite vein centered at 660 feet from Well 64-16.	62
Figure 4.14. Graphs of H ₂ O and CO ₂ for Karaha Well K-33. Note the peaks all correspond to location of vein at 5458 feet.	64
Figure 4.15. FIS log a) and fracture log showing fracture width and the temperature gradient (b) for Steamboat Springs Well 87-29.	66
Figure 4.16. FIS log for Steamboat Springs Well 87-19 and vein locations (after Hulen) in the primary production zone.....	67
Figure 4.18. FIS logs for existing Well 77-13 and the new Well 57-13 at Beowawe, Nevada.	70
Figure 4.19. FIS logs for Well 68-20 and 68-20RD which was drilled seven years later. Note the difference between the two well logs particularly the peaks in	

the data at approximately 3650 feet, and 5250 feet in Well 68-20 versus lack of peaks in Well 68-20RD.	72
Figures 4.20(a) through 4.20(e) present the differences in various compounds between Well 68-20RD and Well 68-20. Note the significant peak at about 2900 foot depth, which corresponds to break in well casing.....	74
Figure 4.21 a and b. Temperature logs for Wells 38C-9 and 51B-16. Note the continuously sloping temperature profile in Well 51B-16 versus the variable sloping profile for Well 38C-9 indicating lower permeability and heat flow by conduction in Well 51B-16.....	77
Figure 4.21 c and d. Temperature logs for Wells 67-17 and 84-30. Note the near vertical temperature profiles indicating convection and high permeability. However note the lower temperatures when compared to Well 38C-9 in Figure 4.13 a.	78
Figure 5.1. FIS mudlog for Well 38C-9 with major breaks in chemistry identified.....	81
Figure 5.2. FIS mudlog for Well 51B-16 with major changes in chemistry identified.....	84
Figure 5.3. FIS mudlog with select mass spectra plotted versus depth for an injection well, Well 67-17.	85
Figure 5.4. FIS mudlog with select mass spectra plotted versus depth for Well 84-30 located at the southern margin of the field and non-producing.....	86
Figure 5.5. Finer detail in mass spectra for Well 38C-9. Arrows point to areas of potential fractures.	87
Figure 5.6. Flow chart illustrating the determination of fluid types.	91
Figure 5.7. Fluid logs for Wells 33-7, 58A-18, 46A-19RD, and 73-19 that occur on the western side of the field.	92
Figure 5.8. Fluid logs for Wells 67-17, 67-17C, 52-20, 68-20, 68-20RD, and 84-30 that occur on the middle southern portion of the field.	93
Figure 5.9. Fluid logs for Wells 34-9RD2, 38C-9, 38D-9, 51B-16 and 58A-10 located on East Flank of the Coso field.....	94
Figure 5.10. Interpreted fluid types for Well 38C-9.....	95
Figure 5.11. Interpreted fluid types for Well 51B-16.....	96
Figure 5.12. Interpreted fluid types for Well 67-17.....	97
Figure 5.13. Interpreted fluid types for Well 84-30.....	98
Figure 5.14. The CO ₂ /N ₂ vs. Total Gas Diagram. Boiling trends plot with a negative slope whereas condensation trends plot with a positive slope, Norman et al (2002).....	101

Figure 5.15. The CO ₂ /N ₂ vs. Total Gas diagram for Wells 38C-9, 67-17, and 33-7.....	103
Figure 5.16. Correlation of ratios with temperature. Note for N ₂ /Ar and CO ₂ /CH ₄ there are higher ratios only with higher temperatures. Low ratios exist throughout the range of temperatures.....	106
Figure 5.17. N ₂ /Ar and CO ₂ /CH ₄ ratios versus depth for four wells. High values for ratios may correspond to fractures.....	110
Figure 5.18. Temperature log versus FIS logs for Well 38C-9. Note correlations between changes in all the logs.....	113
Figure 5.19. Temperature log and FIS logs for Well 51B-16.....	114
Figure 5.20. Temperature log versus FIS logs for Well 67-17.....	115
Figure 5.21. Rock types plotted with gas analyses for Well 34-9RD2. Rock types are coded as follows: greens/yellow- diorites, orange-granodiorite, pink-granite, red-microgranite, purple-metasediments, and blue-massive veining. Fluid types are: blue – meteoric, yellow – condensate, grey - background	117
Figure 5.22. Photographs of scale in Well 68-20RD from Moore & Norman, 2006.....	122
Figure 5.23. Legend of fluid types for the cross-sections in Figures 5.24 through 5.28.....	123
Figure 5.24. Cross-section of the East Flank with location map.....	125
Figure 5.25. Cross-section based on FIS of the western edge of the Coso field with location map.....	127
Figure 5.26. Cross section of the middle portion of the field with location map.....	129
Figure 5.27. Cross-section based on FIS diagonally across the Coso field from the southwest to the northeast with location map.....	131
Figure 5.28. West to east cross-section based on FIS logs with location map.....	132
Figure 5.29. Fence Diagram of Coso Field based on FIS logs.....	134

This dissertation is accepted on behalf of the
Faculty of the Institute by the following committee:

Andrew Campbell

Advisor

[Signature]

Nancy Blaney

[Signature]

JAMES B. Johnson Cor Dr. Robert Bowman

June 4, 2009

Date

I release this document to the New Mexico Institute of Mining and Technology.

Abril M. Diller

Student's Signature

6/4/09

Date

This dissertation is accepted on behalf of the
Faculty of the Institute by the following committee:

Andrew Campbell

Advisor

[Handwritten signature]

M. J. Blaney

[Handwritten signature]

J. A. B. Johns - Cor Dr. Robert Bowman

June 4, 2009

Date

I release this document to the New Mexico Institute of Mining and Technology.

Student's Signature

Date

CHAPTER 1. INTRODUCTION

The purpose of this research is to adapt Fluid Inclusion Stratigraphy (FIS), a new well logging method used in the petroleum industry, to geothermal fields. Fluid Inclusion Stratigraphy uses bulk fluid inclusion gas analysis from well cuttings systematically sampled with depth to differentiate fluid horizons (Hall 2002). Petroleum well FIS analysis identifies hydrocarbon-bearing horizons; seals that limit fluid flow; occurrence of hydrocarbons missed by other means of borehole logging; and fluid interfaces (Hall 2002). Intervals of hydrocarbon fluids can be traced from hole to hole when several boreholes are analyzed, hence the use of “stratigraphy” in the process name.

The type of information required to assess a geothermal well differs from that used to interpret petroleum wells. Fluids of interest are present in the system at the time of drilling. These geothermal fluids include plume fluids, condensate, and groundwater, which do not have a single distinguishing gaseous species as is the case with hydrocarbon fluids. Rather the various types of fluids have common aqueous gaseous species and can be identified by differences in relative amounts of species (i.e. gas ratios). Also in hydrocarbon reservoirs, fluids fill interstitial spaces of highly porous and permeable rock. Geothermal fluids principally flux through fractures.

The study started with several working hypotheses to be tested:

- 1) Fluids fluxing through fractures diffuse into wall rock through microfractures; therefore, fluid flowing in major fractures will affect enough rock to be detected in well cutting gas analysis.
- 2) Fractures can be identified by a high fluid inclusion density, therefore FIS analyses when plotted verses depth will show a peak at fracture locations.
- 3) Present-day fluids will add to and in some cases destroy fluid inclusions from previous geothermal events.
- 4) Bulk fluid inclusion gas analysis of well cuttings can distinguish several types of geothermal fluids that include meteoric or groundwater, condensate, and plume fluids.
- 5) The boundary between convective, upward flow of deep plume fluids and the low permeability cap rock that directs upwards flowing plume fluids laterally can be identified by FIS analyses.

Nine well cutting samples from the Coso geothermal system were initially analyzed to determine if fluid inclusion volatiles could be observed in wall rock chips as there were no published analyses other than for oil fields. Fluid inclusion volatiles from the well cuttings were measured and found to be similar in composition to gas analysis of Coso vein minerals. Well cuttings and vein minerals both show fluid inclusions that are mainly filled by water with small amounts of admixed carbon dioxide, nitrogen, hydrogen sulfide, argon, methane, hydrogen, and helium with trace amounts of C₂ to C₆ hydrocarbon species.

The overall goal of this project was to develop a methodology for applying well cuttings fluid inclusion gas analysis to geothermal exploration.

Specific objectives were to:

- Identify geothermal fluid type using fluid inclusion gas analysis and develop a procedure for analyzing and displaying FIS mass spectrometer analyses.
- Verify that FIS analysis indicates fractures.
- Optimize FIS sample frequency to minimize cost and maximize information obtained.
- Verify that FIS done on multiple holes will show a “stratigraphy” (vertical sequence) of subsurface fluids that can be traced, or correlated, between wells.
- Test the developed geothermal FIS methodology on wells drilled during the project period and evaluate the value of the method.

In addition to these practical goals, the scientific goals were to:

- Gain a better understanding of fluid flow within a geothermal system.
- Create a fluid model of a geothermal system.

CHAPTER 2. BACKGROUND

2.0 Geothermal Systems

Volcanic hosted geothermal systems are divided into island arc systems, typified by New Zealand systems; rift systems, typified by East Africa and Iceland systems; and California-Sierran mixed with extensional and transverse fault systems such as Coso and Imperial Valley (Grant et al. 1982). In each of these systems there is a heat source, either from current or recently solidified magma bodies. In addition there are the Basin and Range systems such as Beowawe and Dixie Valley in Nevada where there is no firm evidence of an underlying magma, but rather heating is attributed to deep circulation of meteoric fluids in the crust with above normal heat flow. The temperature and fluid distribution in reservoirs are determined by hydrothermal convective fluid flow (Ellis & Mahon 1977).

Geothermal systems are also classified as either vapor-dominated or liquid-water systems. Vapor-dominated systems have steam with minor admixed gaseous species, temperatures greater than 455°F (235°C), and production wells typically 1 to 4 km in depth. Steam is brought to the surface and it is used directly to create electricity. Liquid-water systems have typical temperatures ranging from 300°F (150°C) to 572°F (300°C) (DOE 2003). A flash steam power plant is most common in liquid-water systems.

Geothermal fluids are brought to the surface through production wells as deep as 4 km.

Fluids are highly pressurized; up to 40 percent of the water flashes to steam in a series of steps. The steam is separated and used to turn the turbines. Lower temperature reservoirs, those between 212°F (100°C) and 400°F (225°C) typically require a binary cycle power plant. In the binary plant, geothermal fluids are passed through a heat exchanger heating a secondary working fluid that vaporizes which turns the turbines (DOE 2003). Coso and Beowawe are liquid-water systems.

Although Coso is a liquid-dominated field, a vapor reservoir is developing. It was shown by Moore et al. (1998) that The Geysers in California formed from a liquid-dominated field much larger than Coso. He proposed that vapor-dominated fields should be thought of as heat pipes. Once boiling starts a drop in water levels occur. Rock is left with heat that is above saturation temperature (boiling point). Liquid forming as condensate at the reservoir cap flow downward encountering hot rock, and boils. The rock's heat is lost in boiling and a steady-state is achieved, with salinity increasing with time as steam is lost from the reservoir. Condensate at the top is low in salinity and slightly acidic. As this liquid moves downwards it results in corrosion of calcite and quartz as observed in The Geysers (Moore et al. 1998). Similar process may be creating the vapor phase in the Coso Field. Water levels drop as a result of production and/or lack of recharge.

Henley & Ellis (1985) proposed a generalized model (Figure 2.1) of a liquid-dominated geothermal system in a silic volcanic environment, similar to Coso. The model shows that chloride waters, which are created by chemical interactions of water-rock-magma at depth, rise and boil, and the resultant steam migrates to the surface. Near-surface

condensation and oxidation of transported H_2S produces sulfate-dominated, steam-heated waters and condensate. Near-neutral pH chloride springs occur sparingly on the surface.

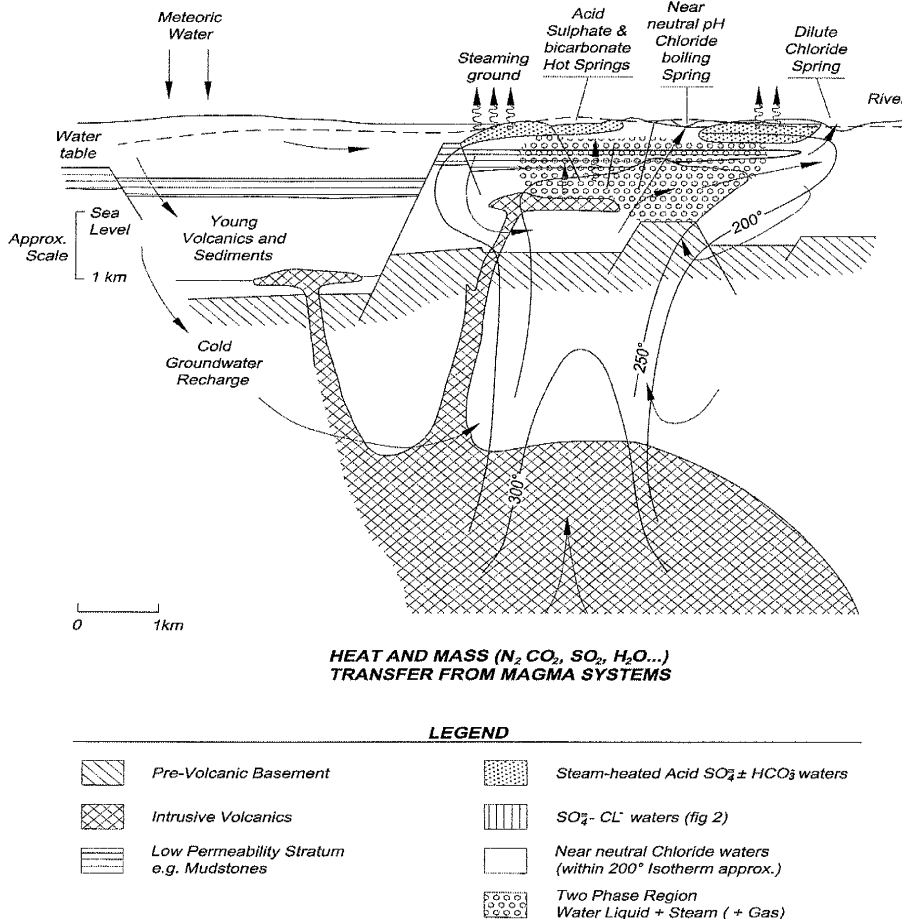


Figure 2.1. Typical geothermal system in silicic-volcanic environment. Temperature distribution is based on the system at Wairakei, New Zealand. (From: Henley & Ellis 1985).

Geothermal systems exploit concentrated heat sources in the crust. The feasibility of a system for exploitation is based on the flow of groundwater through permeable rocks. Introducing a heat source, such as an igneous intrusion into the crust creates a heat engine for the formation of a geothermal system (Figure 2.2). Groundwater in the vicinity of the heat source is heated by conduction. As the groundwater heats up, fluid density and

viscosity decreases. The changes in density and viscosity are dependent upon temperature, pressure and concentration of solute (Bredehoeft and Norton 1990). Convection cells are created due to the differences in the fluid density and viscosity. The convecting cells move heat away from the heat source and are the source of production in a geothermal field (Nielson 2001). The region where conduction is heating the groundwater and convection starts is the plume zone; whereas most convection occurs in the mixed zone. The meteoric zone with cooler waters occurs at the top of the system. Separating the zones are caps that are created by chemical changes (Reed & Spycher 1985).

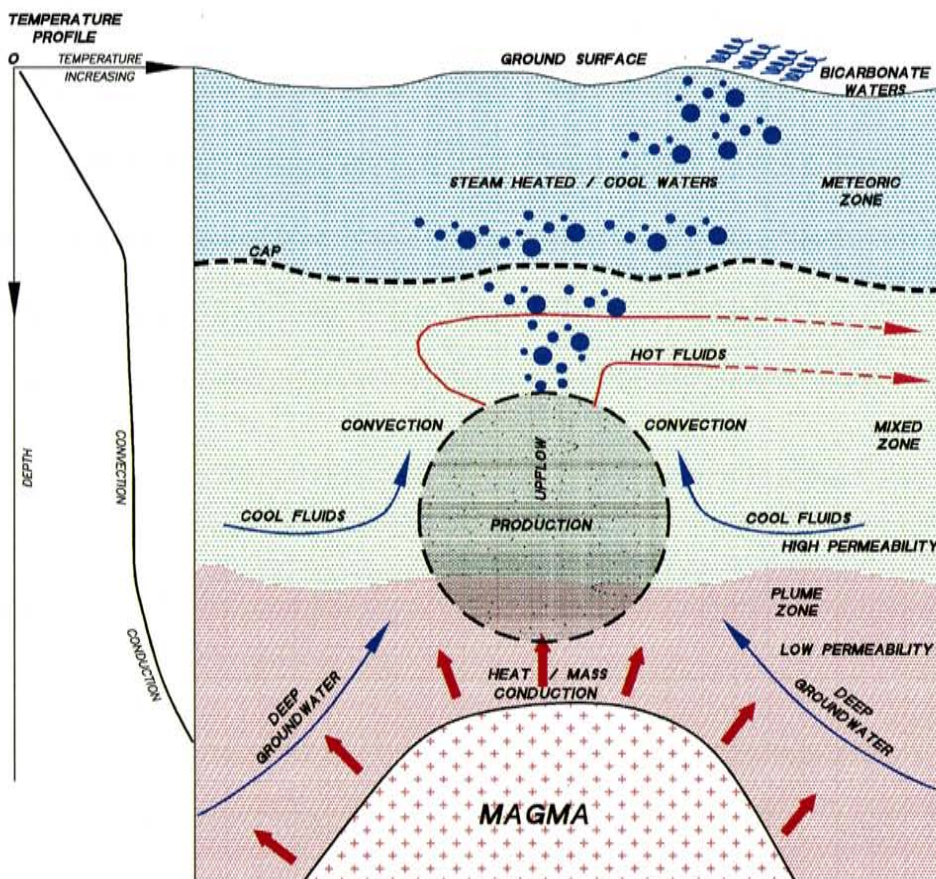


Figure 2.2. Fluid flow model in a geothermal system. Modified from Henley & Ellis (1985).

Permeability in geothermal systems is typically greater than 10^{12} m² resulting in fluid flow. As permeability increases convection as opposed to conduction of heat and solute dominates (Manning & Ingebritsen 1999). Pore pressure is affected by changes in pore volume and temperature. The properties of water allow for significant changes in pore pressure when heat is introduced (Bredehoeft and Norton 1990). As pore pressure increases rock failure occurs resulting in shearing or hydraulic fracturing. Fractures increase the permeability of the rock and the high pore pressure dissipates. Boiling of fluid and deposition of minerals may occur at this point within the fracture.

Conduction occurs in low flow areas, allowing temperature to increase rapidly with depth. Conduction is indicated on temperature versus depth plots by sloping lines. Larger flow rates produce near vertical profiles on temperatures versus depth plots indicating convection (Manning & Ingebritsen 1999). A simplified temperature profile showing depth with convective and conductive heat flow is present on Figure 2.2.

Geothermal systems are more complicated than the simple models presented. For example, how and why reservoir caps form is poorly understood. They may be lithologic (based on low permeability rock types) or the result of enhanced mineral deposition at boundaries between reservoir fluids and cooler ground waters (Moore et al. 2001). Fluid movement is complicated in geothermal systems. Entrances (inflow zones) of steam-heated and cool surface waters into the lower mixed and plume zone is common at the Coso field (Brian Berard personal communication) and can be identified in some systems

by changes in alteration and vein mineralogy (Moore et al. 2001). Cool, low-salinity groundwater is denser than the typical hot geothermal fluid; therefore, when cold water enters a fracture bearing hot waters the cold water will sink and mix with the hot water. Gas composition in geothermal systems is also complicated such as vapor development that fractionates gaseous species. Species with low solubilities like H₂ and Ar readily partition to a vapor phase, whereas more soluble gaseous species that commonly interact with water, like CO₂ and H₂S, remain in solution.

Geothermal fluids deposit minerals in open fractures. High strain rates common in geothermal systems continuously reopen fractures (Blewitt et al. 2002; Moore, Morrow et al. 1987) allowing for episodic mineral deposition. Boiling, dilution and fluid-rock interactions can change the chemical composition of fluids, resulting in mineral growth and formation of fluid inclusions within the minerals. Fluids trapped in inclusions during mineral growth are generally faithful chemical indicators of fluids at the time of crystal growth. A small change in fluid temperature and/or pressure can create a rapid deposition rate (particularly in areas of high fluid flow) due to the near saturation of silica, calcite, and calcium sulfate. A well in Tongona, Leyte Philippines developed aragonite scale at the rate of 1 mm/hour (Ellis & Mahon 1977). Field experiments at Wairakei, New Zealand indicated that over 570,000 pounds of amorphous silica could precipitate in 10 years from flashed fluids reinjected containing 530 ppm silica (Mroczek, White and Graham 2000). This rapid deposition of minerals seen in wells may also occur in fractures within the present-day geothermal system.

2.1. Fluid Inclusion Gas Analysis – Previous Work

Carbon dioxide (CO₂), hydrogen sulfide (H₂S), hydrogen (H₂), nitrogen (N₂), ammonia (NH₃), methane (CH₄), and inert gases are the major gaseous species in geothermal fluids (Ellis & Mahon 1977; Henley et al. 1984). Basic geothermal equilibrium gas chemistry is discussed by Giggenbach (1980). In 1986, Giggenbach calculated the effects of boiling on CO₂-CH₄-H₂ ratios in geothermal fluids and presented the idea that fluid inclusion gas analysis can be used to identify a magmatic component in inclusion fluids. Since that time, Norman, Moore, Giggenbach and a number of collaborators have used fluid inclusion gas analysis to expand the science of geothermal gas chemistry and understanding of geothermal processes (Norman and Sawkins 1987; Graney 1994; Giggenbach 1997; Moore 1995; Moore 1997; Norman 1994; Norman 1996; Norman et al. 1997; and Norman & Moore 1999). Norman and Musgrave in 1995 showed that the nitrogen/argon (N₂/Ar) ratio in fluid inclusion gas analysis is an important indicator of magmatic components. Follow-on work by Norman et al. (1997) showed that steam-heated waters are distinguished by high concentrations of more soluble gaseous species, including CO₂, benzene (C₆H₆) and H₂S. The ratio of CO₂/CH₄ in fluid inclusions has also been showed to be high in fluids with a magmatic component (Giggenbach 1986; Norman & Musgrave 1995; Norman et al. 1996; Lutz et al. 1999; and Moore et al. 2001).

Distinctive assemblages of gases can assist in defining fluid types. Alkaline chloride plume fluids, condensate, and shallow bicarbonate waters have different gas chemistries (Ellis & Mahon 1977; Henley, et al. 1984). Specific gases can be derived from high-temperature reactions within the system or may be introduced from external recharge

waters. Reactive gases such as H₂, H₂S, CH₄, and NH₃ are derived from water/reactions with organic chemical species or with mineral phases in a geothermal reservoir (Henley, Truesdell & Barton 1984). The species CO₂, H₂, SO₂, H₂S, HF, N₂, Ar, He and HCl are recognized in volcanic gases and geothermal systems (Giggenbach 1986). High concentrations of CO₂, H₂S, and HCl are noted in Icelandic geothermal fields and are thought to be derived from active magmatic chambers at depth (Armannsson et al. 1982).

Geothermal fluid types are named by fluid origin and chemistry. These include meteoric water, plume fluids, bicarbonate waters, steam-heated waters, condensate waters, and acid sulfate waters. Meteoric fluid is the term generally used for shallow, young groundwater that originated as rainwater. Plume fluids are deep circulating groundwater heated to the point they can be produced profitably for electric power generation. They are chemically modified by water-rock reactions and commonly admixed with limited amounts of magmatic volatiles. Plume fluids are near-neutral pH chloride waters (Henley, Truesdell & Barton 1984). Steam-heated waters are formed by fluxing steam from boiling alkali-chloride waters bearing geothermal gaseous species through shallower waters. Generally these are meteoric waters hence steam-heated waters have low chlorine. Steam can heat groundwater to a maximum of 455⁰F (235 C). Steam can condense and collect at the base of steam zones; this fluid is similar in gas content and chlorine content to steam-heated waters. Poorly understood is the flux of super critical “steam” from cooling intrusives that can mix with shallower waters. Because of their high enthalpy, supercritical fluids can heat groundwaters to 572⁰F (300 C). For want of a better term such fluids are called deep condensate or condensate because of additions of

condensed supercritical fluid. The gas signature of condensed supercritical fluids and boiled fluid are nearly identical with the exception that the liquid phase becomes enriched in H₂S. In both cases there is a vapor and liquid phase present. Based on modeling, plots of CO₂/N₂ vs. total gas are used to separate the two (Norman et al. 2002). It is expected that magmatic vapor will be high in typical magmatic gaseous species like CO₂, H₂, SO₂, and HCl. Mixed fluids have shared characteristics of several fluid types.

Gas analyses of steam and water samples from various geothermal fields have used N₂/Ar ratio to determine fluid origins. These studies have included Mazor & Wasserburg (1965) and Gunter (1973) evaluation of Yellowstone and Lassen; Hulston & McCabe (1962) study of New Zealand fields, Giggenbach (1997), and Shukolyukov & Tlstikhin (1965) study of Russian geothermal fields. These studies mainly focused on identifying the meteoric component of the fluids. Meteoric waters (air saturated waters) contain a distinctive suite of gases including Ar and other noble gases, which are useful in identifying meteoric water influx in active geothermal systems (Norman and Musgrave 1995). Meteoric fluids in fluid inclusions have N₂/Ar ratios between 38, value of ratio from air saturated water, and 54 by additions of some air in vadose zone. These values are empirically determined with values as high as 110 from N₂/Ar fractionation by boiling or additions of organic N₂, (Norman et al. 1997).

Giggenbach (1986) introduced the use of the N₂/Ar ratio to indicate the presence of magmatic gaseous constituents in geothermal fluids based on the occurrence of N₂/Ar ratios greater than 100 in silicic volcanic gases (Giggenbach 1986) Giggenbach proposed

that N_2/Ar ratios greater than groundwater indicates magmatic gas components in geothermal fluids. Additional work by Norman and Musgrave (1995) determined that the N_2/Ar ratio is an important indicator of magmatic components when used in fluid inclusion gas analysis.

In addition to the high N_2/Ar ratio, magmatic gases generally have high CO_2/CH_4 content (Giggenbach 1986; Norman and Musgrave 1995; Norman et al. 1996). Plume fluids that circulate in non-organic rocks (like Coso) have CO_2/CH_4 ratios higher than 4. However, if basement rock is rich in organic compounds methane can be an important geothermal species. The ratio of CO_2/CH_4 in fluid inclusions was used by Lutz et al. (1999) to evaluate the origins of fluids at Dixie Valley geothermal field in Nevada where there is evidence of an intrusive at depth. Basement rocks are organic-rich marine clastics. Most of the geothermal vein samples from the wells were interpreted as mixtures of shallow meteoric and plume fluids. They determined that if the CO_2/CH_4 ratio is less than 4 the fluid is plume fluids that circulated deep in the organic-rich sediments. Moore et al. (2001) also found that in The Geysers field in California, the plume fluids had CO_2/CH_4 ratios of less than 4 as do nearby Wiber Springs waters; and the host rock is the Franciscan Formation, which is very organic-rich. The Geysers fluids also have N_2/Ar ratios greater than 100 and mantle He_3/He_4 ratios.

Boiling and condensation are important processes that occur within geothermal systems. Fluid inclusion gas analyses by Norman et al. (2002) indicate that vapor-filled inclusions will be enriched in methane, ethylene, and other similar less soluble species.

Condensation will concentrate more soluble species including aromatic organic species, H₂S, and CO₂. Through successive crushing and extraction of gases from a single mineral, Norman (1997) showed that there is an evolution in the composition of gases within fluid inclusions trapped during boiling. Methane, ethylene, nitrogen, and other insoluble species are initially trapped. As boiling continues, these components are removed from the system until inclusions with mostly CO₂ are left. Norman et al. (2002) developed an open system boiling model and showed that as total gas is decreased the ratio of CO₂/N₂ increases with time in both liquid and vapor inclusions.

Deeper meteoric fluids typically have H₂, He, H₂S, CO₂, CH₄, or heavier organic species derived from fluid interaction with organic-rich sedimentary rocks. These fluids have decreased oxygen and reflect a reducing environment when compared to shallower meteoric fluids. Giggenbach (1986) also showed that these fluids are enriched in CH₄, other hydrocarbons, and N₂/Ar ratios up to 150. Fluids from metamorphic processes are dominated by CO₂, with lesser amounts of CH₄ and H₂S (Landis and Hofsta 1991).

Norman et al. (2002) also showed by analysis of samples from Karaha Telegas Bodas geothermal system and Coso geothermal system, that various organic compounds occur in fluid inclusion gases and range in concentration from about 1 ppm/v to almost 900 ppm/v. The concentrations and type of organic species measured indicate inorganic processes as the source. Biogenic processes typically occur at less than 100 °C and produce mostly methane. Inorganic sources include pyrolysis of organic material producing alkanes and heavier hydrocarbon species and Fischer-Tropsch reactions

produce lighter hydrocarbon species and alkenes (Norman et al. 2002). Wall rock reactions with alkanes can produce alkenes. Norman et al. (2002) concludes that the ratio of alkanes/alkenes (C_{n+1} / C_n) can be used to indicate source of geothermal hydrocarbon gaseous species.

At higher temperatures (300 to 350⁰C) H₂S is in equilibrium with pyrite and magnetite (Henley & Brown 1985). Thus H₂S is in concentrations of $\sim 10^{-3}$ m or 34 ppm/v (0.0034 mol%) in plume fluids. Norman et al. (1997) showed that steam-heated waters are distinguished by high concentrations of more soluble gaseous species, including CO₂, benzene (C₆H₆), and H₂S, and that H₂S is low or absent in groundwater. However, highly evolved (older) groundwater may have high concentrations of H₂S above 1000 ppm/v as well as He and CH₄.

In summary, previous work on interpreting fluid sources and fluid processes from geothermal gas chemistry has shown the following (Table 1): (1) meteoric-air saturated water (shallow groundwater) has low concentrations of gaseous species and N₂/Ar ratios of between 38 to 54; (2) plume fluids that are the deep circulating alkaline chloride waters typically have N₂/Ar ratios greater than air, CO₂/CH₄ ratio greater than 4 (if low organics in reservoir rocks like Coso), and H₂S in near equilibrium with pyrite and magnetite; (3) steam-heated waters have high concentrations of the more soluble gaseous species such as H₂S, CO₂, and benzene; steam caps have inclusions rich in gaseous species and much less water than assemblages of aqueous inclusions (Moore et al. 2001); (4) boiling creates inclusions with trapped vapor resulting in higher gas/water ratios and

condensation results in higher concentrations of more soluble gaseous species including H₂S, CO₂, and aromatic organic species. Both boiling and condensation result in increased CO₂/N₂ ratios.

Table 1. Summary of Fluid Inclusion Gas Chemistry and Fluid Types.

Fluid Types	N ₂ / Ar	CO ₂ / CH ₄	H ₂ S	Other
1) Meteoric-Air Saturated Waters	38 -54	Low <4	Low	Low total gas Alkanes/alkenes high
2) Geothermal Fluids w/ plume fluids	>110	>4	Present maybe high	High CO ₂ , Total gas >0.1
3) Steam-heated waters/steam caps		Typically >4	High >0.01 mol%	Soluble gases, H ₂ S/N ₂ >0.1
4) Boiling/ Condensation	>110	>4	Present Condensation high	Gas/Water high, CO ₂ /N ₂ high versus Total Gas

2.2. Well Logging/Testing

Vital to the management and sustainability of a geothermal reservoir is an understanding of fluid movements and controlling structures within the reservoir. Tools currently available to understand the behavior of the fluids within a reservoir are well log data, alteration patterns, and fluid inclusion thermometry. Geophysical data such as seismic, magnetotelluric, and resistivity are used to image the geometry of controlling structures in the subsurface and areas of clay mineral alteration (Newman et al. 2005). Well log data provide information on the temperature and flow of fluids and on fracture patterns (Ellis & Mahon 1977; Roberts et al. 2001). Alteration patterns describe past behavior of fluids and identify the chemistry of fluids. Fluid inclusion gas chemistry and microthermometry provide information on the chemistry, temperatures, and salinities of the fluids. Each of these techniques is expensive and time consuming. Well logging

typically averages on the order of hundreds of thousands of dollars per well for a suite of logs (Berard 2003). Temperature logging requires many days to run several tests at various pumping rates to obtain accurate temperature profiles of the borehole.

Determining alteration patterns requires detailed geological study of the core. Fluid inclusion gas chemistry has to this point been performed only on limited samples using high-precision mass spectrometers that require several days to obtain results. Fluid inclusion thermometry requires detail analysis and skilled interpretation. A goal of this project was to develop a methodology to show that FIS can provide a rapid (within the time frame of drilling the well), inexpensive (on the order of \$5,000 to \$10,000 per well) technique that will produce the same type of data as the above techniques on a detail scale and be useful to understanding a geothermal system.

A geothermal well will typically cost between \$5 million and \$13 million, and there may be 10 to 100 or more wells in a fully developed field. Drilling can readily account for 30 to 50 percent of the total financial outlay of a geothermal project. Testing during drilling of the well and after well completion is essential for determining reservoir and fluid properties. This project hopes to demonstrate FIS as a tool to be used while a well is being drilled, that will provide information on fluid types. FIS does not affect the well environment like testing and logging tools do and therefore FIS provides a picture of the well prior to development.

2.3. Coso Geologic Setting

The Coso geothermal system was chosen for the demonstration for several reasons. First, it is one of the larger geothermal systems in production. Second, with approximately 100 wells in production, the field offers a great variety of wells to choose from for study, including high-production geothermal wells that produce about 25 megawatts (MW) down to the geothermal wells that produce in the 2- to 3-MW range. Third, Coso is a young system, less than 10,000 years old (Kurilovitch et al. 2003), with recent deposition overprinting that of an older geothermal system. Fourth, it is also one of the best-documented silicic dome systems in the world (Ross and Yates 1943; Dupuy 1948; Bacon and Duffield 1980; Bacon et al. 1981; Adams et al. 2000).

The Coso geothermal system is approximately 30 miles north of Ridgecrest, California, within the western extent of the Basin and Range province (Figure 2.3). The system occupies approximately 30 square kilometers of the Mojave Desert. The reservoir has sustained 240 MW of electricity from fractured Mesozoic rocks that consist primarily of granitic plutons and metamorphics. Pliocene and Pleistocene volcanics with an age range of 4 to 0.04 Ma overlie the Mesozoic rocks.

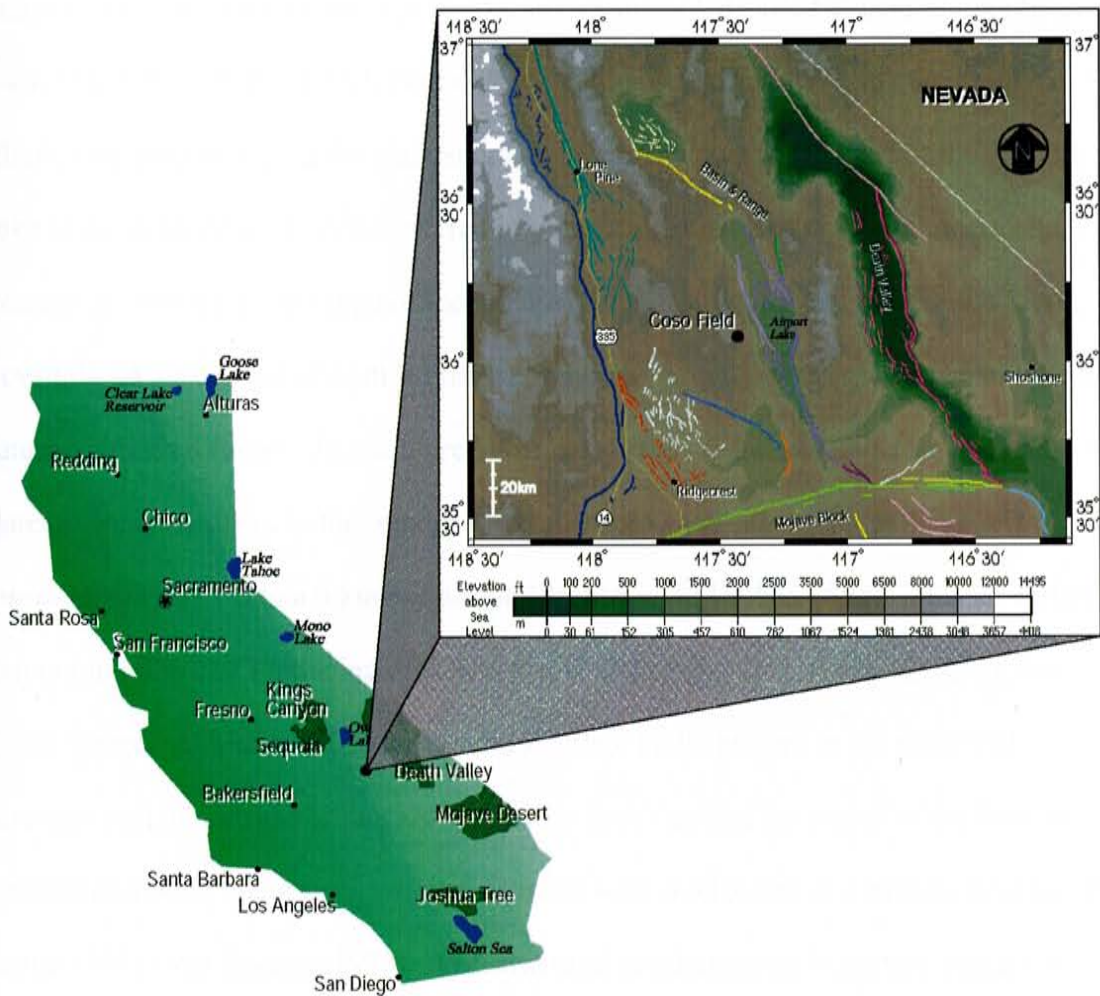


Figure 2.3. Map of California with location of Coso Geothermal Field. Top photograph modified from Southern California Earthquake Data Center indicating the Basin & Range and Mojave Block as well as location of major fault zones.

The geology of the Coso area results from the complex interaction of Basin and Range extensional forces with the right-lateral strike slip movement of the San Andreas fault system. The Sierra Nevada Range to the west and the Argus Range to the east are north-south trending ranges bounded by normal faults reflecting the east-west extensional nature of the Basin and Range area. The irregular and ill-defined boundaries of the Coso

Range reflect the complex tectonic history of the area. A detailed structural map (Figure 2.4) of the area indicates a high fault density. Three sets of faults create the dramatic relief of the area including the giant staircase stepping down to the west of the Airport Lake area. A set of west-northwest trending vertical faults occur in the southern and western parts of the Coso range reflecting the regional structure that ends in the Sierra Nevada's. A second set of north-northeast trending normal faults indicate the basin and range extensional forces. Dramatic relief of the Airport Lake area, consists of a series of plateaus stepping down to the west in Pliocene rocks. Vertical offset in this area is approximately 650 m in a 9 km wide zone (Wohletz and Heiken 1992). This set of faults step out into the east producing the Coso Basin, separating the Coso Range from the Argus Range. A third set of faults are the accurate faults present in the north and northeast part of the field which are concentric faults around the center of the field and dip inward toward the center. Originally, these were interpreted as a caldera structure by Austin (1971) and Koenig (1972). The structural relationship is important because it allows for development of faults that are part of the continual expression of the movement of the magma body below the geothermal field.

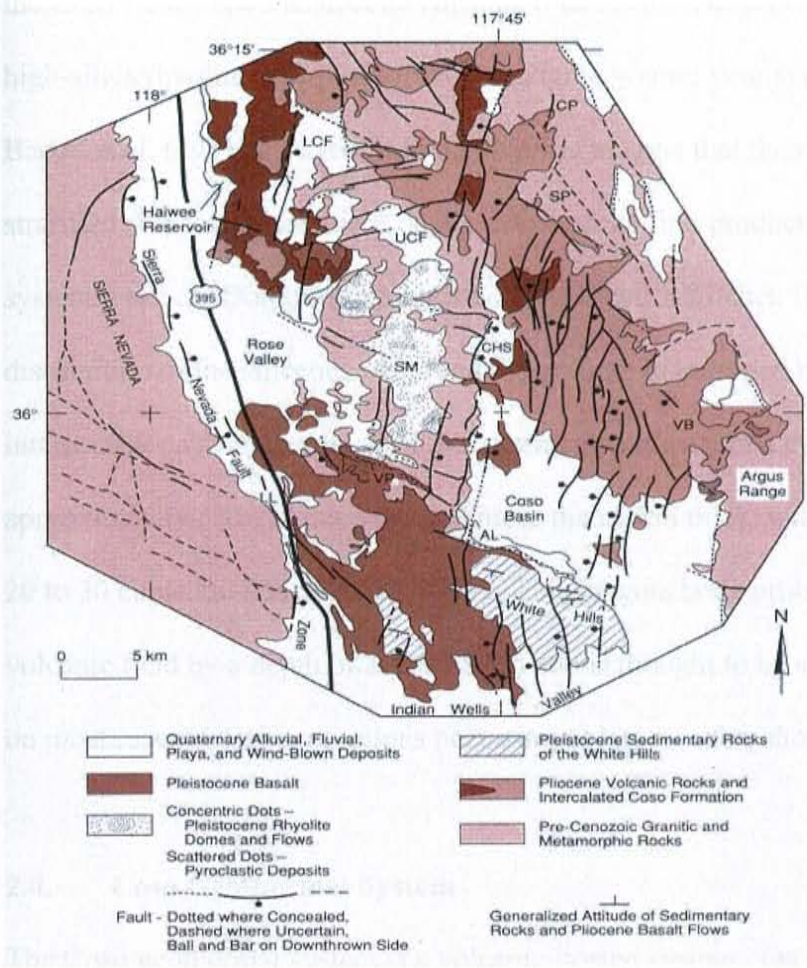


Figure 2.4. Geologic Map of the Coso volcanic field indicating the three sets of faults in the region. Abbreviated locations: CP=Coso Peaks, LCF=Lower Cactus Flat, UCF=Upper Cactus Flat, SP=Silver Peaks, CHS=Coso Hot Springs, SM=Sugarloaf Mountain, VB= Volcanoe Butte, VP= Volcano Peak, AL=Airport Lake, and LL = Little Lake (From: Wohlez K. and Heiken G. 1992).

Pliocene and Pleistocene volcanic rocks are the most voluminous and widespread of the rocks in the area. There are approximately 400 km³ of lava flows and domes. The relationship of the volcanic rocks to the underlying granitic basement was documented by Duffield et al. in 1980. Sugar Loaf Mountain is a rhyolite dome in the middle of the Coso field, surrounded by a series of basalt rocks. The older granitic and metamorphic rocks of the Sierra Nevada's and the Argus Range are both to the east and to the west of

the Coso field. The Pleistocene volcanic rocks consist of 38 separate domes and flows of high-silica rhyolite, and most of them are quite young; younger than 300,000 years. Bacon et al. (1981) inferred from the rhyolite magma that there was a chemically stratified siliceous reservoir at depth. Most of the first production of the geothermal system was near Dome 53, which is near the Devil's Kitchen fumarolic area. The distribution of the siliceous vents and the volume of extruded magma combined with interpretations from geophysical measurements indicate that the siliceous magma body is approximately 5 km in diameter and more than 1 km thick, with a total volume of about 20 to 30 cubic km (Bacon et al. 1980). This magma body probably underlies the Coso volcanic field by a depth of at least 8 km and is thought to be still partially melted, based on most recent basaltic eruptions occurring as late as a few thousand years ago.

2.4. Coso Geothermal System

The Coso geothermal system is a volcanic-hosted system. On the basis of the rocks observed on the surface, there appear to have been three episodes of thermal activity. Fossil fumaroles (travertine deposits) on the eastern side of the field are dated using U/Th dating to 307,000 years old and represent the first episode of thermal activity (Adams et al. 2000). Sinter deposits dated at about 238,000 years old in the eastern and southern parts of the present-day field record the second episode. The most recent thermal episode began approximately 10,000 years ago (Kurilovich et al. 2003), based on potassium/argon dating of well chip samples. Fluid inclusion data from Lutz (1999) suggest that the first episode was a large-scale system but of low to moderate temperature. The second episode was produced by magmatic activity beneath the dome

field that resulted in a large high-temperature system. The most recent event has heated up the eastern flank by 212°F (100°C) and reactivated the high-temperature center beneath the southern part of the field.

Chloride isotopic compositions indicate that crustal waters from nearby sedimentary formations were probably the original waters in the first system. (Adams et al. 2000). Convection of the fluids caused the thermal fluids to flow longitudinally and upward to the north for much of the first and second thermal episodes. A non-thermal groundwater system capped the thermal system. The low-salinity groundwater disappeared, most likely at the end of the last glacial period. (Adam et al. 2000) The last pluvial period in the area occurred approximately 10,000 years ago. After this period the Mojave Desert became drier. The present-day geothermal system is partitioned into at least two reservoirs that are weakly connected and one that is isolated. The segregation of the reservoir and the components may have occurred when the groundwater disappeared (Adam et al. 2000).

Fluid inclusions from the Coso geothermal system record a broad range of temperatures and salinities. Adams et al. (2000) indicates that fluid inclusions related to current geothermal activity have homogenization temperatures ranging from 69°F (76°C) to 622°F (328°C) and salinities of 0 to 3.4 weight percent in chlorine (Cl) equivalent. The highest temperatures are found near the southern end of the field, where they define a shallow up-flow zone in the area that contains no surface manifestations. The variations

Initial gas data from 41 wells prior to extensive production and drilling was provided by Coso Operating Company. Once production and additional drilling occurs, the gas ratios change rapidly due to changes in pressure and fluid levels. Table 2 presents the initial gas data gathered from fluid samples in 40 Coso wells:

Table 2. Initial Gas Data (ppm/v) from the fluid samples collected in 40 wells in Coso Field

Species	High	Low	Average	Std Dev
CO ₂	52900	640	11,900	12,900
H ₂ S	1,110	2.43	183	269
NH ₃	8.14	0	1.18	1.90
Ar	1.71	0.05	0.46	0.52
N ₂	1,030	3.03	58.6	161
CH ₄	11.0	0	1.56	2.29
H ₂	14.6	0.008	1.10	2.51
N ₂ / Ar	170	33.6	127	
CO ₂ / CH ₄	21,000	3,400	7600	

A series of active acid-sulfate springs and mud lakes comprise the main Coso Hot Springs area. The hot springs occur along the north–northeast trending fault on the east side of the main fault block. Austin and Kringle (1970) measured up to 3000 parts per million (ppm) chloride in deep well waters in this area. Downhole temperatures were measured at 288°F (142°C). The Devil’s Kitchen area consists of a series of fumaroles on the tuff ring at Dome 53, and there is a present-day deposit of sulfate, native sulfur,

and cinnabar. Various fumaroles become active at different times, and it was noted during the site visit in 2003 that a new fumarole had developed in this area.

2.5. Beowawe Geology

Part of the project was conducted using data from Beowawe, Nevada. A new production well was being drilled in Beowawe by Coso Operating Company and it was decided that this well would be a good test case of applying FIS to well drilling decisions. A major fault location in the well could not be identified. The drill rig was on standby. FIS was used to identify the fracture in less than a week. Also, core samples were studied from Karaha Telga Bodas, Indonesia and Steamboat Springs, Nevada to determine if fractures can be identified by FIS analysis. There is virtually no available core from Coso and Beowawe wells.

The Beowawe geothermal field is located in northern Nevada within the Basin and Range geologic province. Miocene volcanic rocks overlie older chert, shale and quartzite of the Valmy Formation (Garside et al. 2002). The reservoir is associated with the normal Malpais fault that cuts across the northern Nevada rift. Production occurs in the Valmy Formation within highly fractured rocks. The Malpais fault is the major conduit for geothermal fluids to rise from a deeper reservoir (Figure 2.6). Two production wells drilled in 1985 provided the production capacity of 16.7 MW. A third production well 77-13 was placed on line in 1991 (Rose & Adams 1995).

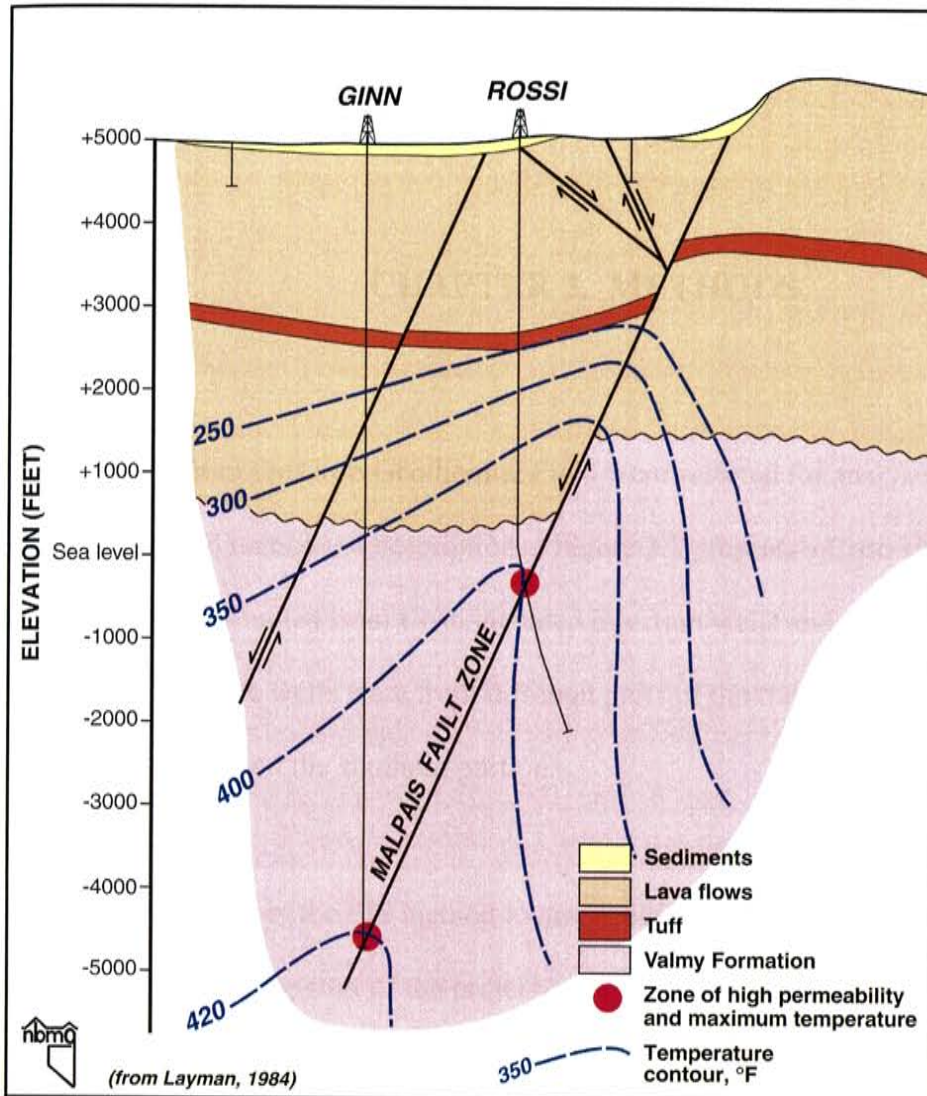


Figure 2.6. Cross-sectional model of the Beowawe geothermal system. Note the Rossi well cuts the Malpais fault at about 5500 feet and the zone of high permeability lies within the Valmy Formation (From: Layman, 1984).

CHAPTER 3. METHODS

3.0 Wells

Fifteen wells from the Coso Geothermal Field were selected for analyses. Table 3 presents the well names and descriptions. Figure 3.1 presents a Coso site map and well locations. Wells studied from Coso included injection wells and non-producers to 8-MW capacity wells. The wells were from different parts of the field including the East Flank, the western edge, and the southern portion.

One goal was to apply the FIS method to new wells being drilled. Coso Well 38D-9 was drilled shortly after the start of the project, and the FIS method and interpretation were performed during drilling. Samples were collected in the first 6,000 feet and submitted for analysis. Additional samples were collected from the remaining footage drilled and analyzed as the well was being completed. The purpose was to evaluate the turnaround times and what if anything the FIS method indicates about production zones while the well was being drilled. In 2006 a new well drilled in the Beowawe field was selected as the second test well. The charge was to determine the fault location and if the production zone had been encountered. Cuttings from a different Beowawe production well where the fault location and the production zone are known were analyzed for comparison.

Well names are on Table 4.

In May 2003, four Coso wells (33-7, 84-30, 58A-18, and 38C-9) were analyzed to determine if the technique would work. Drilling was planned for Well 38D-9 during this time. Samples were collected by a mud logger while this well was drilled in 2004. In late 2004, Coso Wells 51B-16, 34-9RD2, 67-17, and 52-20 were sampled by a Coso geologist from stored drill cuttings. Well 46A-19RD was sampled in March 2005 by a Coso geologist. The final Coso sampling was conducted in October 2005 at the core laboratory at Energy & Geoscience Institute (EGI) at the University of Utah by the author. Drill cuttings from Wells 68-20, 68-20RD, 67-17C, and 73-19 stored at the EGI laboratory were sampled. Beowawe wells were sampled by a company geologist in January 2006.

Table 3. Coso Geothermal Field Well Names and Descriptions. Low temperature wells have temperatures of 212 to 428⁰F (100 to 220 C), medium temperature wells have temperatures of 428 to 572⁰F (220 to 300 C) and high temperature wells have temperatures > 572⁰F (300 C). Well temperatures are not exact and change with time and well depth.

Well Name	Type	Temperature (Enthalpy)	Capacity (MW)	Sampling Interval (ft)
33-7	Producer	Low	2	760-9860
38C-9	Producer	Medium	8	100-9180
84-30	Non-Producer	N/A	-	540-7820
58A-18	Producer	Low	4	2580-8660
38D-9	Producer	Medium	7	6100-9450
58A-10	Non-Producer	Unknown	-	60-9860
51B-16	Non-Producer	High	-	780-9800
34-9RD2	Injection	High	3+	1590-4080
67-17C	Injection	Low	-	540-7780
67-17	Injection	Low	-	497-9020
46A-19RD	Non-Producer	High	-	2360-13020
68-20	Injection	Low	-	1000-6380
68-20RD	Injection	Low	-	2600-6960
52-20	Producer	Low	3	520-7780
73-19	Producer	High	3	800-6050

Table 4. Beowawe, Nevada, Geothermal Field Well Names and Descriptions.

Well Name	Type	Temperature	Capacity (MW)	Sampling Interval
77-13	Producer	Medium	Unknown	0 - 8,300
57-13	New Well	Unknown	Unknown	0 - 10,600



Figure 3.1. Location of wells used in the study and surface features of Coso Field. CHS=Coso Hot Springs. Colors represent topography with pinks being high areas and grays and whites low areas.

3.1. Rock Cores

Additional samples from borehole cores were collected to determine if increased gas concentration corresponds to fracture zones. There is only limited core from one Coso well, hence the exercise was supplemented by core available from other geothermal fields. Samples were collected from a select interval from the one well at Coso, select intervals from two wells at Karaha Telga Bodas, Indonesia (Karaha) as well as one well at Steamboat Springs. The cores were located at EGI laboratory, and were sampled in October 2005. The interval along each core was selected based on the presence of a distinct fracture or vein. The veins were typically composed of quartz and/or calcite. Chip samples were collected at 1- to 2-foot spacing along the core for about 10 to 20 feet in both directions away from the center of the fracture or vein. The wells and sampling intervals are presented in Table 5. Samples were crushed and sized to 1 to 5 mm grains similar in size to chips obtained from rotary drilling.

Table 5. Sampling Interval of Rock Cores

Field	Well Name	Type	Sampling Interval (ft)
Karaha	K-33	Producer	4339-4347
Karaha	K-33	Producer	5449-5459
Karaha	K-33	Producer	5460-5467
Karaha	T-2	Producer	3512-3521
Karaha	T-2	Producer	3549-3567
Karaha	T-2	Producer	3650-3659
Karaha	T-2	Producer	3669-3699
Steamboat	87-29	Producer	20 – 4000
Coso	64-16	Unknown	560-720

3.2. Sampling

Sampling of the wells consisted of obtaining 10 to 20 grams of well cuttings at 20-foot intervals. The cuttings ranged in size from coarse-sand to fine-sand. At each sampling interval, 10 to 20-gram samples were randomly pulled from the well cuttings. No effort was made to collect a specific chip size or specific minerals within the well cuttings.

Select intervals of Well 38C-9 were resampled at 10-foot intervals to evaluate sampling intervals. Coso well, Well 38D-9 and Beowawe Well 57-13 were sampled during drilling; all other wells were sampled from stored well cuttings several years after drilling and logging had occurred. One well, 84-30, was sampled since it was considered a dry hole and was located outside of the geothermal system. Two wells, 68-20 and 68-20RD, were drilled seven years apart. The two wells started at the same location and deviated from each other at most about 150 feet at 5500 foot depth. These wells were sampled to determine if there was a difference in the fluid inclusion gas chemistry after seven years of injection that was known to result in scaling and loss of well permeability.

3.3. Laboratory Analysis

Over 5,000 samples from the wells were submitted to Fluid Inclusion Technology (FIT) laboratory in Oklahoma for analyses. Fluid Inclusion Technology has developed a proprietary system for rapid bulk analysis of fluid inclusion gases and uses the method for evaluating petroleum reservoirs. Analyses are performed by first cleaning the samples, if necessary, then crushing a gram-size sample in a vacuum and analyzing the volatiles with a quadrupole mass spectrometer.

Fluid Inclusion Technology analyses are provided as is. In order to evaluate FIT analyses about 100 analyses of chips from Coso's Well 58-A10 were performed both at the FIT and the New Mexico Tech facility, which makes quantitative analysis of fluid inclusion volatiles.

Generally the geothermal samples are clean when sampled and therefore did not require additional cleaning at the laboratory. The samples are loaded into a 630-hole tray with appropriate standards and placed in a vacuum oven at elevated temperatures for a minimum of 24 hours, followed by another vacuum oven at lower temperatures for a minimum of 24 hours (Hall 2006). This removes adsorbed organic and inorganic volatile materials from the samples. The volatiles released from crushing by an automated mechanical crusher, are dynamically pumped through four quadrupole mass spectrometers where molecular compounds are ionized by electron bombardment and separated according to the mass/charge ratio. The separation occurs by a combination of RF (radio waves) and DC (direct current) electrical fields. Electronic multipliers detect the signal, which is processed creating a mass spectrum for each sample. The output data for each sample is the magnitude of mass peaks for masses 2 to 180. A volatile like CO₂ has a gram formula weight of 44 and will be measured by a peak at mass 44. Ionization can break up gas species molecules into charged fragments. Nitrogen (N₂) for example yields a mass peak at 28 from N₂⁺ and a mass peak at 14 from N⁺. Table 6 presents the formula and chemical species associated with the more common mass peak.

FIT returned the raw data within about three weeks of each submittal. The data package from FIT consists of an ASCII file with values for all 180 masses analyzed in the mass spectrometer per sample. Appendix A contains these files.

Table 6: Common chemical species and their mass number

Mass #	chemical species
2	H_2^+
4	He^+
14	N^+ CH_2^+ CO^{++}
15	C_1 fragment (CH_3^+), methane
16	CH_4^+ (methane) O^+
18	H_2O^+
28	N_2^+ C_2H_4^+ (ethylene) CO^+
30	C_2H_6^+ (ethane)
34	H_2S^+
39	C_3H_3^+ (propene)
40	Ar^+ C_3H_4^+
43	C_3H_7^+ (propane)
44	CO_2^+ C_3H_8^+
48	SO^+
50	C_4H_3^+ (cleaved from benzene)
56	C_4H_8^+ (butylene)
58	$\text{C}_4\text{H}_{10}^+$ (butane)
64	SO_2^+
70	C_5H_8^+ (cyclopentane)
78	C_6H_6^+ (benzene)
86	$\text{C}_6\text{H}_{14}^+$
92	C_7H_8^+ (toluene)

CHAPTER 4. DATA

4.0 Data Quality

Data from FIT and quantitative analyses conducted at New Mexico Tech (NMT) were compared to evaluate the quality of the FIT data. Understanding the quality of the data depends upon understanding the differences in the analytical processes used by FIT and NMT. Both laboratories crush samples in a vacuum chamber attached to high-vacuum pumps. Crushing releases a brief puff of inclusion volatiles, including water, that are recorded by quadrupole mass spectrometers scanning at rates of 5 to 10 times per second. Species with high volatility and low melting points such as the noble gas species are quickly removed from the vacuum system hence the mass peak is on the order of a second or two in width.

FIT crushes the sample once and applies a uniform crush. Burst size varies at most by a factor of 20. FIT analyses indicate inclusion density assuming drill chips all have the same mechanical properties. NMT sequentially crushes a sample several times by hand. Burst size varies by a factor of 1000. Sequential crushing gives information about inclusion heterogeneity. The amount of volatiles released by NMT crushing varies with the force applied. NMT's procedure is to vary the crush force so that a burst size of about 1×10^{-6} is achieved, which gives maximum measurement precision. NMT integrates the area under mass peaks that corrects for gas sorption, whereas FIT reports peak heights.

NMT measures selected mass peaks to maximize precision and calibrates the system with known gas ratios and natural fluid inclusion standards. Calibrating the analytical system allows NMT to make quantitative analyses. NMT analyses are presented in mol % or parts per million (ppm) of various species. Currently, NMT uses two mass spectrometers and measures 12 species at a time. FIT runs internal standards to control analytical drift. These standards include oil inclusion reference standards; clean quartz sand devoid of hydrocarbons; and clean quartz sand heated to 1000°C (1832°F) to remove a large percentage of fluid inclusion population (Hall 2006). The oil inclusion standards are used to verify effectiveness of the crushing process and sample position. Both of the clean sand standards are used to check the post-analytical processing software.

FIT does not process the data to determine abundances because the relative concentrations are found to be sufficient. Prior to starting this project it was thought a “calibration factor” would be needed so that values from FIT could be compared with quantitative values developed by NMT. Ultimately, the FIT data were used without processing. Comparing relative ratios proved adequate for seeing differences in fluid sources. Prior to starting this project a select number of samples from Coso Well 83-16 were submitted to both FIT and NMT facilities to evaluate the differences in the data.

Figure 4.1 presents plots developed by Norman et al. (2004) for the FIT analyses versus the NMT analyses for the samples from Well 83-16. Although there are differences in the exact values, the overall patterns appear similar. For N₂/Ar ratio (the first graph in

each group) the majority of the peaks occur below 6000 feet. The propane/propene ratio graphs (second graph in each group) indicate peaks for chips from above 6500 feet in both graphs. The graphs are also similar for the CO₂/CH₄ ratios, with peaks occurring in the upper portion of both graphs. From this study, it was concluded that although exact values are not obtained, the FIT data provides relative gas ratios that can be comparable with results obtained by NMT's more quantitative process.

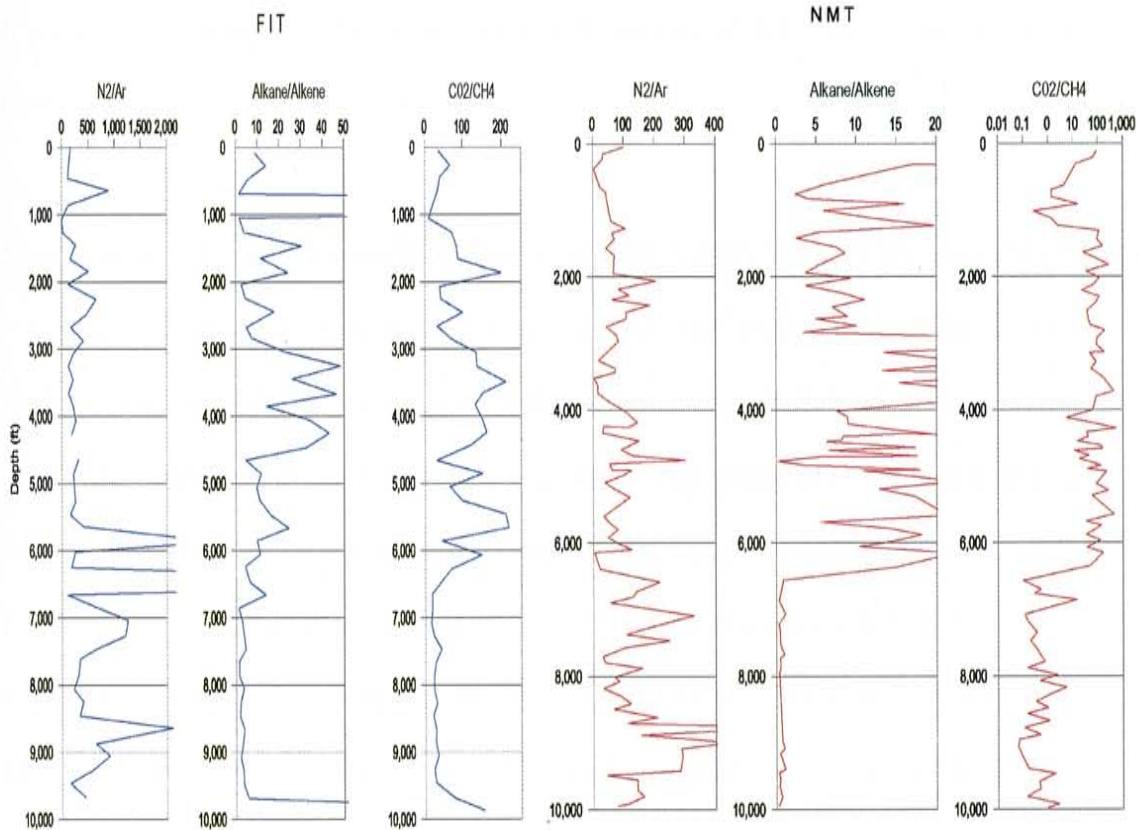


Figure 4.1 FIT and NMT data for several ratios for samples from Coso Well 83-16. Although the absolute abundances differ, the patterns of high and low concentrations are similar.

4.0.1. Mass Spectra Fragmentation

Of principal concern in the FIT analyses was overlap of mass peaks. Most of the gaseous species present in fluid inclusions exhibit one or more gas peaks when ionized in a mass spectrometer with little interference. Volatiles fragment during ionization. The fragments are measured at mass peaks m_i/e_i where m is the mass of the fragment and e is the charge. Carbon dioxide for example commonly yields fragments of C^+ ($m/e = 12$), O^+ ($m/e = 16$), CO_2^{++} ($m/e = 22$), CO^+ ($m/e = 28$) and CO_2^+ ($m/e = 44$). Organic species fragment by splitting C-C bonds and loss of H atoms, which results in complex mass spectrums.

Measurement of nitrogen potentially has a problem because there is overlap of the N_2 $m/e = 28$ peak with organic molecule fragments and CO^+ from the fragmentation of CO_2 . Carbon dioxide is commonly the principal gaseous species in fluid inclusions hence its fragment could mask N_2 which is generally one or two orders of magnitude lower in concentration. To determine if mass 28 represents nitrogen or carbon dioxide, the values for mass 28 are plotted against mass 14 (N^+ , N_2^{2+}) and against mass 44 (CO_2) (Figure 4.2). Hence if $m/e=28$ represents mostly N_2 it should strongly correlate with $m/e=14$. A linear trend for mass 14 against mass 28 for analyses from 4 wells, and lack of correlation of mass 28 with 44, indicates that the mass 14 represents nitrogen and not carbon dioxide (Figure 4.2). The slope of the line is based on the fragmentation process in the individual machine. The theoretical fragmentation of N_2 produces about 15 percent N_2^{++} . The slope on this data varies from about 25 to 35 percent.

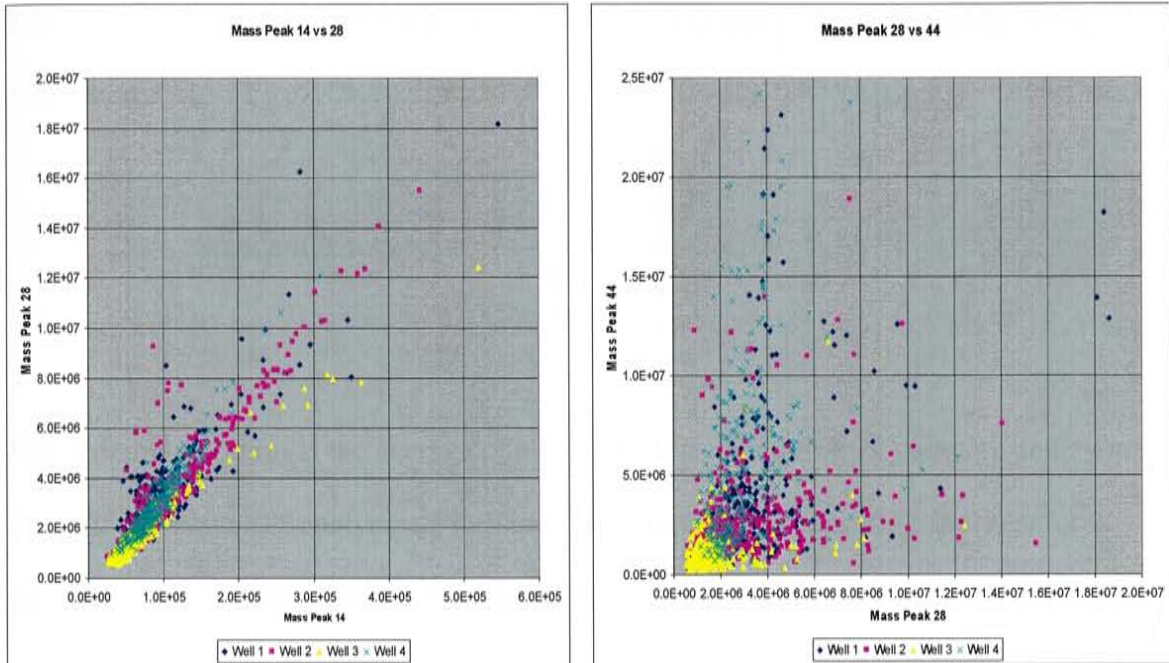


Figure 4.2. Plots of mass 28 against mass 14 and against mass 44. Blue: Well 33-7; Pink Well 38C-9; Yellow: Well 84-30; Light Blue: Well 58A-18

4.0.2. Calculating Precision

Replicate analysis measures homogeneity of sample material, homogeneity of sample shape and of fracturing, impact repeatability, and machine measurement factors, in addition to analytical precision. Samples taken from the same bag of well chips is expected to show some sample to sample variation. No effort was made to select specific mineral grains or types during the sampling. One hundred and twenty-four replicate analyses were made over a time period of 3 years.

Precision of FIT analyses from Well 58A-10 duplicates was calculated using the expression:

$$\text{Standard Error (\%)} = \frac{\sqrt{\frac{1}{k} \sum_{i=1}^k (x_{1i} - x_{2i})^2}}{\frac{1}{2k} \sum_{i=1}^k (x_{1i} + x_{2i})} \times 100$$

The denominator term is the average of all values. k is the number of pairs. x_{1i} and x_{2i} are a pair of duplicate FIT analyses. Precision was calculated for repeating analyses for 2 major mass peaks 28 and 44 and two minor peaks 34 (H₂S) and 78 (benzene) (Table 7). Analysis repeatability is a function of inclusion heterogeneity, analytical precision and uniformity of crushes. The calculated precision duplicating gas ratios is done because our interpretation plots use gas ratios.

Table 7. FIT analytical precision determined on 124 replicate analyses for repeating measurement of individual species and repeating gas ratios.

	N ₂	CO ₂	H ₂ S	Benzene	N ₂ /Ar	CO ₂ /H ₂ O	CO ₂ /N ₂	H ₂ S/N ₂
standard error (%)	41	46	123	67	39	30	27	68

4.0.3. Standards Analyses

Analyses of standards gas ratios analyzed by FIT and NMT were compared (Table 8). The NMT facility measures duplicate N₂/Ar of air in artificial inclusions with a standard error (precision) of about 1 percent. However, natural standards all show heterogeneity that in part masks the analytical precision. The value of the standards is that some values are quite repeatable, and they are useful in monitoring long term machine stability.

Standards HF1, SCLQ, and BHQ-1 have gas ratios that are repeatable at 20 percent or better; standard SCLQ N₂/Ar is repeatable to 3 percent. Table 8 shows that FIT analyses have lower precision than NMT analyses. Because of sample to sample heterogeneity in fluid inclusions it is hard to place an exact figure on the precision, however analyses of over 100 sample replicates suggest (Table 7) a precision for major species is better than 50 percent and ratios of major gaseous species at better than 30 percent. Hence FIT will show order of magnitude differences in gaseous species, but the analyses as shown in Figure 4.1 show more noise – sample to sample variation- than NMT analyses.

Table 8. Comparison of standard errors (%) of NMT and FIT. The standard error is the precision in measuring gas standard's gas ratios. The standard error in NMT analyses in part reflects sample to sample variations in gas ratios.

Standard Type		N ₂ /Ar	CO ₂ /H ₂ O	CO ₂ /N ₂	H ₂ S/N ₂
HQ-1	FIT	69	131	59	103
	NMT	54	33	49	94
SCLQ	FIT	56	39	20	102
	NMT	3	36	16	52
HF-1	FIT	24	181	50	73
	NMT	20	15	17	67
BHQ-1	FIT	40	96	66	49
	NMT	13	26	18	38

The FIT gas ratios are not the same as obtained from NMT facility because FIT is not calibrated. NMT measurement of N₂/Ar commonly shows ratios typical of groundwater from 30 to 100; FIT ratios of N₂/Ar are in the range of 200 to 450. Multiplying the FIT gas ratio by 0.5 yields a N₂/Ar value close to that measured by NMT. A few FIT analyses show some interference of the N₂ (28) mass peak, but this little affects plots of

N₂/Ar ratio. Other interferences are negligible because of the low fragmentation in FIT mass spectrometers and low amounts of organic species.

4.1. Sampling Interval

Well cuttings are generally obtained during drilling at 10-foot intervals. The package of well cuttings obtain represents the entire 10-foot interval. For example, for a 100-foot interval, a well would have 10 packages of well cuttings collected representing each of 10-foot intervals. Initial sampling for this project was set at collecting a sample at 20-foot intervals. The 20-foot interval sample is not a composite of the entire 20 feet but is the sample at the 20-foot depth and represents a 10-foot interval, for instance from 20 to 30 feet and then the next sample would be from 40 to 50 feet. For the 100-foot interval five of the packages (every other package) were sampled as oppose to all 10 packages.

To determine whether sampling intervals (frequency) might significantly change the FIS results, a sensitivity exercise was conducted using Coso Well 38C-9. Analyses using a 10-foot sampling interval data are compared to analyses from a 20-foot sampling interval data to determine if the smaller sampling interval would produce comparable results to the 20-foot sampling interval. The species and gas ratios selected for comparison are H₂O, N₂/Ar, and CO₂/CH₄. Figure 4.3 shows the comparison of the select species and ratios for the two sampling intervals. The 10-foot sampling in general provides more peak detail for H₂O. Mass peaks that are not evident in the 20-foot sampling interval are shown in the 10-foot sampling; see intervals 7500, 7690, and 7830 feet. Also, from about

8250 to 8410 the broad peaks recorded by 20-foot sampling show more detail when a 10-foot interval is used.

For the remaining ratios, the smaller sampling interval did not appear to offer significant improvement in detail. For the N_2/Ar ratio, some of the minor peaks are missing or are subdued in the 20-foot sampling interval, but in general most of the peaks are similar in the 10-foot and 20-foot sampling intervals. The CO_2/CH_4 ratio peak was missed at 7050 feet, but all of the other peaks appeared with the 20 foot sampling interval. For this ratio there were a few low points (7390, 7800, and 8050 feet) indicated in the shorter sampling interval that did not appear in the larger sampling interval. Based on the sampling interval analysis it appears that 20 feet is considered a reasonable sampling interval for the collection of FIS data and the 10-foot interval analyses are not worth the cost increase. For more detailed analysis it would be beneficial to sample at the smaller sampling interval. The nature of the problem would define the sampling interval. In general it appears that for evaluating the wells for fluid types a 20-foot sampling interval will provide the necessary details. If the problem is to identify certain zones than as with other logging tools, a more detailed sampling interval would be needed.

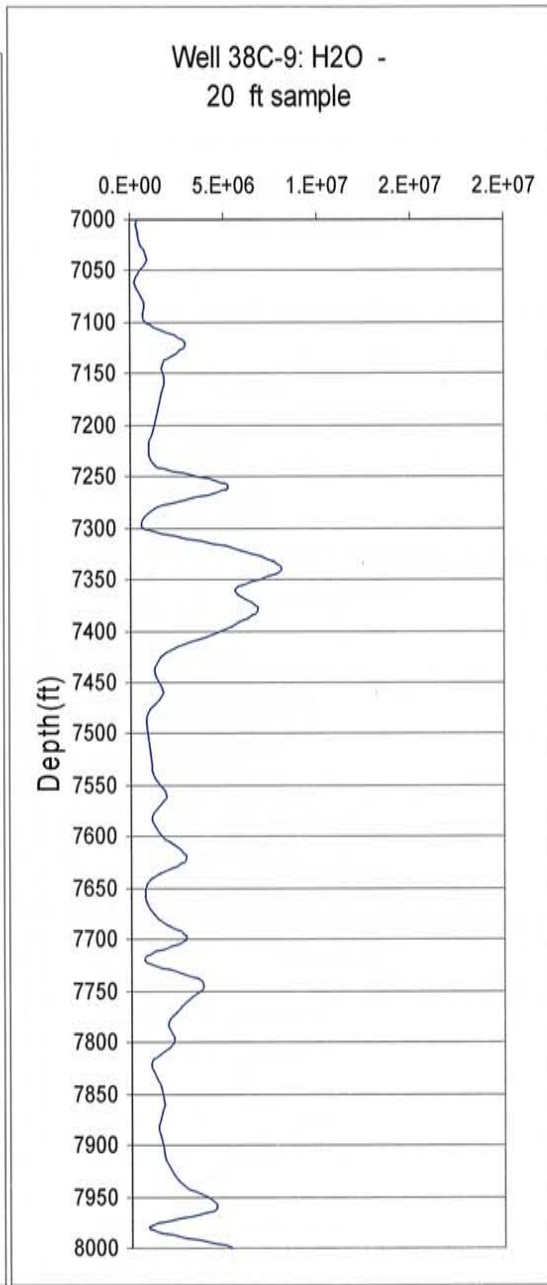
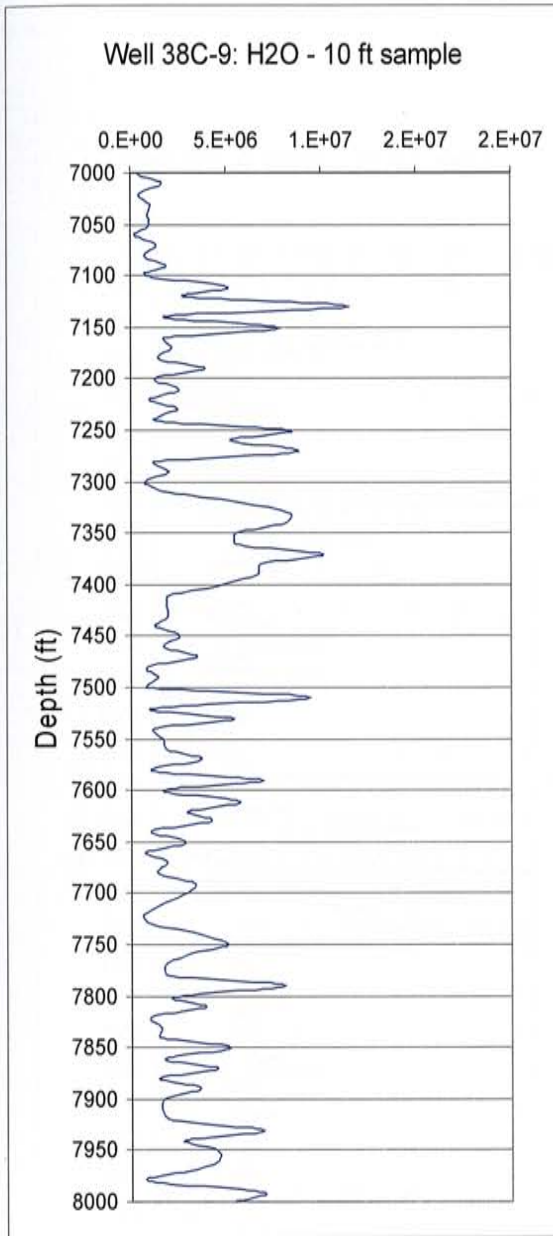


Figure 4.3. Graph of H₂O for 10 feet and 20 feet sampling.

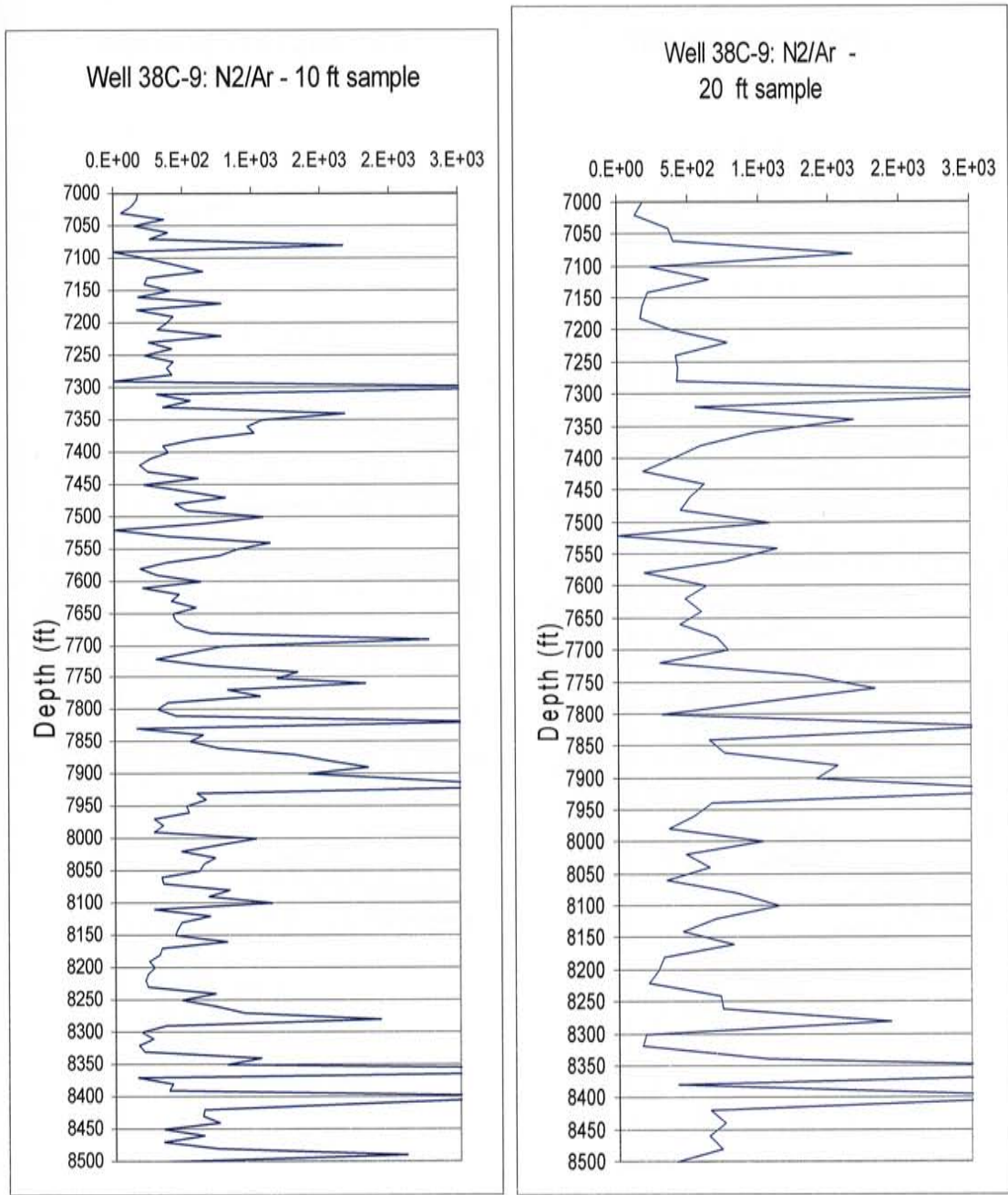


Figure 4.3 (continued). Graphs of N₂/Ar for 10 feet and 20 feet sampling.

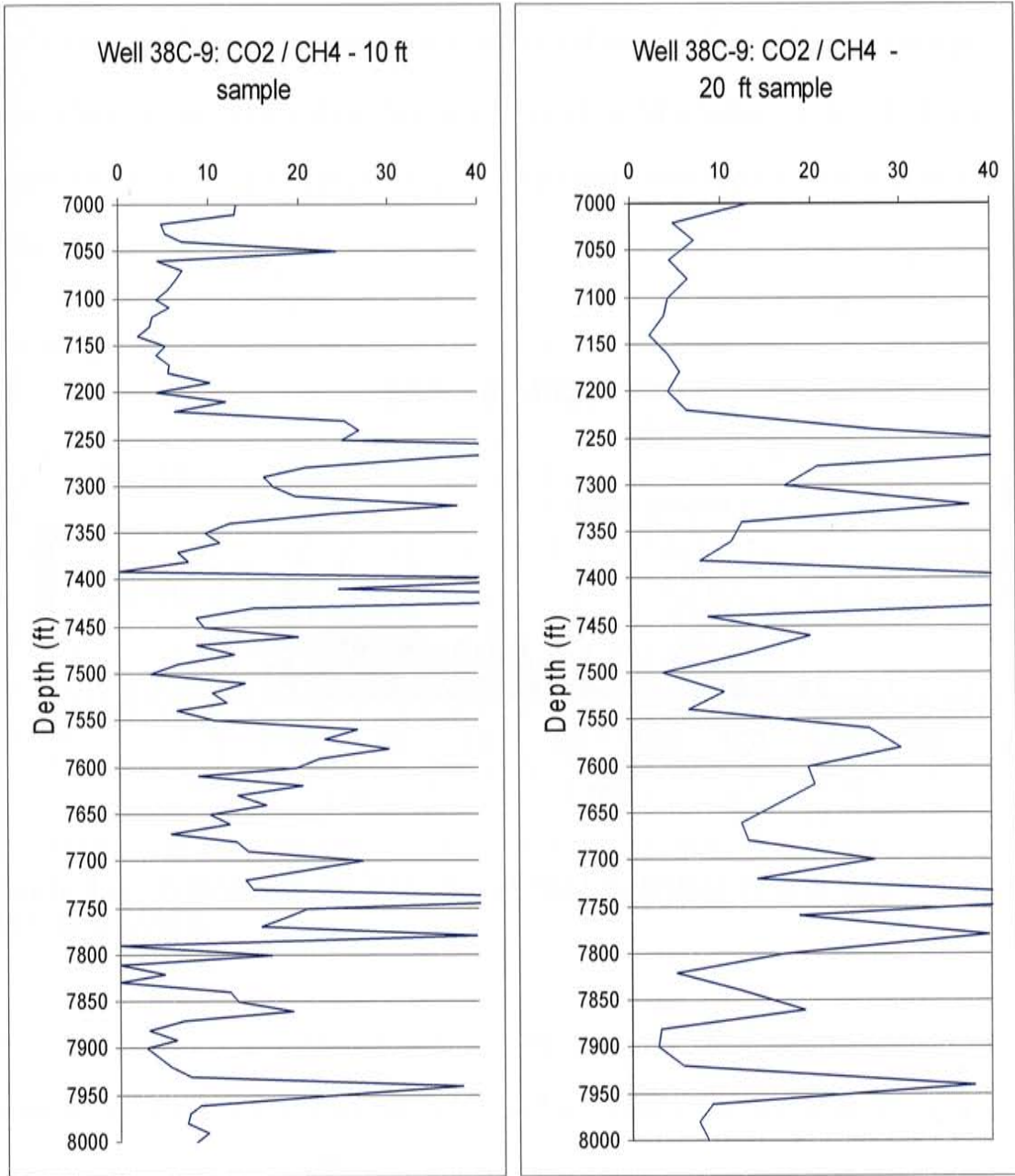


Figure 4.3 (continued). Graphs of CO₂/CH₄ for 10 feet and 20 feet sampling.

4.2. Displaying the Data

Geothermal fluid inclusion mass spectra generally show major peaks at 2 (H_2), 18 (H_2O), 28 (N_2) and 44 (CO_2), with other mass intensities at lower values. The peaks at high mass/charge values (above about 60) are typically heavier organic compounds. Intensities range up to 8 orders of magnitude. Figure 4.4 presents mass spectra for one sample at 4350 feet from Well 58A-10.

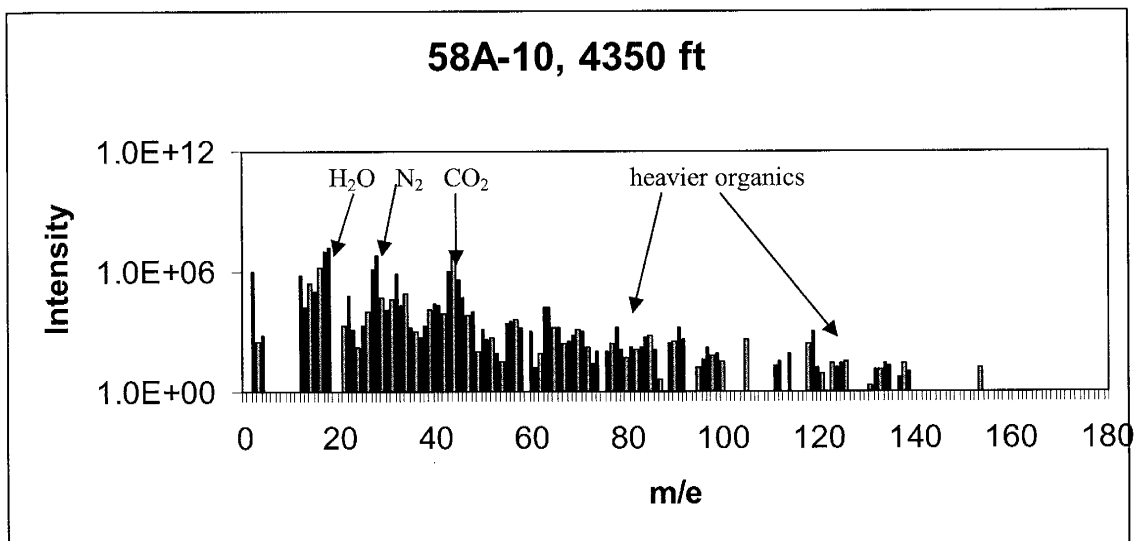
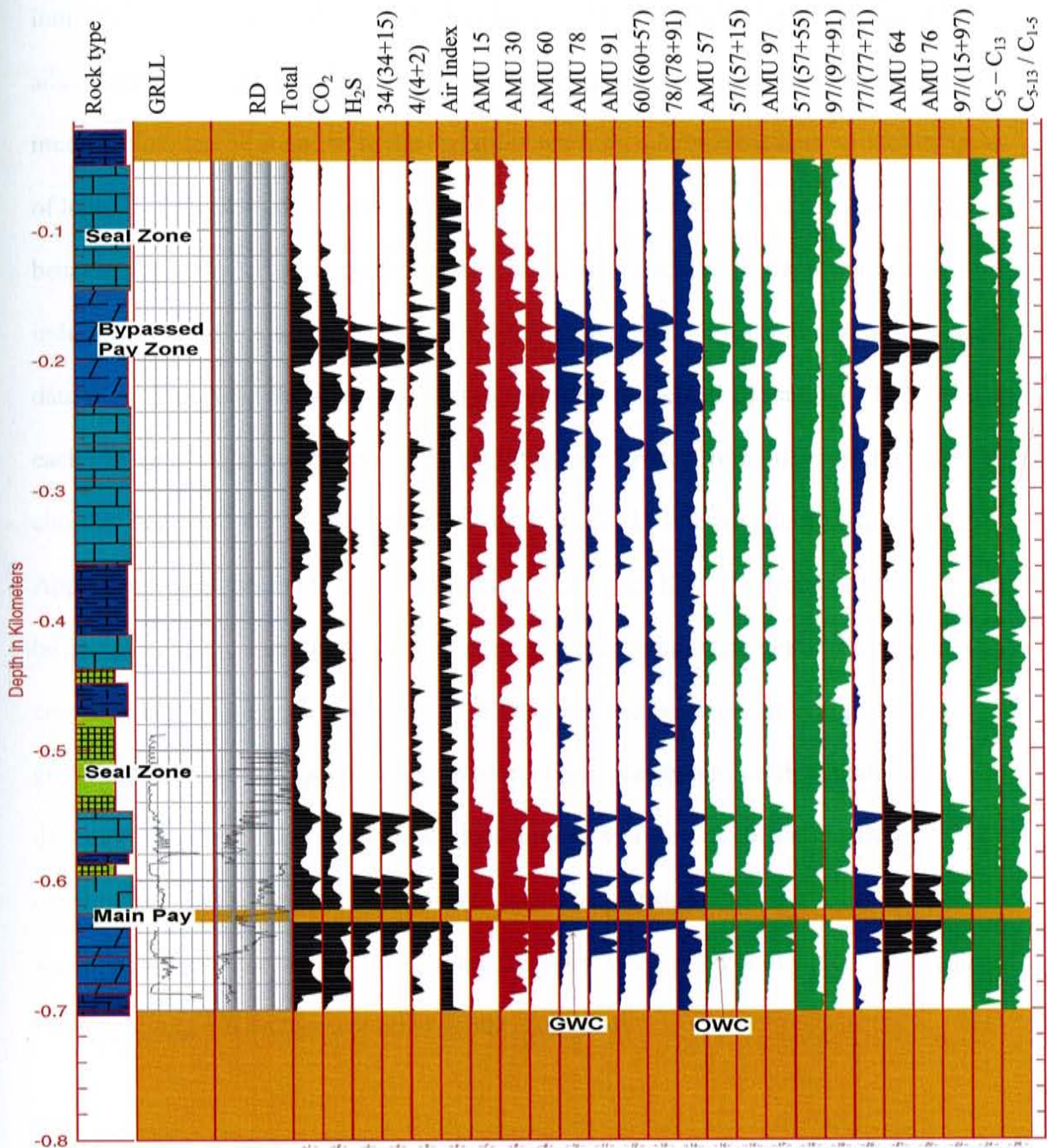


Figure 4.4. Typical FIT mass spectra of fluid inclusions in drill chips from Well 58A-10 at 4350 ft.

Due to the extensive amount of data (mass peaks from 2 to 180 for each of the over 5000 samples), data processing is required and a tool is needed to display the data. Figure 4.4 would not be useful for plotting the data for interpretation for each well. FIT generates mudlog type graphs as seen in Figure 4.5 and provides a report with interpretations (Hall 2002)



Fluid Inclusion Technologies, Inc.
<http://www.fittulsa.com>



UWI# 999999999994
 FIS# F19808206

Figure 4.5. FIT's mudlog type graph presentation of mass spectra

In order for FIS analyses to be useful and economically applied to the geothermal industry an approach similar to FIT was adopted. Mudlog graphs have two significant advantages: 1) a large number of variables can be easily compared and analyzed, and 2) mudlog plots can be supplied to the end users who can combine the data with other types of logs. The Rockware program Logger® was selected for plotting the mass spectra because it was low cost, adequate for the job, and data files can be transferred into industry programs. Logger® produces graphic strip logs from user-created or imported data files. The data files were created in Excel from the ASCII file supplied by FIT. For each gas species a major gas peak that had little interference from other species were chosen. For example for methane this is mass 15, not 16 (the weight of methane). Appendix B presents the Excel data files and the Logger file. The format of the logs can be designed by the user. For each well a mudlog displaying mass peaks of various compounds were plotted (Norman et al. 2005). For each species, the scaling of the graphic strip is set using as a maximum as the mean plus two times the standard deviation. That scaling is used for all the analysis from Coso so that all wells are comparable. The scale used for Beowawe was changed since the scale used for Coso wells did not produce suitable logs. Some changes in scaling will most likely be required when applying FIS analyses to other geothermal fields.

On the mudlogs developed (Figures 4.6 through 4.12) the species are grouped by chemical type, which are plotted in different colors. The species plotted (23 total of the 180 mass spectra available) were based on the previous research work described in Chapter 2.1. Helium and water are plotted in blue with water distinguished by a lighter blue color. The inorganic species N₂, Ar, and CO₂ are plotted in red. The C₂-C₆ straight

chain organic species are plotted in green (C_2H_6 , C_3H_6 , C_3H_8 , C_4H_8 , C_4H_{10}); the sulfur species are plotted in orange; and organic aromatic peaks are plotted in gray. Sulfur species plotted are H_2S (mass 34), SO_2 (mass 48) and mass 64. Mass 64 is a major peak for SO_2 and CS_2 , and it is a minor fragment peak for some organic species. Hence mass 64 is distinguished by a different color than orange used for mass 34 and mass 48. Mass peaks 70, 78 and 92 are respectively the principal peaks for cyclopentane, benzene and toluene. Mass peak 50 is a common fragment peak for aromatic compounds.

Quantitative analysis of fluid inclusion organic species shows concentrations are in the low ppm and ppb range (Norman et al. 2004).

Figures 4.6 and 4.7 present the FIS mudlogs for producing Well, 38C-9 and a high temperature but non-producing Well 51B-16. Figure 4.8 presents the FIS mudlog for an injection Well 67-17, and Figure 4.9 presents the FIS mudlog for Well 84-30 which is located beyond the southern extent of the field, in the meta-igneous rocks. Figures 4.10 through 4.12 present the remaining FIS mudlogs for the remaining wells. They are grouped according to the well locations. The FIS mudlogs are also presented in combination with other logs in Appendix C.

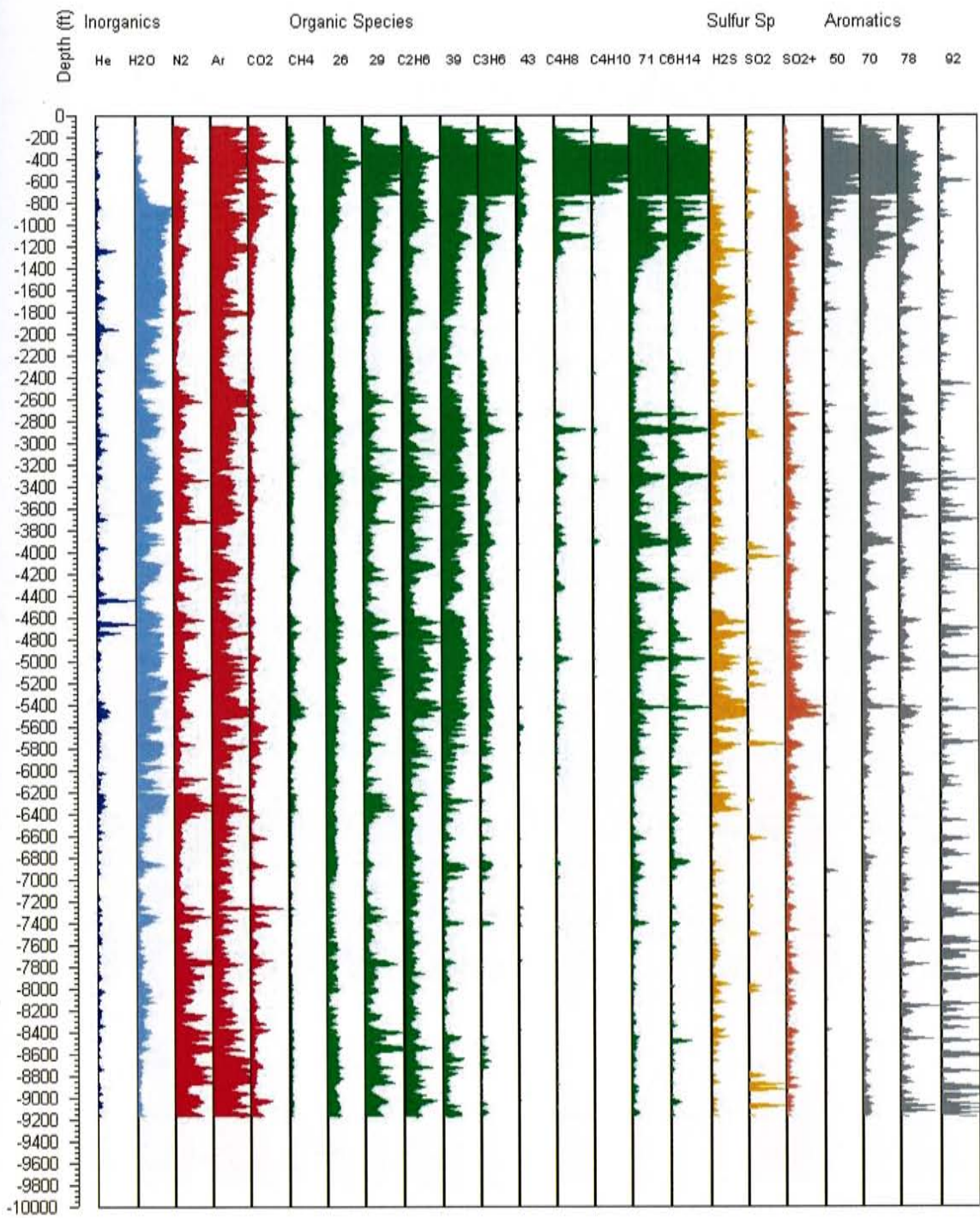


Figure 4.6. FIS log with select mass spectra plotted versus depth for Well 38C-9 a major producing well.

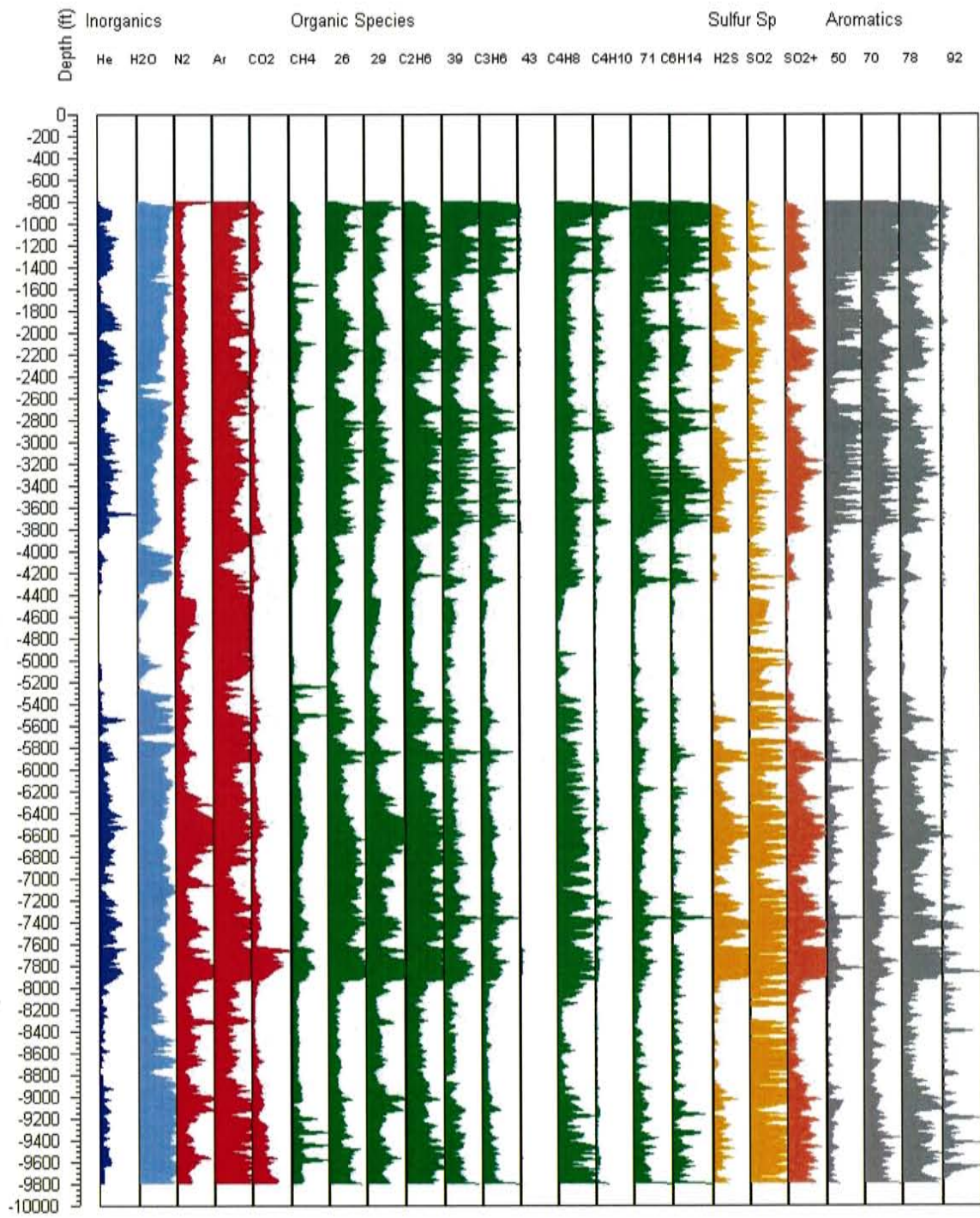


Figure 4.7. FIS log with select mass spectra plotted versus depth for Well 51B-16, a high temperature, non-producing well.

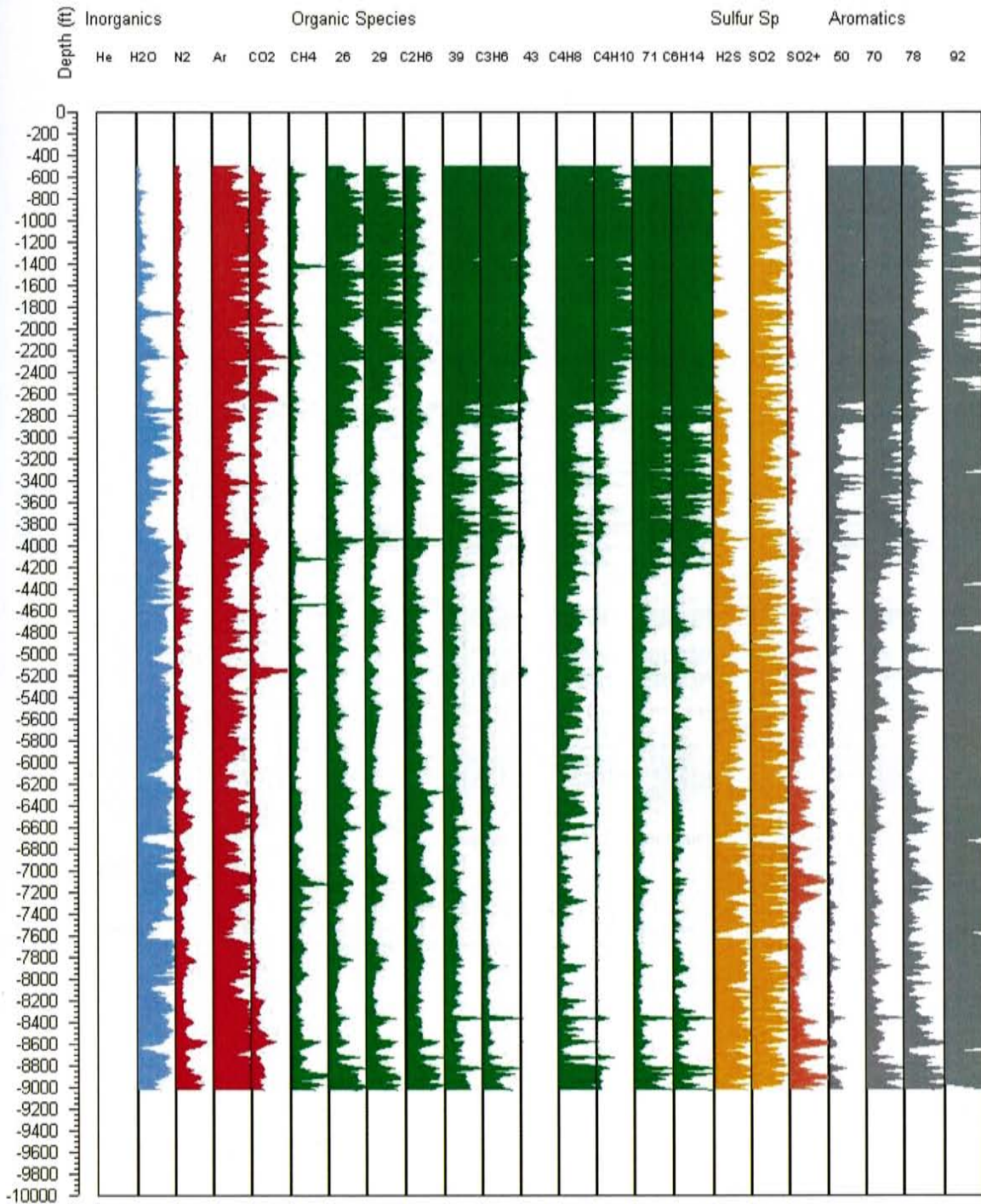


Figure 4.8. FIS mudlog with select mass spectra plotted versus depth for an injection well, Well 67-17.

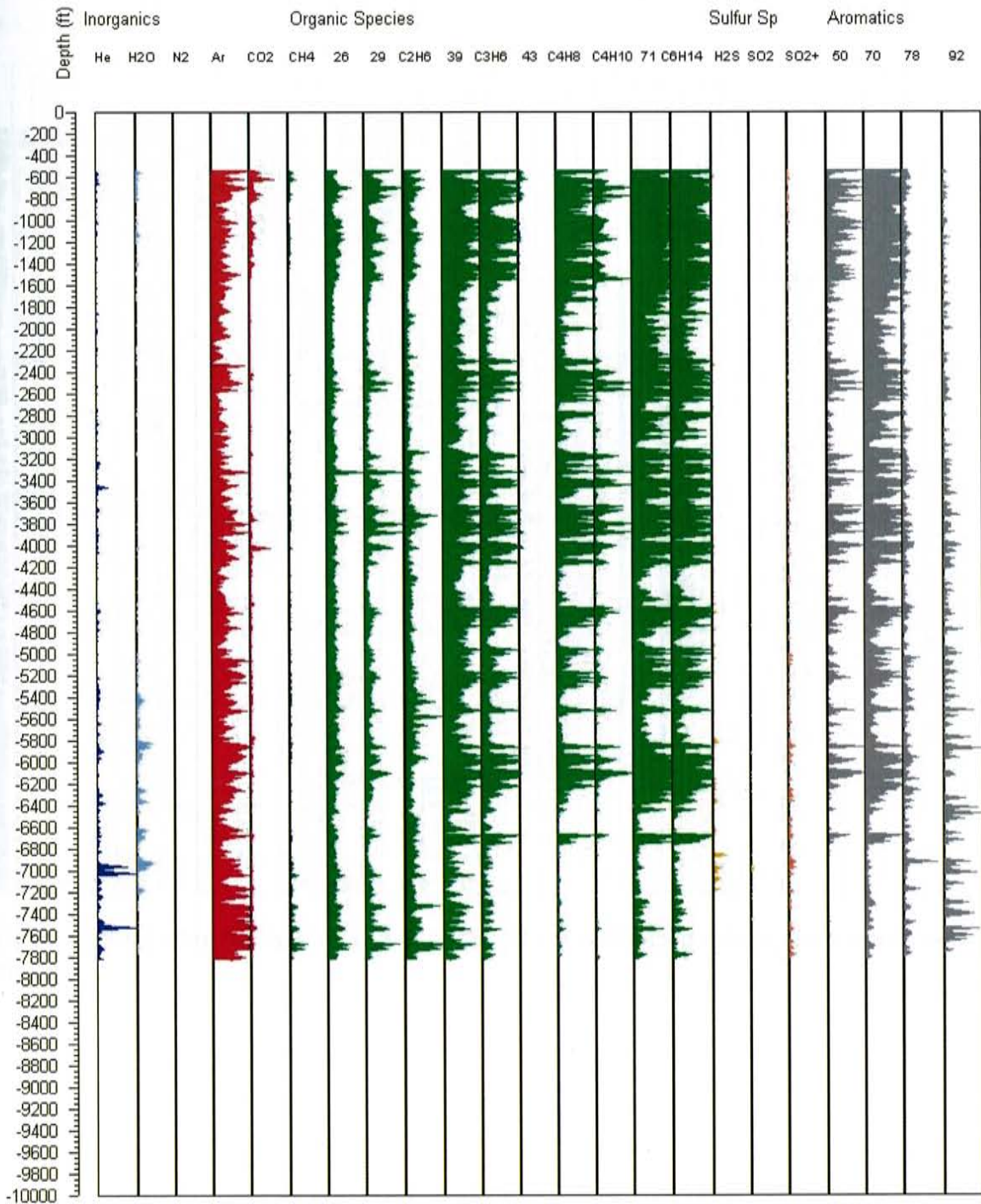


Figure 4.9. FIS log with select mass spectra plotted versus depth for Well 84-30 (a non-producing well) located at the southern margin of the field.

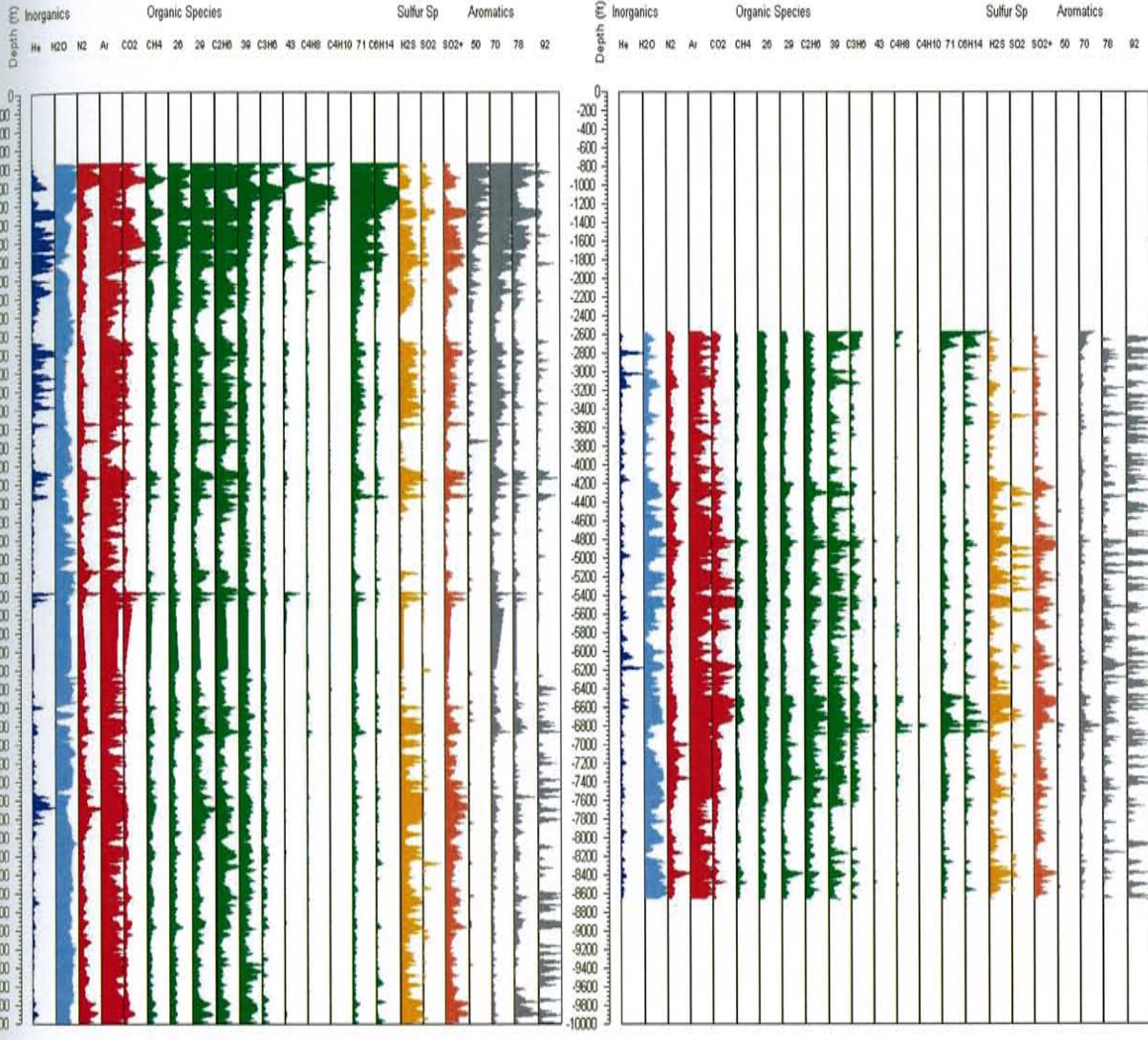


Figure 4.10. FIS logs for Wells 33-7 and 58A-18. These wells occur along the western side of the field.

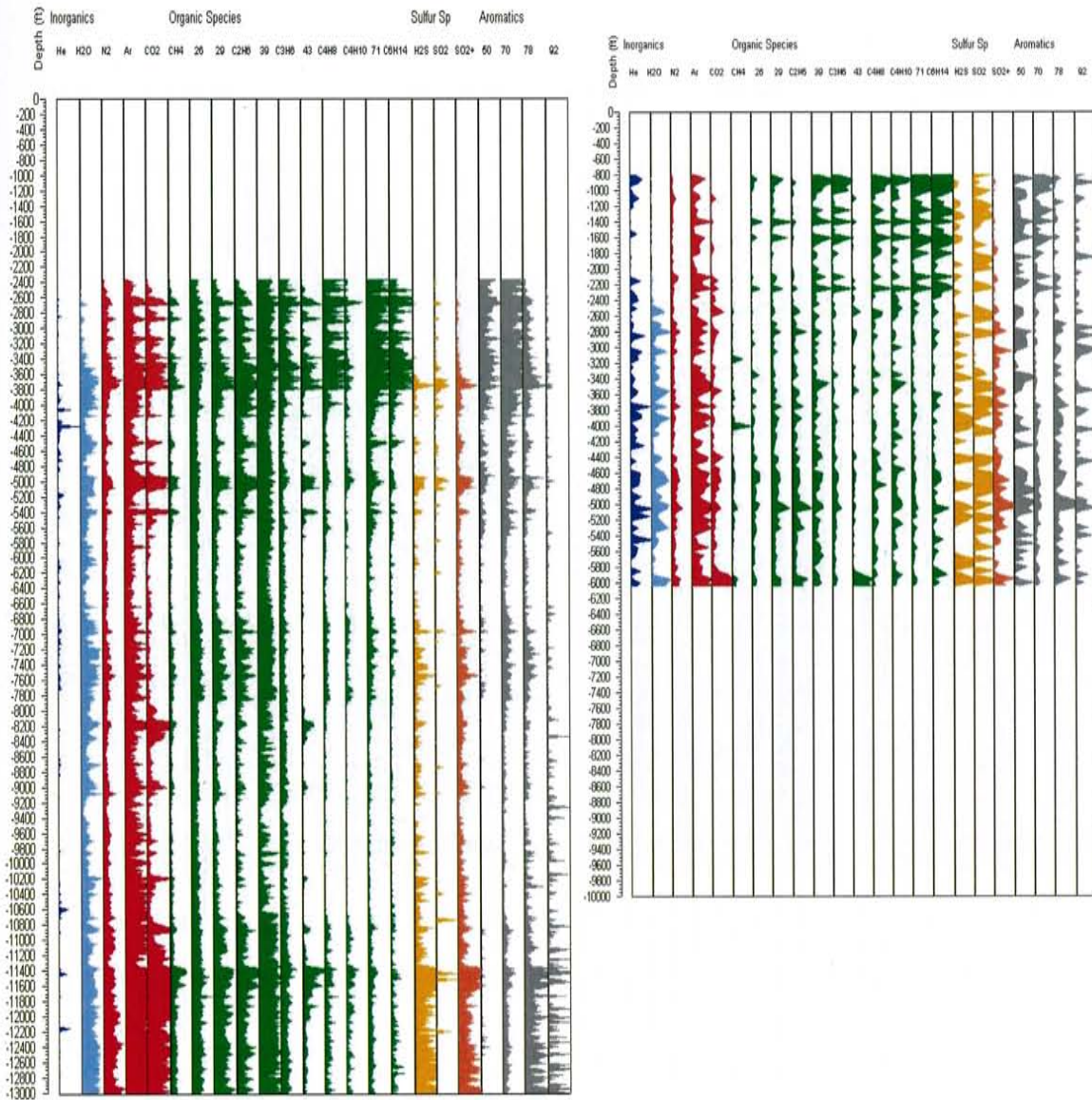


Figure 4.10 (continued) FIS logs for Wells 46A-19RD and 73-19, which occur along the western side of the field.

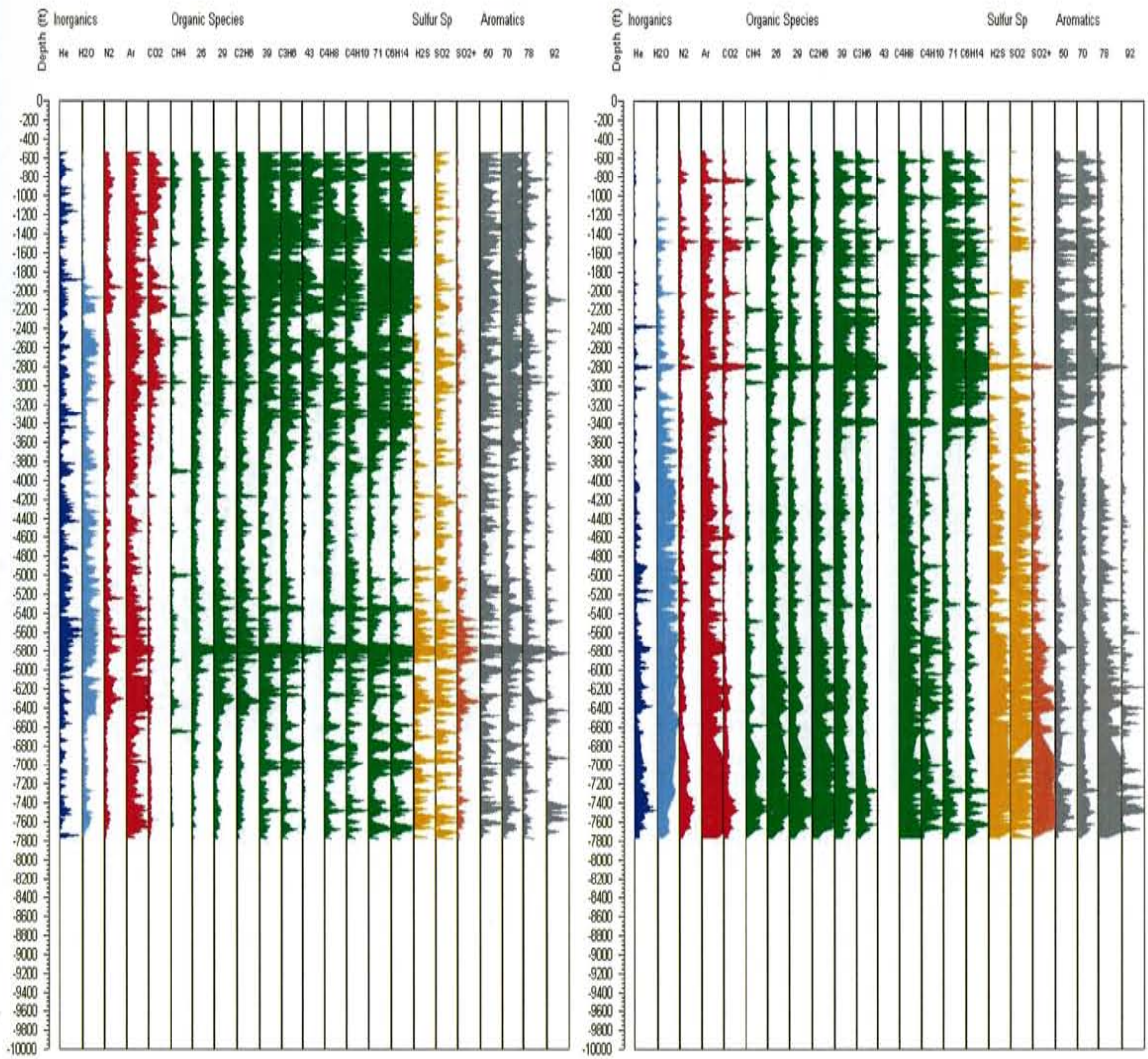


Figure 4.11. FIS logs for Wells 67-17C and 52-20, located in the middle southern portion of the field.

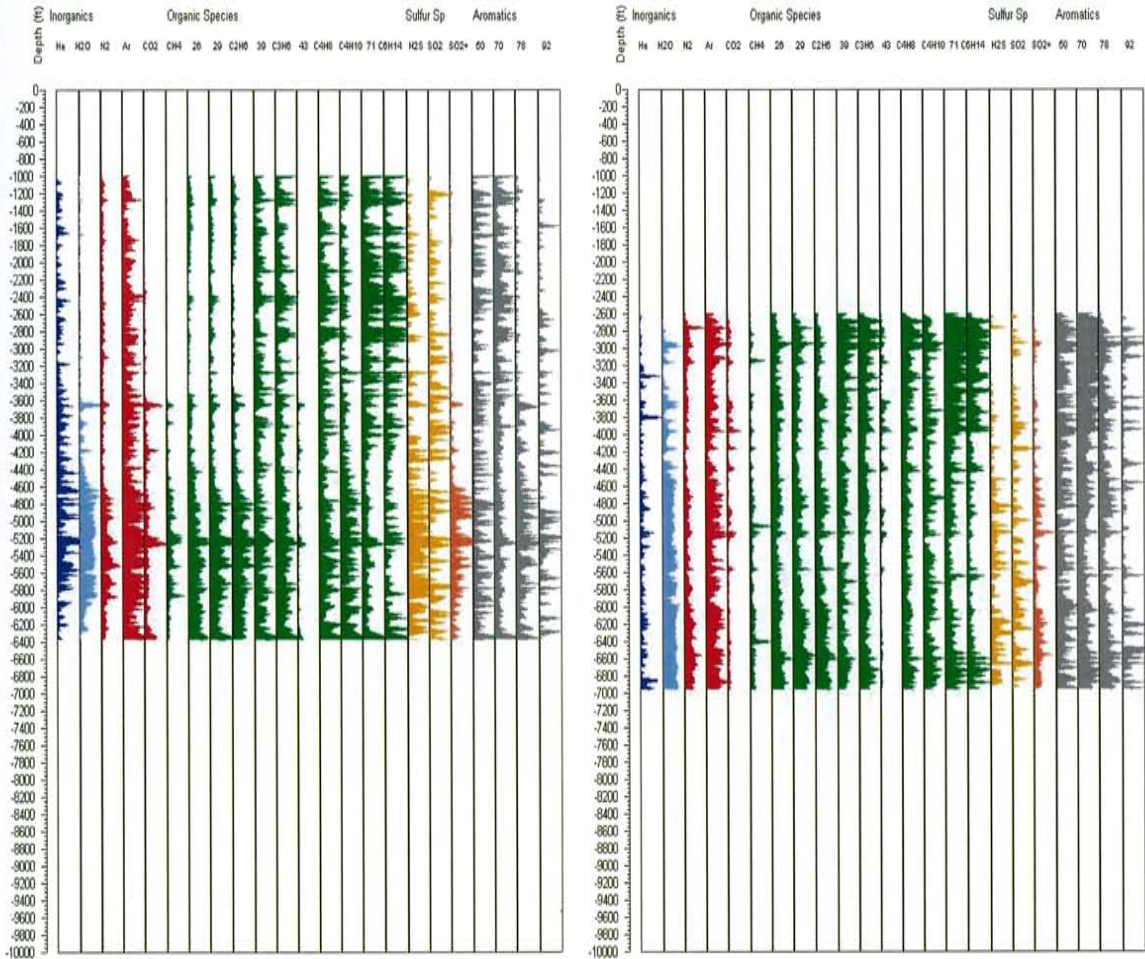


Figure 4.11 (continued) FIS logs for Wells 68-20 and 68-20RD located in the middle southern portion of the field.

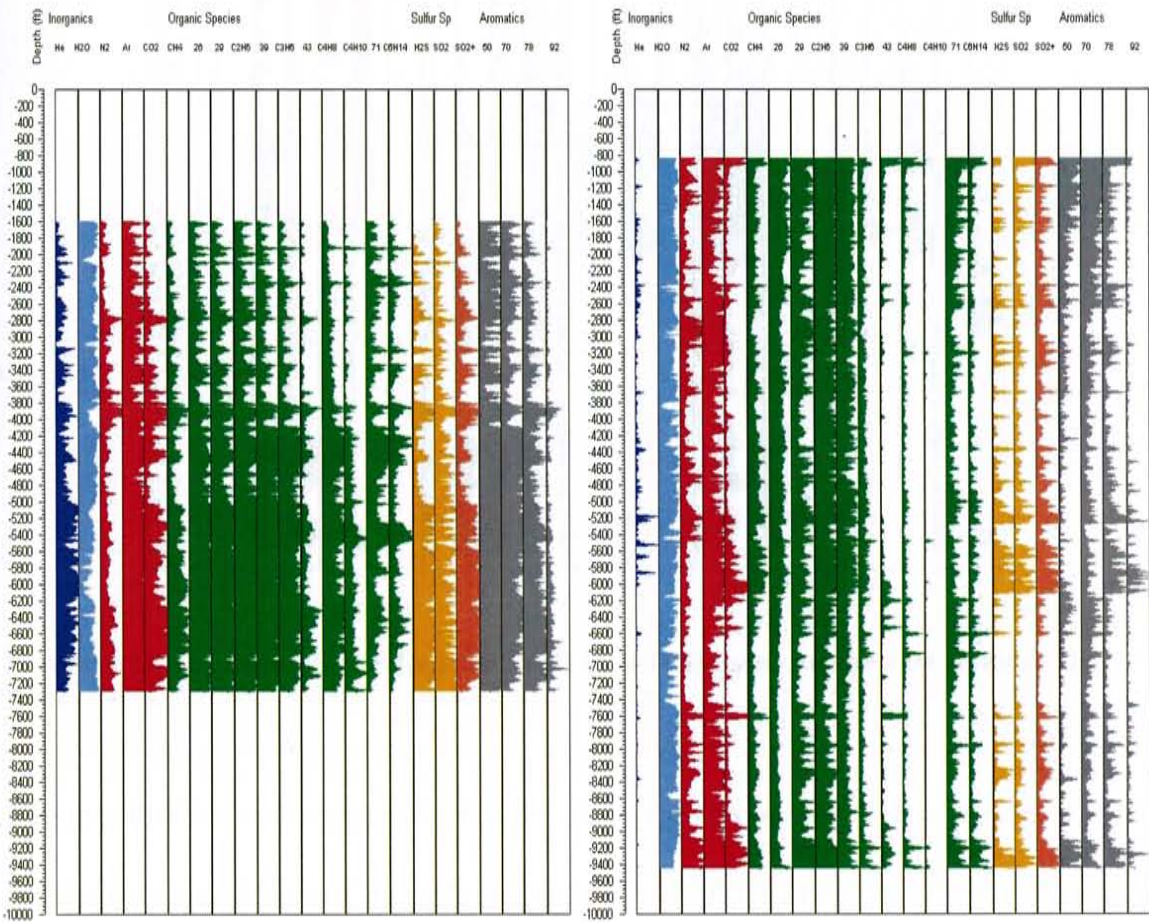


Figure 4.12. FIS logs for Wells 34-9RD2 and 38D-9 located on the east flank of the field.

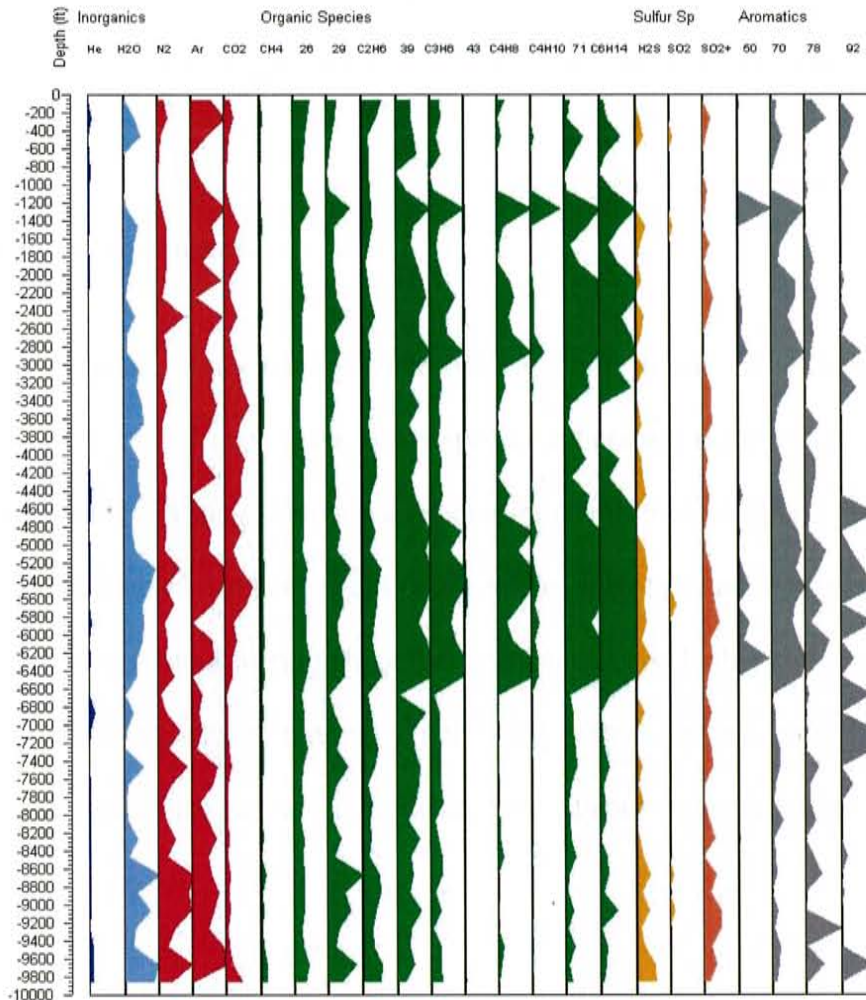


Figure 4.12. (continued) FIS logs for Well 58A-10 located on the east flank of the field.

The amplitude of each mass peak changes with depth for each well (Figure 4.6 to 4.12). Species data vary from well to well. For instance, He intensities plot differently in each well. Another observation is that at specific depths, mass peak intensity shows high values for several species. For example, in Figure 4.6 at 400 feet a number of gases particularly the organic species (green), and aromatic species (gray) all show peaks in intensity and sulfur species are low. Figure 4.7 has low intensities for a number of the

species from about 4400 to 5200 feet except for N₂, Ar, and SO₂. This could represent a low number of inclusions suggesting a seal or cap at this depth in the geothermal system

4.3. Relation to Fractures

What causes the peaks in intensities seen in FIS log plots? It can not be chance because peaks occur in several, in most cases, many species at the same depth. Undoubtedly the peaks are the result of a sample having a greater number of inclusions and that the difference in the species that have peaks is due to the type of fluid that formed the inclusion. We assume as a working hypothesis that peaks and higher concentrations of inclusions are related to fractures along which fluids flowed. In order to test this hypothesis, analyses were performed in material for which fracture locations were known.

4.3.1. Coso Wells

Rock samples were obtained from Coso Well 64-16 core that has a noticeable calcite vein between 659 and 662 feet. The purpose of the sampling was to determine if FIT analysis shows a peak over the vein, and how far from the vein chemical species signatures could be observed. The sampling interval ranged from 20 feet at 600 feet to 1 foot at the vein center. The 660-foot sample is calcite; all other samples were green altered host rock. Figure 4.13 presents the mass spectra for H₂O, CO₂/CH₄, and N₂/Ar.

It can be seen that for H₂O there is a peak centered at 683 feet. For CO₂/CH₄ and N₂/Ar, the peaks are broader and the highest points of the peaks are above the center of the vein. For CO₂/CH₄, the width of the peak is about 15 feet, while for N₂/Ar the width of the peak is about 10 feet. The peaks observed in the mass spectra for CO₂/CH₄, and N₂/Ar shows that these species indicate the calcite vein and that the FIT analysis can be used to indicate veins and fractures with some mineral infilling.

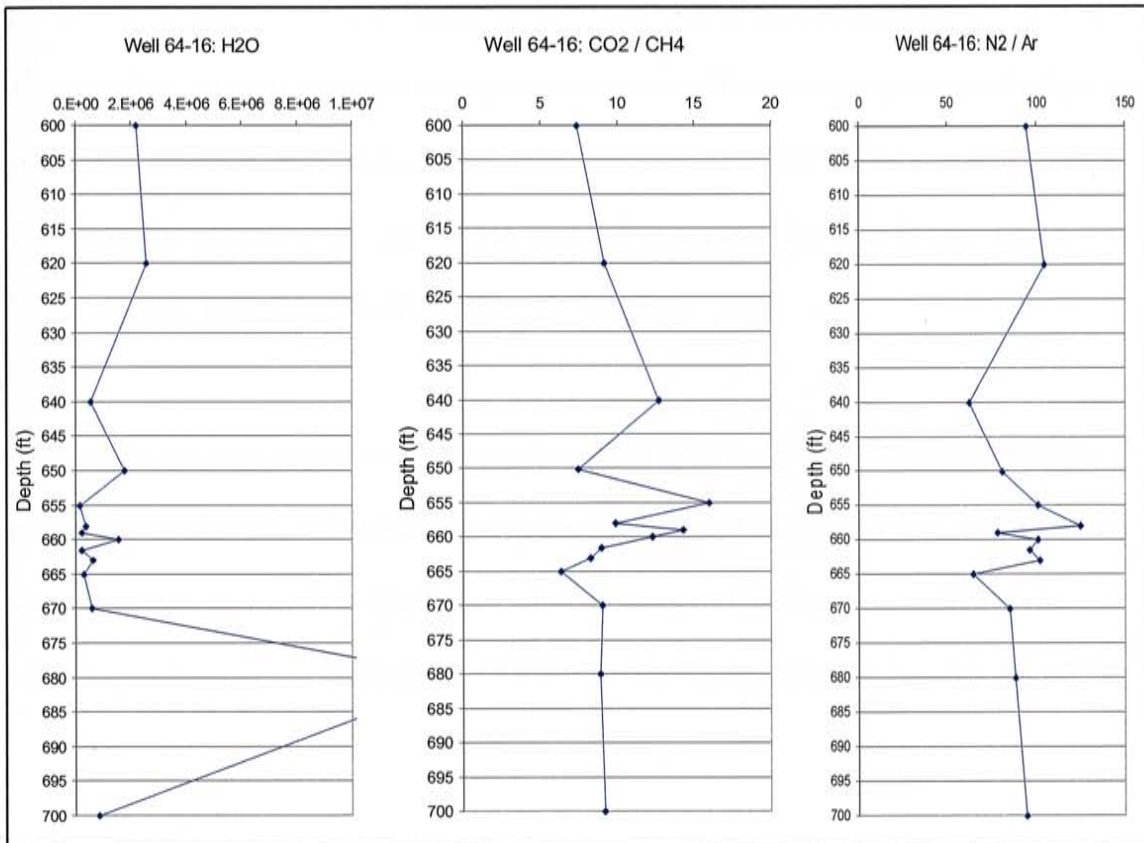


Figure 4.13. Graphs of H₂O, CO₂/CH₄, and N₂/Ar for a calcite vein centered at 660 feet from Well 64-16.

4.3.2. Karaha Wells

Because of the limited core from Coso, cores from Karaha were used as an additional test that gas peaks are related to fractures. Six fracture zones were selected from the Karaha wells. The fracture zones typically consisted of a zone approximately one to two feet with multiple veins composed of single or combination of minerals and open spaces of $\frac{1}{4}$ to 1 inch. The fracture filling minerals were variable amounts of calcite, quartz and pyrite. The fracture zones were sampled at 2 foot intervals above and below single veins. The sampling interval decreased to 1 foot intervals within three feet above and below the vein. A sample was also taken at the approximate center of the fracture zone. Figure 4.14 shows select results for Well K-33, with a fracture at 5458 feet. It can be seen that H₂O, and CO₂, indicate distinct peaks at this location.

Plotting the six fracture zones similar to Figure 4.14, it became apparent that multiple gaseous species produced peaks near the fracture and that fluid inclusion gas chemistry varied with vein mineral. Table 9 presents a summary of the locations of the peaks for various gaseous species in relation to the mineral(s) that occurred in six fracture zones.

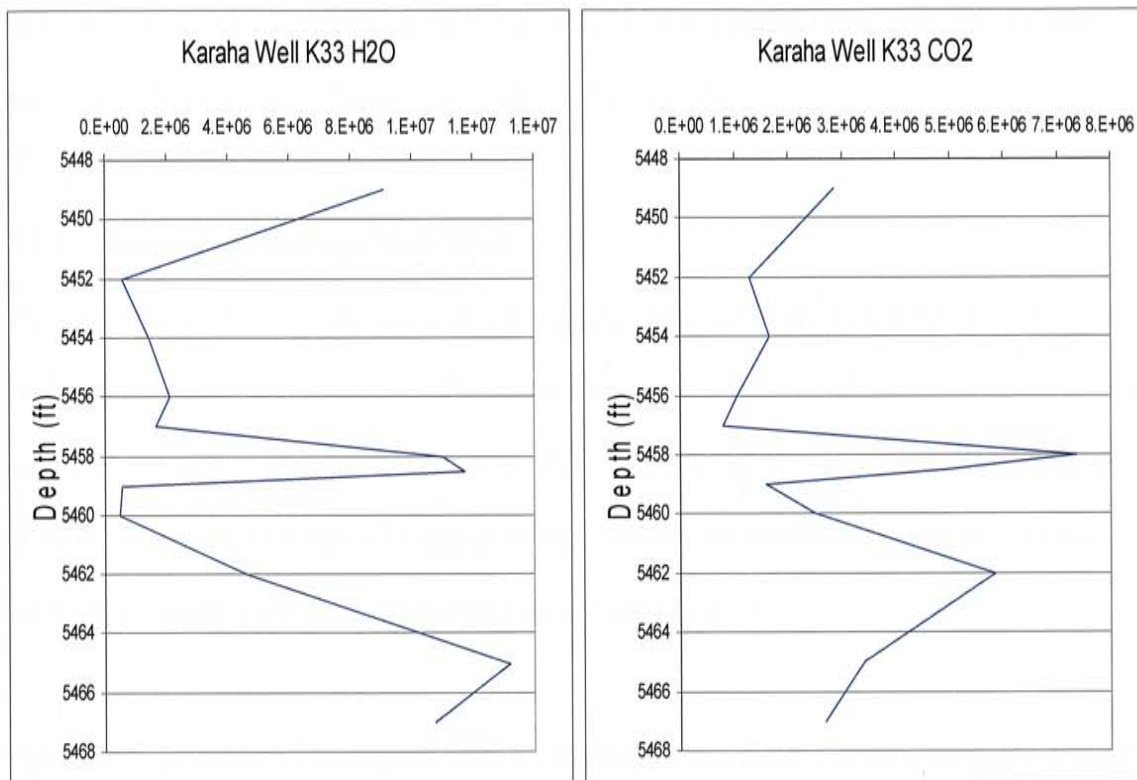


Figure 4.14. Graphs of H₂O and CO₂ for KaraHa Well K-33. Note the peaks all correspond to location of vein at 5458 feet.

Table 9. KaraHa Cores: Select chemical species and their occurrence in relation to the fracture.

Mineral	CH4	H2O	N2	H2S	Ar	CO2	Gas/H2O	N2/Ar	CO2/CH4
Calcite	X	X	-	X	X	Above	X	X	Above
Quartz	X	X	X	X	X	X	-	-	-
Pyrite	X	-	X	X	X		-	-	-
Calcite & Pyrite	-	X	X	-	X	X	X	-	X
Quartz & Pyrite	X	Above	Above	-	Above	X	X	X	X

Note: X indicates a peak at the fracture: Above indicates peak occurred above the fracture: "-" indicate peaks occurred elsewhere

It can be seen that the peaks for a number of the chemical species and ratios of interest occur near the fracture or a few feet above the middle of the fracture zone. Calcite-

bearing and quartz-bearing fracture zones have the most peaks lying near the fracture. For calcite fracture, the CO₂ peak was above the fracture.

4.3.3. Steamboat Springs Well 87-29

The analyses from Coso and Karaha indicate small fractures are detectable by FIT analysis. However most of the wells studied were sampled at 20-foot intervals, hence gas peaks most likely would require large-width fractures or areas of high density of fractures to be detected. To test this, FIT analyses were made of a Steamboat Springs, Nevada well whose major producing fracture locations are known.

Figure 4.15 presents a FIS log for Well 87-29 from Steamboat Springs, Nevada, plotted alongside the fracture log (Jeff Hulen unpublished data). The primary production zone for this well is from about 500 to about 1,200 feet with the hottest temperatures from about 600 to 850 feet. In the primary production zone from 500 to 1,200 feet there is a broad zone of fractures with maximum size of 10 to 100 millimeters and a few with larger openings. The fractures were logged by Jeff Hulen at EGI prior to this project. In the production zones all the major fractures indicated by Hulen are shown in the FIT analyses. There are several major FIT peaks like the one at 500 feet that are reflected in the temperature log, but not identified by Hulen. Below 3,000 feet, Hulen shows numerous fractures that appear misaligned to the FIS analyses by about 100 feet.

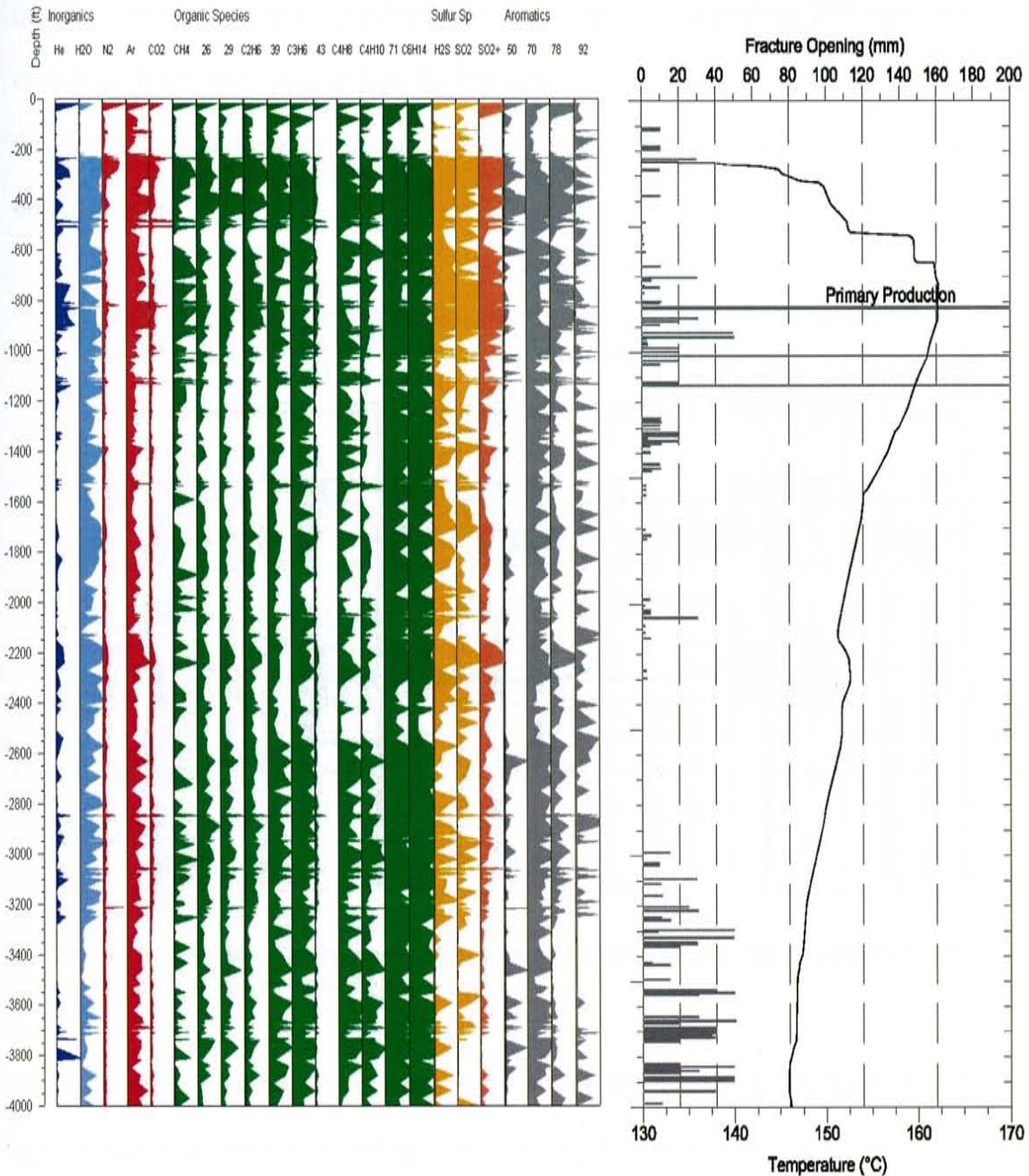


Figure 4.15. FIS log a) and fracture log showing fracture width and the temperature gradient (b) for Steamboat Springs Well 87-29.

Figure 4.16 shows the FIS log and the location of significant veins (from Hulen) for the upper 1,500 feet in Steamboat Springs Well 87-29. The veins are composed of calcite or

quartz. There is good correspondence between mapped fractures and FIS data with one exception at 850 feet. At 500 feet, the FIS peak corresponds to a calcite vein located at this depth. In addition the three large quartz veins correspond to FIS peaks from about 900 to 1150 feet.

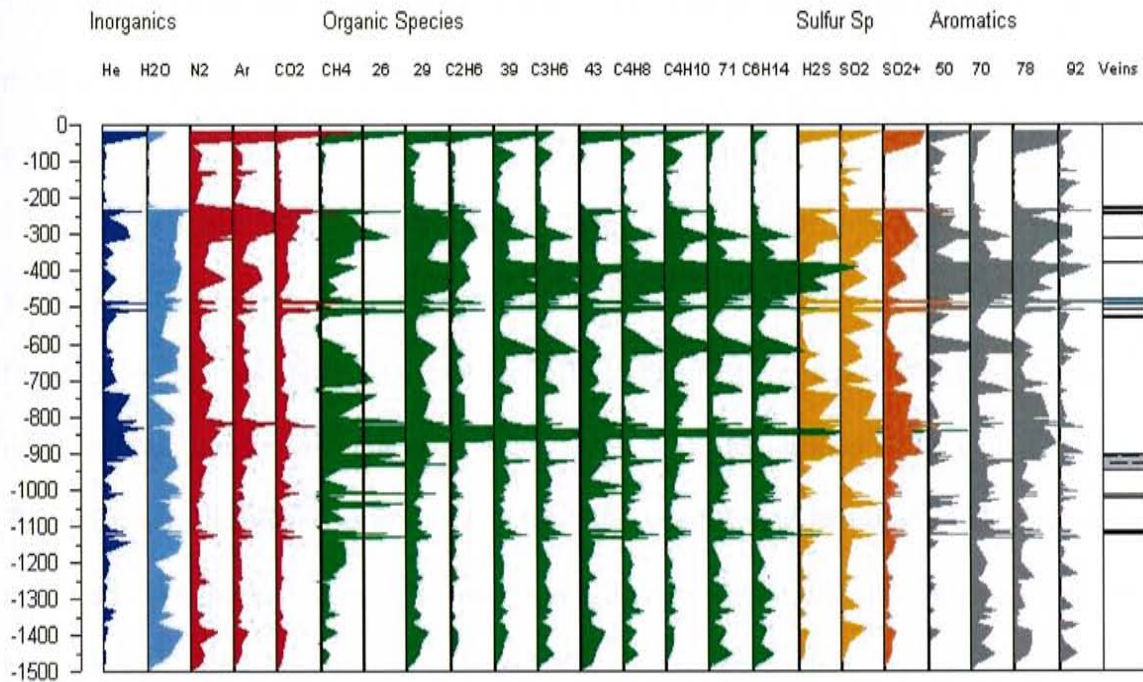


Figure 4.16. FIS log for Steamboat Springs Well 87-19 and vein locations (after Hulen) in the primary production zone.

From the limited fracture study using cores from Coso, Karaha and Steamboat Springs, it can be seen that peaks observed on FIS logs correlate to fractures in the rock. When FIS is used for the petroleum industry, they have assumed that the peaks observed in their data are also fractures within the reservoir. From the Karaha samples it seems not to matter whether the fracture filling material was calcite, quartz, pyrite, or some mixture of the minerals; there were several mass spectra with peaks that corresponded to the filled

fractures. The Steamboat Springs core further suggests that differences in gas chemistry can indicate areas with a number of fractures.

4.4. Beowawe

Two wells at Beowawe, Nevada, 57-13 and 77-13, were provided to determine if the method would work at a different field and also to test if real-time data could be used for well decisions. It was also a test to see if FIT analysis can detect major fractures. Well 77-13 is a principal producer at Beowawe. Temperatures range up to 420°F (215°C). Well 77-13 penetrates a fault at approximately 5500 feet and produces beneath the major Basin and Range fault with 1,000s of feet offset. Figure 2.5 presents a cross-sectional model of the Beowawe geothermal system. Well 57-13 was drilled in December 2005. The purpose of the well was to intersect the fault in a different part of the field and produce below the fault zone. The well was drilled to 10,600 feet, and logging could not be determined if the fault was intersected. FIS analysis of the drill cuttings was conducted to determine if the fault could be recognized. At the time of the analysis, the drill rig was idling on-site costing the company thousands of dollars a day in downtime. The analysis took approximately four days and was used to determine if drilling should continue or if the well should be completed for production.

The FIS log for Well 77-13 (older well Figure 4.18) shows large peaks particularly in the organics and aromatics species from about 4,800 to 5,600 feet. Above 4,700 feet there are small amounts of CO₂, N₂, and CH₄ shown on the FIS log. In addition, the water peak and inorganic species increase in peak height below 4,800 feet. The FIS log for the

newly drilled Well 57-13 is also shown in Figure 4.18. The pattern of peaks is similar to that obtained for Well 77-13, but show greater intensity. From about 5,300 to 6,400 there are large peaks in the organics and aromatics. The water peak and inorganic species are significant from about 5,500 feet and increases in intensity below about 6,800 feet to about 7,500 feet and again from 8,600 to 9,700 feet. The spectra indicate the structure was intersected a few hundred feet deeper than in Well 77-13. The difference in peak intensities may be due to drill chip size, difference in drilling techniques, or to the amount of inclusions in the samples.

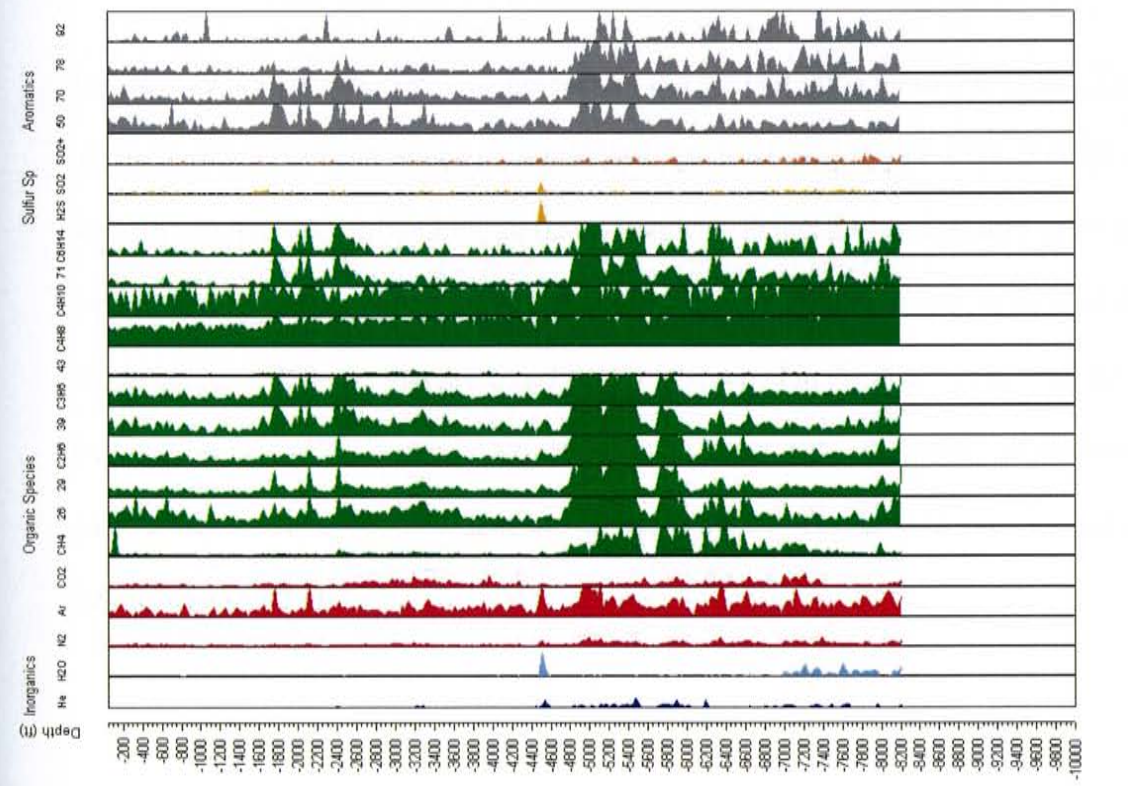
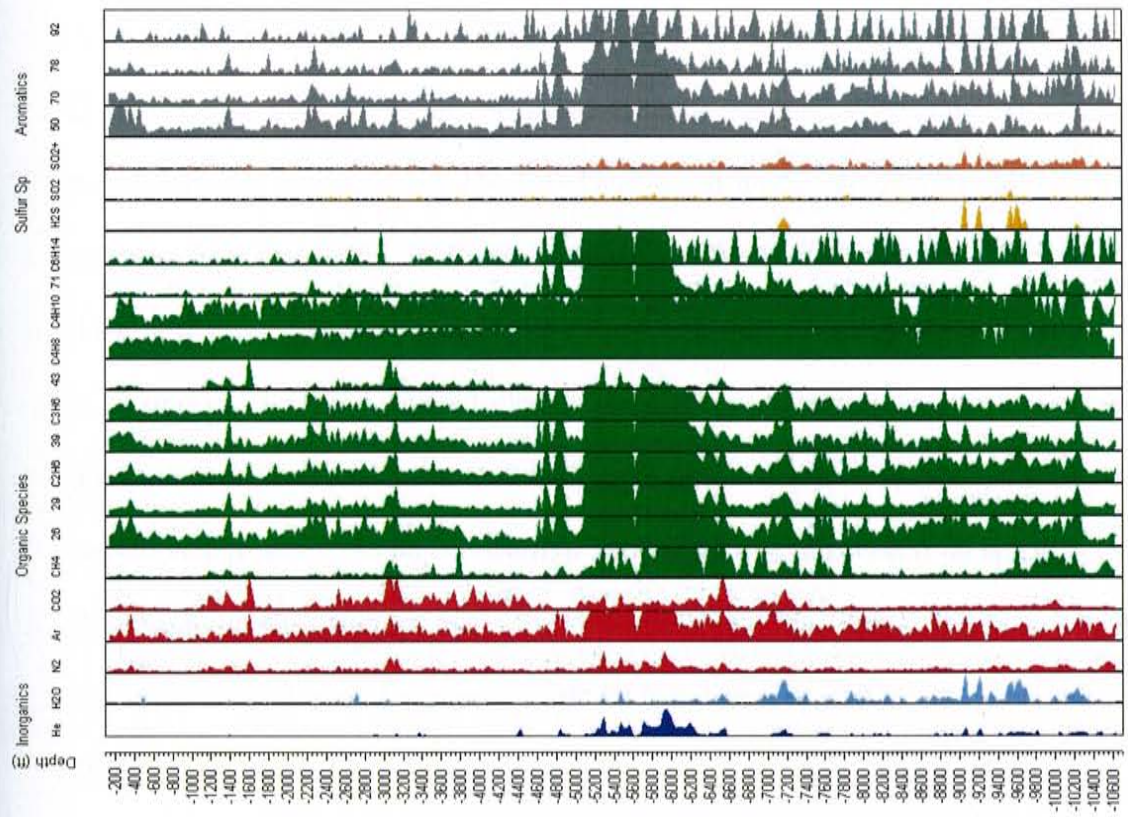


Figure 4.18. FIS logs for existing Well 77-13 and the new Well 57-13 at Beowawe, Nevada.

4.5. Timing

A working hypothesis is that geothermal fluid inclusions mostly reflect recent fluids due to inclusions continually being formed in dynamic geothermal systems. To test the hypothesis well cuttings from a well and cuttings from the same well redrilled 7 years later, were analyzed. Original well cuttings from Well 68-20 and the well cuttings from the redrill, 68-20RD, were collected for fluid inclusion gas analysis. Well 68-20 is used as an injection well and was redrilled due to silica precipitation that resulted in loss of permeability. Well 68-20 and 68-20RD, were drilled at the same location with a deviation at most of 150 feet at depth of 5500 feet. The injection fluid is 230°F (110°C) fluid from the flashed plant and is free of condensable gas. Injection occurred at about 2,900 feet in (wall rock temperature 119°C) in a damaged well casing joint, and at about 5000 feet (wall rock temperature 160°C).

Figure 4.19 presents the FIS logs for each of the wells from 2600 to 6000 feet. The logs are at the same scale. It can be seen that Well 68-20RD is different from Well 68-20 in a number of intervals. In Well 68-20 below about 4700 feet most all species show lower peaks, than in comparison to the redrill chips. Well 68-20 also shows significant peaks at 3650 feet and 5250 feet that are significantly attenuated in the analysis of Well 68-20RD cuttings. Well 68-20RD overall appears to have lower gaseous species concentrations particularly below about 6700 feet and higher amounts of organic species and water at depths near 3000 feet.

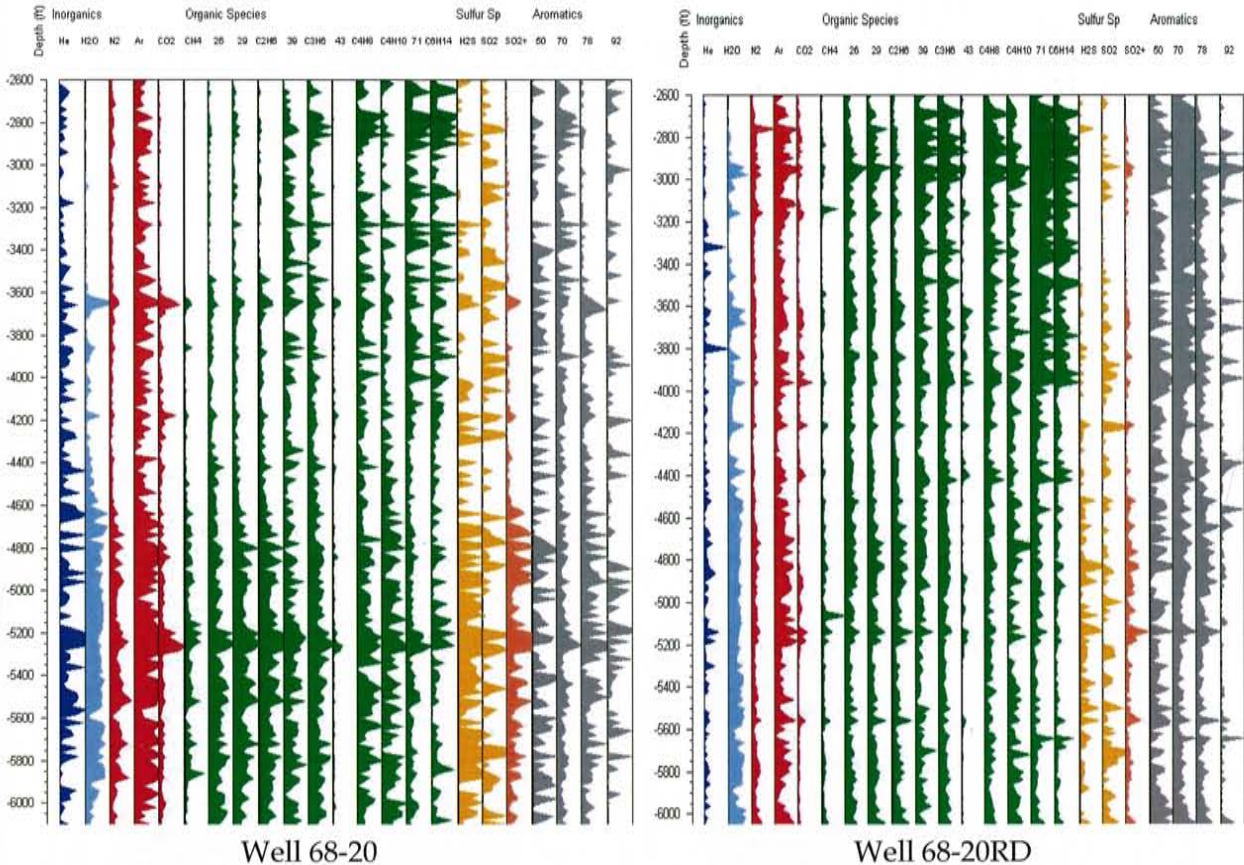


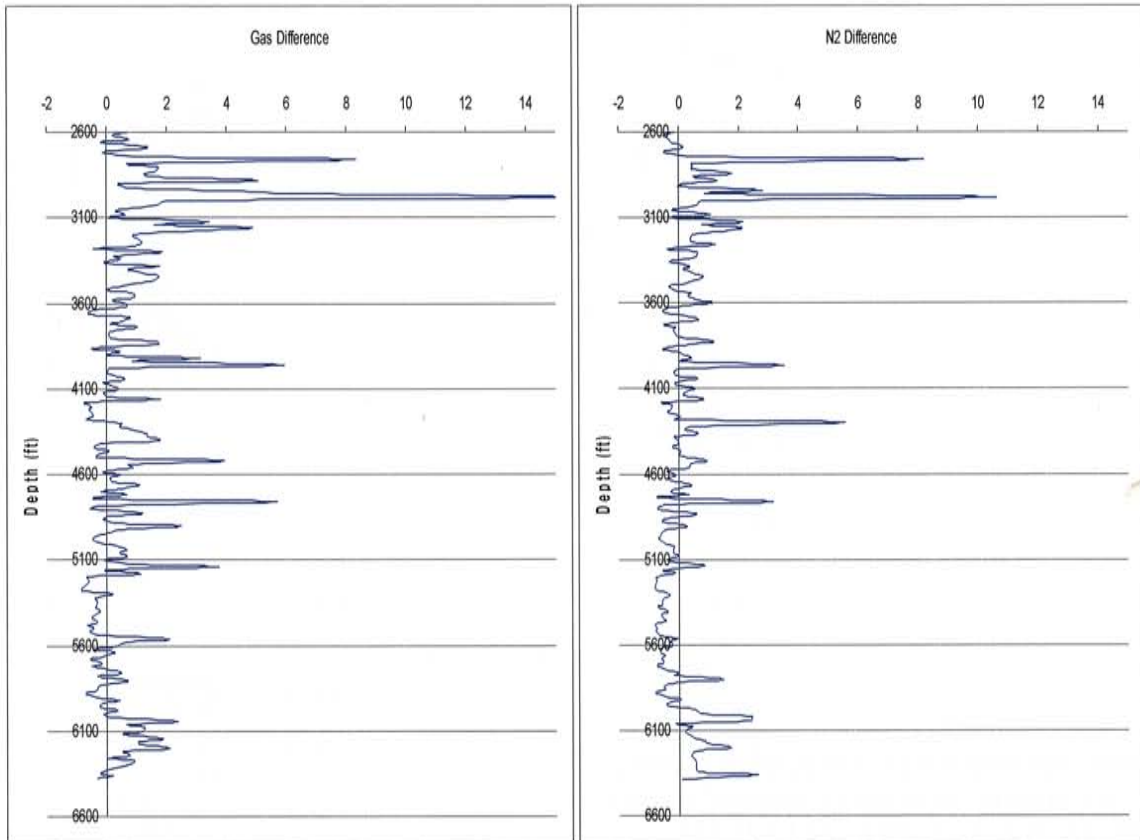
Figure 4.19. FIS logs for Well 68-20 and 68-20RD which was drilled seven years later. Note the difference between the two well logs particularly the peaks in the data at approximately 3650 feet, and 5250 feet in Well 68-20 versus lack of peaks in Well 68-20RD.

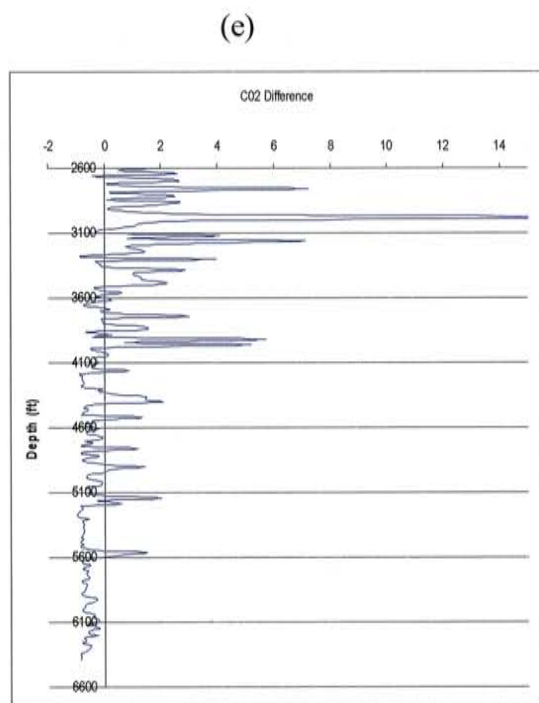
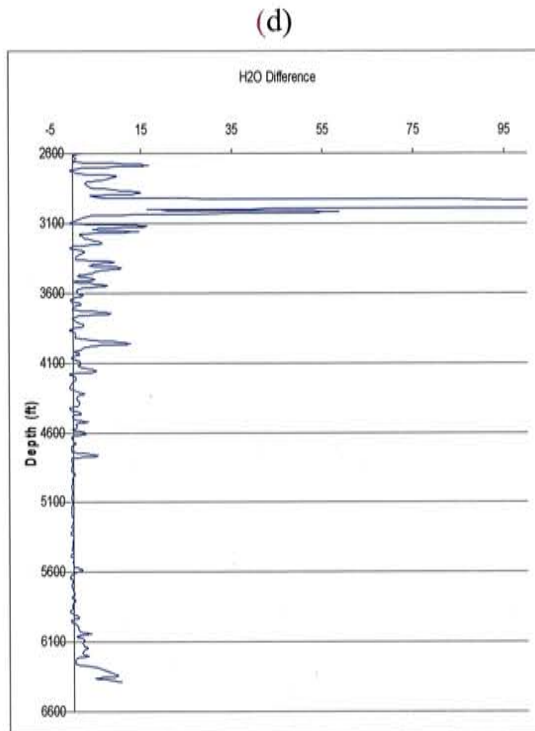
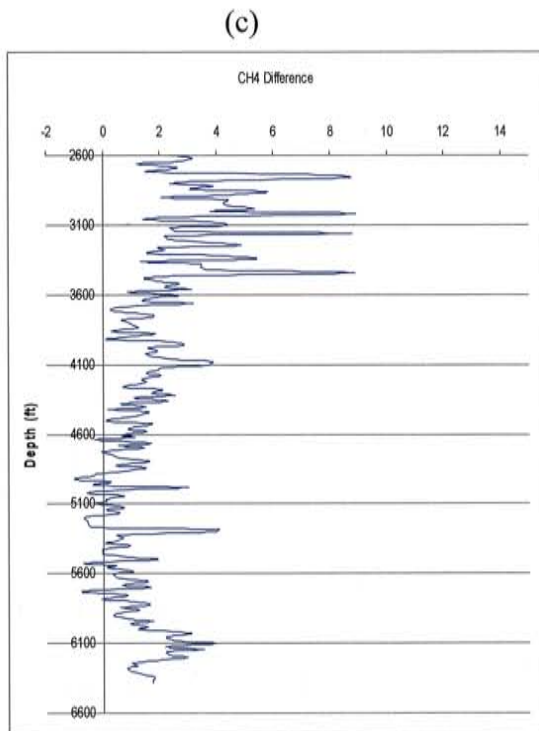
Differences were calculated by subtracting Well 68-20RD from Well 68-20 and the graphs are presented in Figures 4.20a through 4.20e. Negative values indicate more of that species in the original well. The differences shown in Figures 4.20a through 4.20e are also observed in the FIS logs presented in Figure 4.19. The FIS log for Well 68-20 indicates that above 3,650 feet the relative concentration of a number of species (He, H₂O, N₂, Ar, CO₂, CH₄, 26, 29, and others) is very low. The increase in the relative concentrations of these species from the older well 68-20 to the newer well argues that

new fluid inclusions have been formed in the redrill. The location of the largest differences is at approximately 2700 feet and 3000 feet. This corresponds to the break in the well casing that became the injection site.

(a)

(b)





Figures 4.20(a) through 4.20(e) present the differences in various compounds between Well 68-20RD and Well 68-20. Note the significant peak at about 2900 foot depth, which corresponds to break in well casing.

Table 10 shows the percent change in the overall average concentrations and the average concentration at the break in the casing between the original and the redrill wells for H₂O and for CO₂. There is a 74% difference in the H₂O and a negative 18% change in CO₂ overall average concentration. The negative change in CO₂ is indicated in Figure 4.20e where the CO₂ concentration decreases below about 4100 feet in the redrill. In the zone of the break in the well casing there is an 810% change in H₂O and a greater than 110% change in CO₂ concentration

Table 10. Percent change between the original and the redrill well for H₂O and CO₂.

Species	Original Well	Redrill Well	% Change
H ₂ O (overall)	3.3 X 10 ⁶	5.7 X 10 ⁶	+74
CO ₂ (overall)	2.6 X 10 ⁶	2.1 X 10 ⁶	-18
H ₂ O (break)	4.68 X 10 ⁵	4.26 X 10 ⁶	+810
CO ₂ (break)	9.92 X 10 ⁵	2.11 X 10 ⁶	+113

4.6. Temperature Logs

Temperature logs were provided by Coso Operating Company. The temperature logs presented were produced within several months after each well had been drilled. Figures 4.21a through d present the temperature logs for the same four wells that are shown in Figures 4.6 through 4.9. Temperature logs for the remaining wells are in Appendix C. As described in Chapter 2.2, temperature logs are a major tool used to evaluate a well, and to produce a temperature model of the field. Temperature logs are interpreted in terms of conducting versus convecting zones within each well (refer to Figure 2.2). In addition, the slope of the temperature log also indicates well wallrock permeability. A temperature log near vertical or showing convection also indicates high permeability (Figure 4.21c and d) versus a sloping temperature log (Figure 4.21b), which indicates

conduction and thus lower permeability (Manning & Ingebritsen 1999). Interpretations made from the temperature logs were compared to interpretations made from the FIS logs to evaluate the FIS method.

Coso geothermal field production temperatures are typically greater than 482⁰F (250⁰C). The temperature logs presented in Figures 4.21a through d indicate that this temperature is exceeded in Wells 38C-9 and 51B-16 but not in Wells 67-17 or 84-30. Wells 38C-9 and 51B-16 have bottom temperatures that almost reach 600⁰F (315⁰C). Production type temperatures occur in Well 38C-9 starting at approximately 5,800 feet and the temperature continues to rise to a depth about 8,800 feet. For Well 51B-16 the production temperatures occur at approximately 6,200 feet and continue to increase to the bottom of the hole. Reversals in the temperature logs are generally interpreted as cold water inflows.

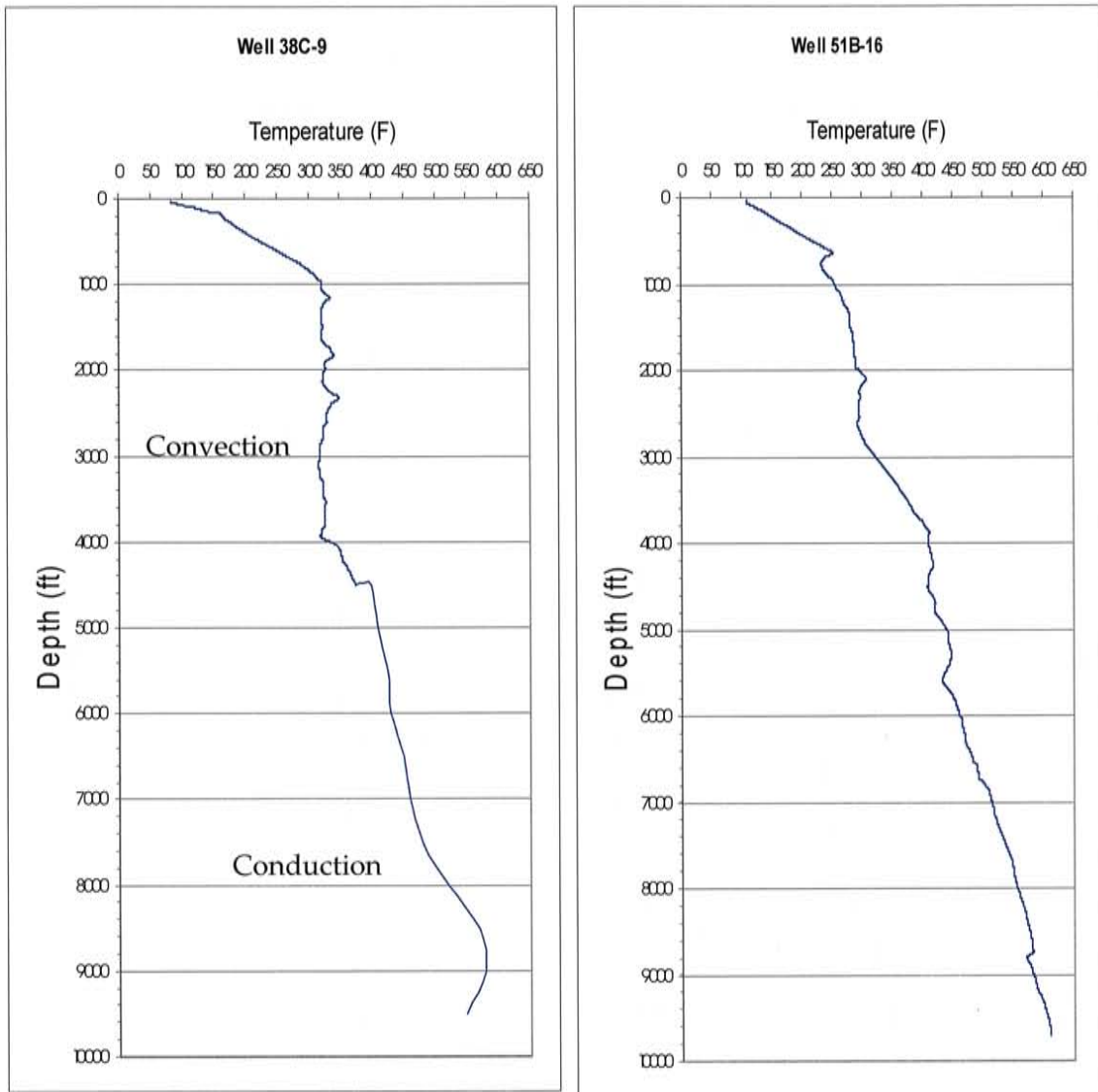


Figure 4.21 a and b. Temperature logs for Wells 38C-9 and 51B-16. Note the continuously sloping temperature profile in Well 51B-16 versus the variable sloping profile for Well 38C-9 indicating lower permeability and heat flow by conduction in Well 51B-16.

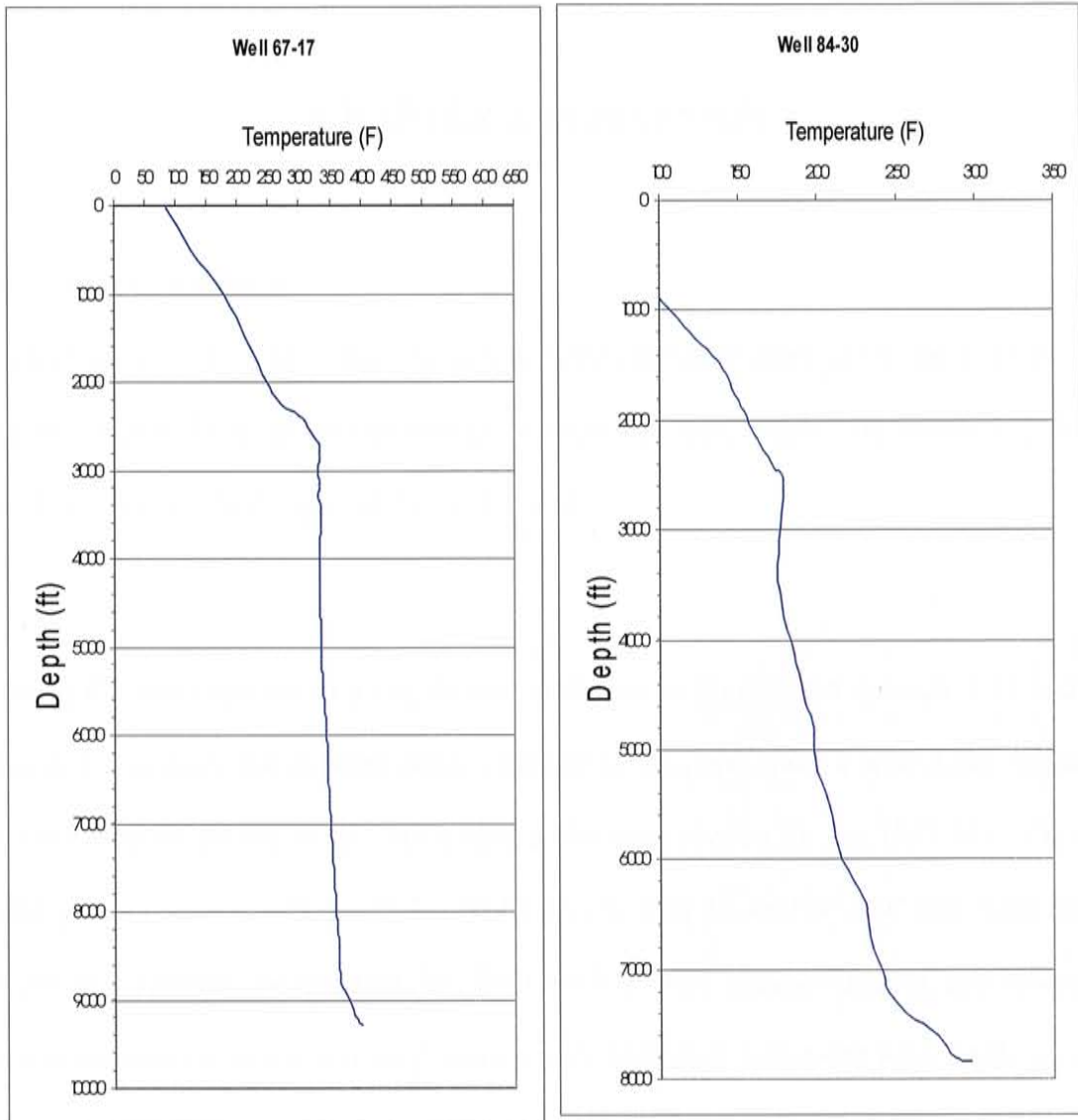


Figure 4.21 c and d. Temperature logs for Wells 67-17 and 84-30. Note the near vertical temperature profiles indicating convection and high permeability. However note the lower temperatures when compared to Well 38C-9 in Figure 4.13 a.

CHAPTER 5. DISCUSSION

5.0 Fluid Chemistry

In order to identify fluid types, changes in fluid chemistry need to be observed on the logs and which chemical species change at about the same depth. By identifying these chemical species, fluid types can be determined.

Plotting the mass spectra in a log format as shown in Figures 4.6 through 4.12 and in Figures 5.1 through 5.4 indicate major changes in the mass spectra with depth between the wells and within the wells. For instance, the mass spectra for He, H₂O, N₂, CO₂ and sulfur group changes with depth for Wells 38C-9, 51B-16, and 67-17C and these mass spectra are virtually nonexistent for Well 84-30. The organic species and aromatic species indicated in green and grey, respectively also show variations with depth in each of the wells including Well 84-30.

Changes in the H₂O spectrum indicate a change in either the abundance of the inclusions or in the type of inclusion from mainly liquid type inclusions to more vapor type inclusions. There is definitely a strong sorption of water in the FIT system. When inclusions are crushed the water vapour released strongly sorbs onto vacuum system walls, which attenuates the mass 18 peak. A typical mass spectrum shows water

($m/e=18$) as a principal peak. Coso geothermal waters are about 99% H_2O , so the $m/e=18$ should be about two orders of magnitude greater than the CO_2 peak ($m/e=44$). But the magnitude of the water peak increases and decreases from sample to sample in the same well and varies from the CO_2 peak. This variation is interpreted as fluctuations in the number of inclusions opened during a crush and therefore the water measurement is useful for indicating if a sample is rich or poor in aqueous inclusions. For instance in Figure 5.1 at about 750 feet, H_2O starts to occur in significant amounts. The zone from 200 to 750 feet is most likely poor in aqueous inclusions and high in vapor rich inclusions due to the presence of other gases as shown on the FIS mudlog.

Upon further examination of the FIS mudlogs it can be seen that several of the mass spectra change at the same depth. In Figure 5.1 there appears to be a decrease in most of the organic and aromatic species and N_2 and CO_2 from about 750 to 2500 feet and then an increase in most of those species. This decrease may represent an area where there is a low abundance of inclusion of any type, which is suggested by the low concentration in many of the gaseous species or more aqueous than vapor inclusions due to the presence of H_2O . At 6400 feet there is decrease in H_2O and a few organic species. Starting at about 7200 feet, there is an increase in N_2 , Ar, and CO_2 to the depth of the well compared to the zone from about 6400 to 7200 feet. At 8400 feet there is a decrease in H_2O , CO_2 , and H_2S and an increase in N_2 , Ar, and several of the organic compounds. Also notice how the sulfur species change throughout the depth of the well.

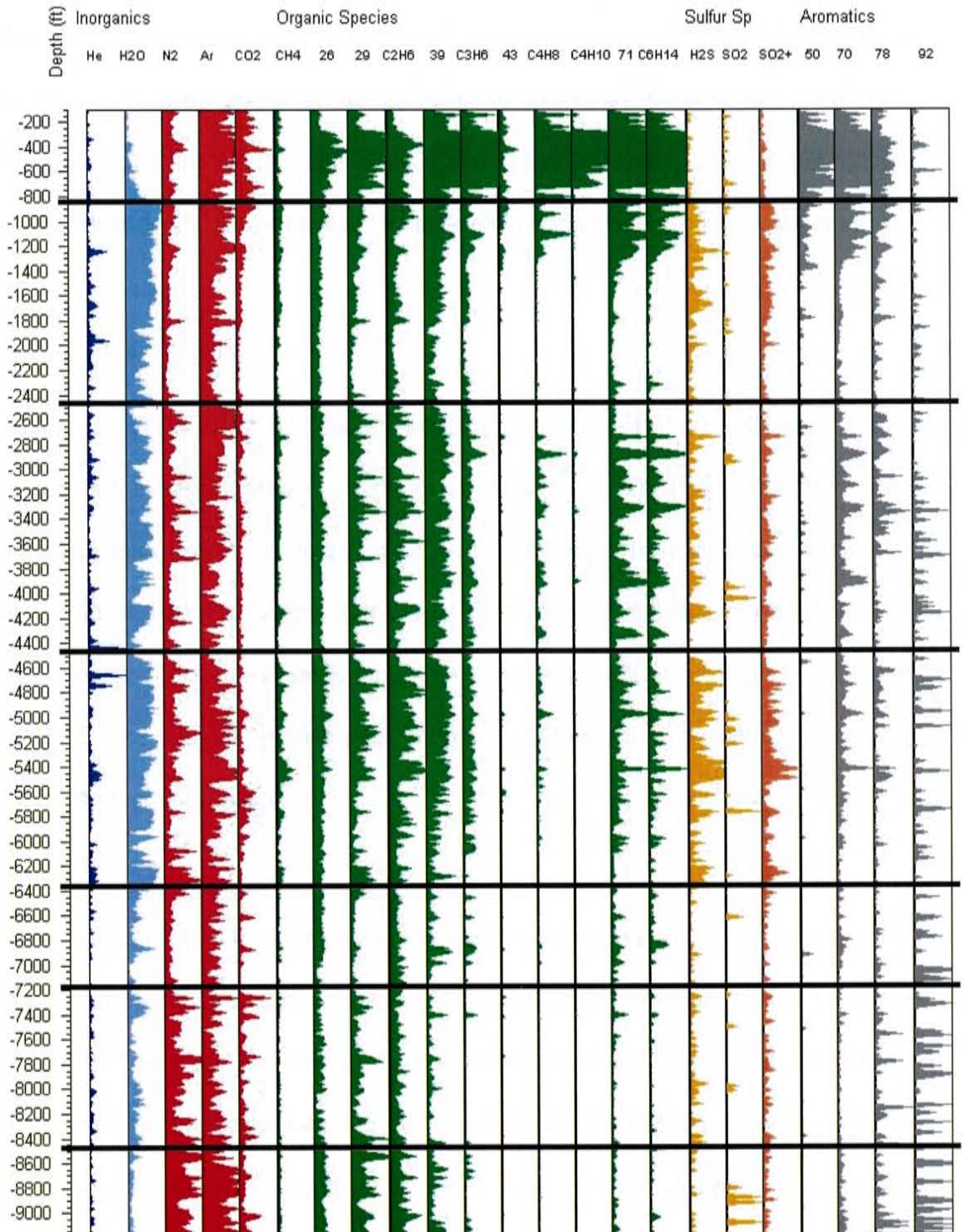


Figure 5.1. FIS mudlog for Well 38C-9 with major breaks in chemistry identified.

As in Well 38C-9, there are different depths where the mass spectra change for Well 51B-16 (Figure 5.2). Most notably from about 4400 to 5200 feet where there is a decrease in most of the species shown and again from about 8000 to 8800 feet. For Well 67-17, as noted on Figure 5.3, changes occur from 2700 to 3900 feet and at 8500 feet. Well 84-30, Figure 5.4, also shows changes in the organic compounds and also in the H₂O peak at depth. These changes indicate changes in fluid chemistry and hence fluid types.

Examination of the FIS logs presented in Figures 4.6 through 4.12 indicates changes in several of the mass spectra with depth in all of the wells. The thickness of the zones where the mass spectra do not change significantly ranges from about 50 feet to several thousands of feet. Production intervals are typically several hundreds of feet thick and therefore the zones chosen on Figures 4.6 through 4.12 indicate changes of at least 500 feet thick. As with interpreting rock stratigraphy, the scale of the analysis is based upon what information is needed.

The gas composition from preproduction wells drilled in the Coso field contained an average of 11,900 ppm CO₂, 183 ppm H₂S, 0.46 ppm Ar, 58.6 ppm N₂ and 1.56 ppm CH₄ (Table 2). The average N₂/Ar ratio is 128, which is well above that of air saturated water or atmosphere. Comparing the FIS logs for Wells 38C-9, 51B-16 and 67-17 in Figures 5.1 through 5.3 to the FIS log for Well 84-30, Figure 5.4 there are significant amounts of H₂O, CO₂, N₂, CH₄, and the sulfur species in the first three wells but not in Well 84-30. This suggests that the fluid inclusions in these wells have incorporated the gases from the

geothermal system. Well 84-30 represents a well that is outside of the geothermal field. The fluid inclusion gas analysis indicates low inclusion concentrations and few peaks representing fractures. Fluid inclusion thermometry and analysis of surface rocks indicate at least three episodes of activity for the Coso geothermal field: 307,000 years ago; 238,000 years ago; and the current episode starting about 10,000 years ago. Based on the FIS mudlogs and temperature logs Well 84-30 does not appear to have experienced these geothermal episodes, while the other three wells have experience at least one of these geothermal episodes.

There is also much finer detail in the mass spectra as shown in Figure 5.5, which presents Well 38C-9 from 4500 to 6800 feet. It can be seen in this diagram that there are multiple peaks in the mass spectra at the same depth, such as at 4900 feet, 5350 to 5450, at 5800 to 5850 feet, and to a lesser extent at about 6250 to 6300 feet. If these peaks are related to fractures then these peaks represent fractures or a series of fractures within that zone. The peaks may also represent the variability in the precision of the measurements which is about 25 to 46 percent. The percent difference between minimum and maximum for these individual peaks ranges from 42 to 100 percent for the various species plotted, suggesting the peaks are significant.

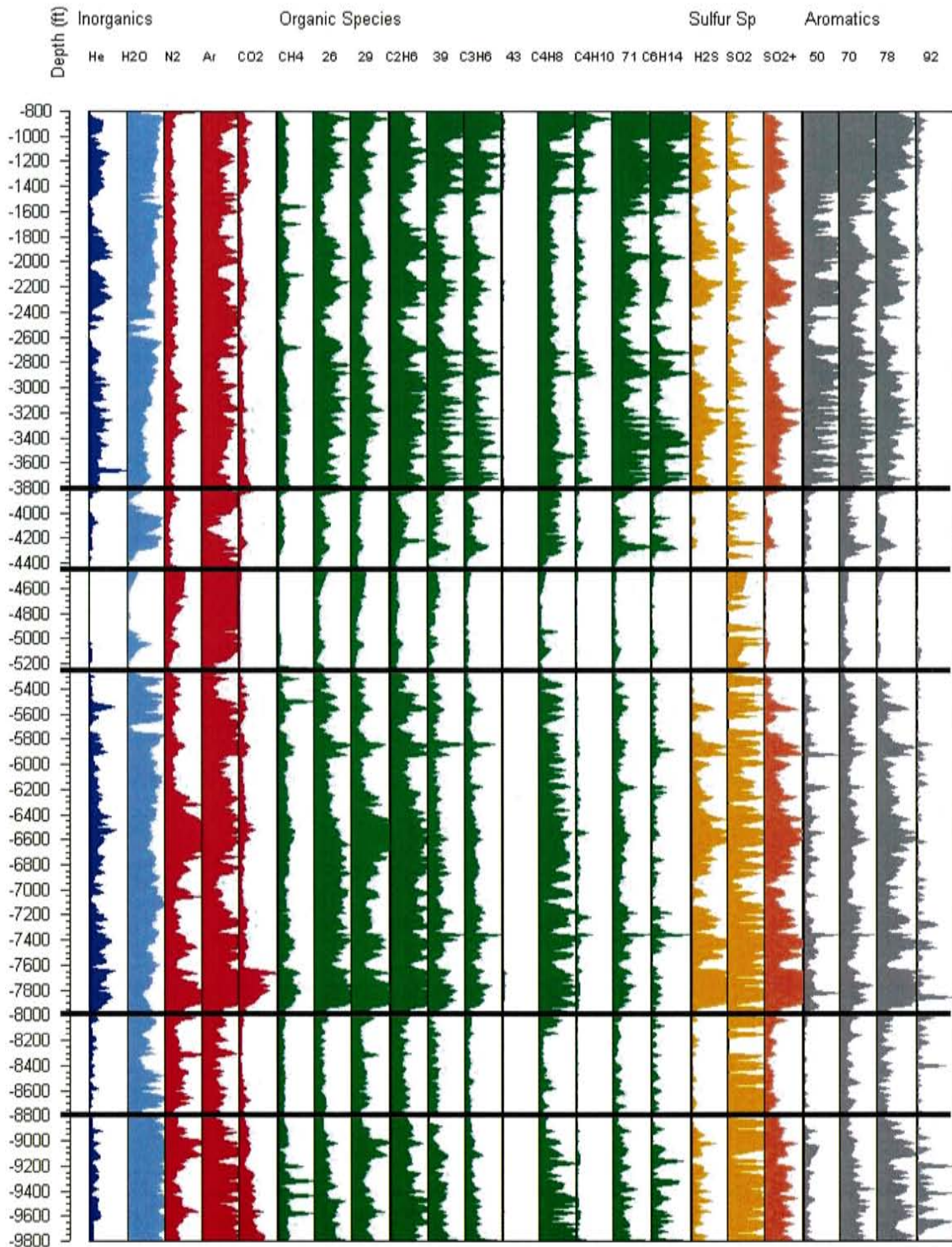


Figure 5.2. FIS mudlog for Well 51B-16 with major changes in chemistry identified.

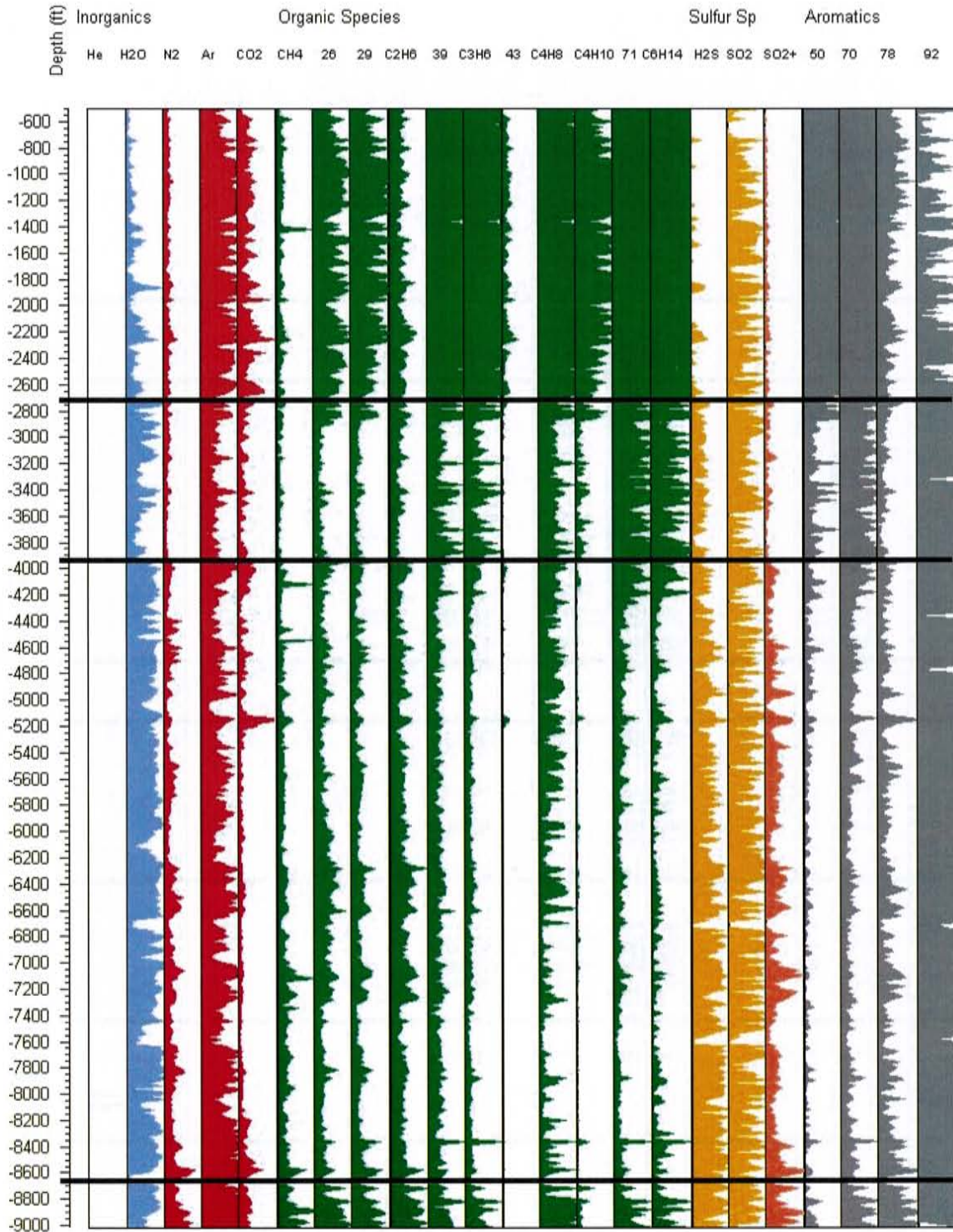


Figure 5.3. FIS mudlog with select mass spectra plotted versus depth for an injection well, Well 67-17.

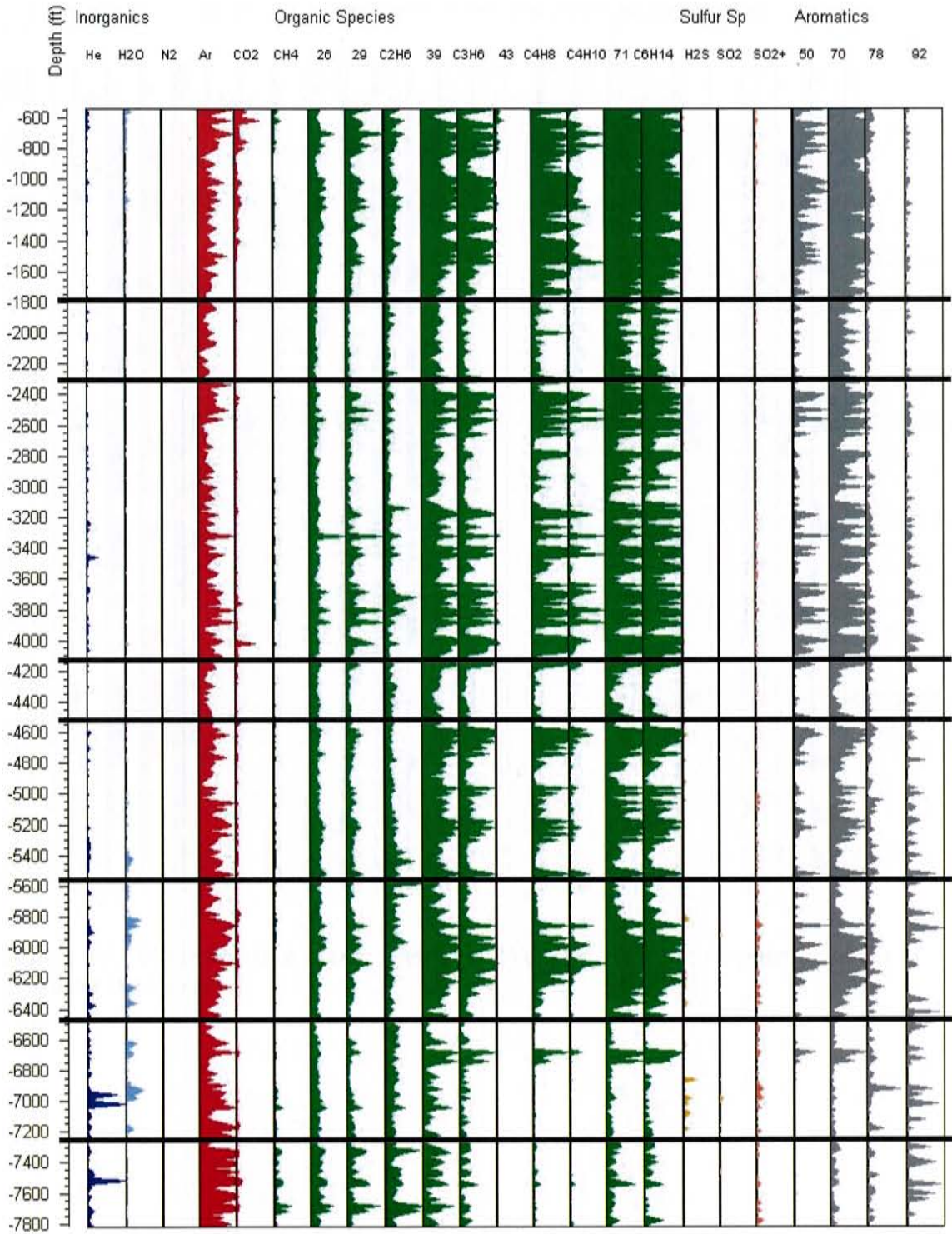


Figure 5.4. FIS mudlog with select mass spectra plotted versus depth for Well 84-30 located at the southern margin of the field and non-producing.

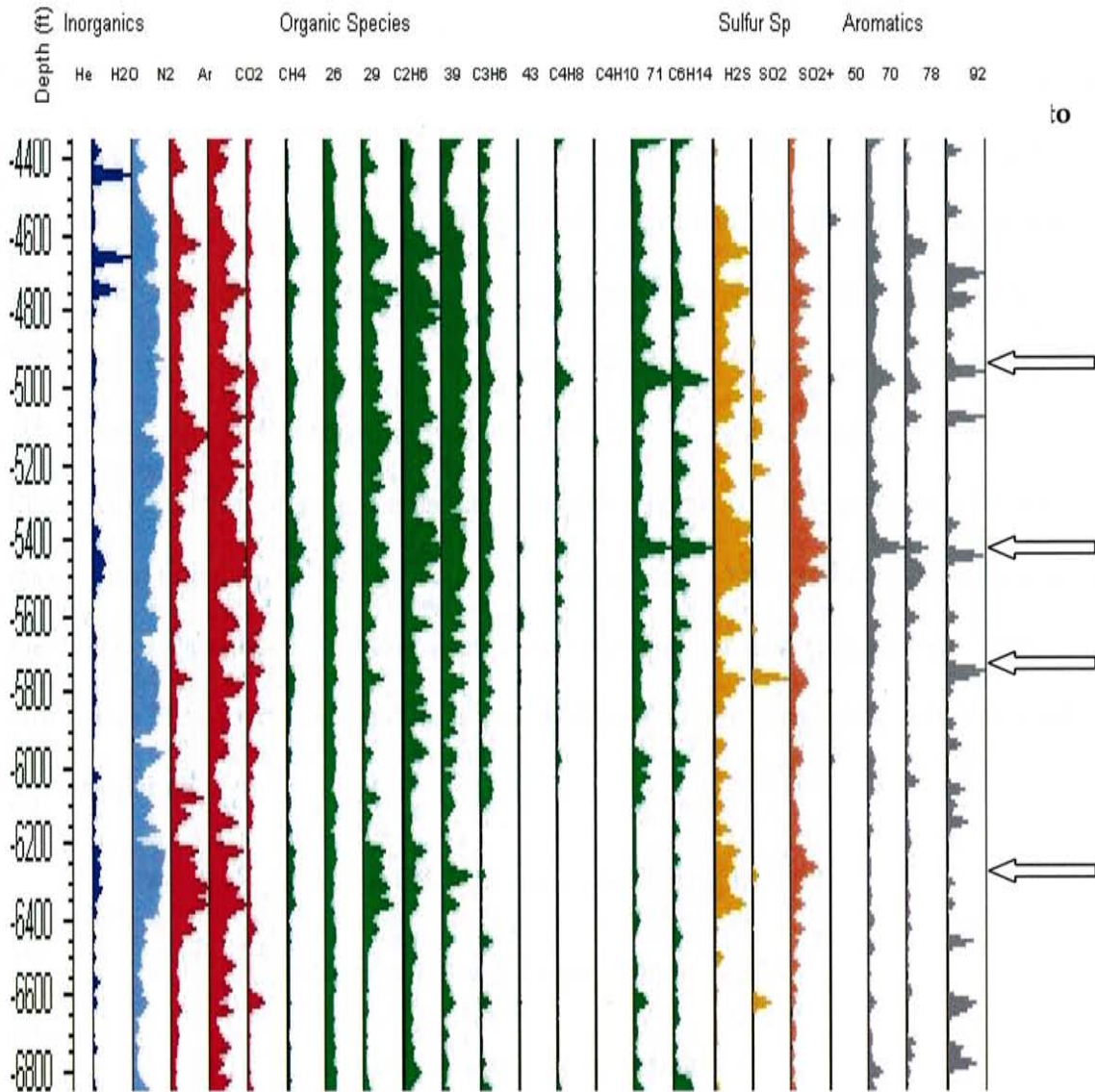


Figure 5.5. Finer detail in mass spectra for Well 38C-9. Arrows point to areas of potential fractures.

5.1. Fluid Source Log

In order to determine fluid type, an additional log was developed that used the gas ratios discussed in Chapter 2.1 and in Table 1. These gas ratios have been used by other researchers to evaluate the type of fluids that were encountered. Based on the discussion in Chapter 2.1 four main fluid types were considered: meteoric, condensate, plume, and background or a zone representing a lack of geothermal activity. Condensate is the term used here forward for both steam-heated waters and condensate. The first step in determining the fluid type represented by the gas analysis was to determine if certain species and ratios were above or below the average concentration for that species or in the case of ratios above or below a particular value for that ratio (Giggenbach 1986; Norman & Musgrave 1995; and Moore et al. 2001). The species, ratios and tests used were the following:

- H₂O – above or below average concentration
- N₂/Ar – above or below 200 (see Table 1)
- CO₂/CH₄ – above or below 4 (see Table 1)
- H₂S – above or below average concentration
- Total organics – sum of mass spectra 26 through 86 subtracting the sulfur species and aromatics – above or below average concentration.

There are several more species plotted on the FIS logs, however the above species and ratios appeared to be the strongest indicators of fluid types.

Next a series of rules were then developed to identify one of the four fluid types: meteoric, condensate, plume or background. Table 11 presents the rules that were developed (see Figure 5.6):

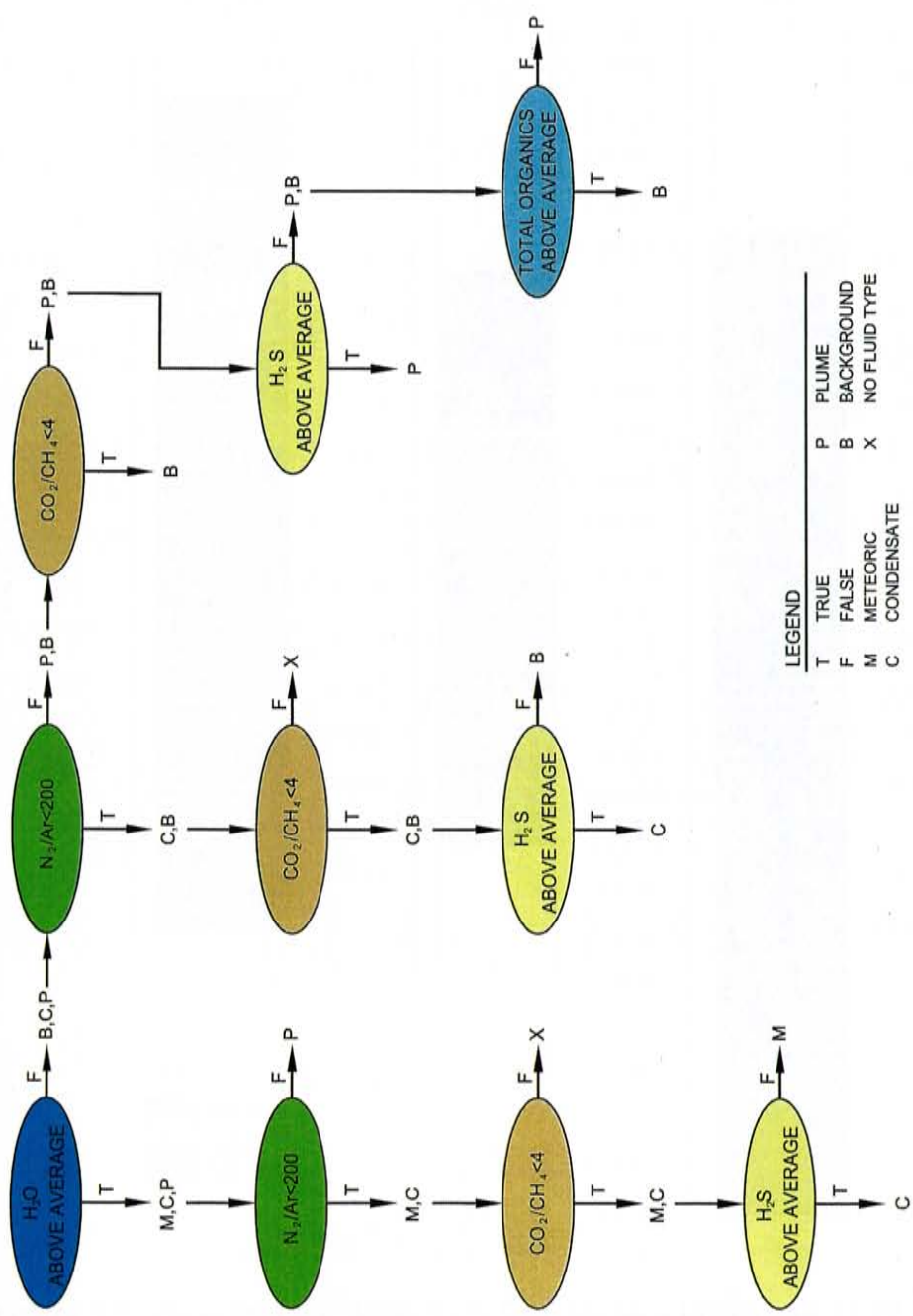
Table 11: Fluid type rules.

Fluid Type	H ₂ O	N ₂ /Ar ratio	CO ₂ /CH ₄ ratio	H ₂ S	Total Organics
Meteoric	Above average	<200	<4	Below average	Below average
Condensate	Does not matter	<200	<4	Above average	Does not matter
Plume	Does not matter	>200	>4	Does not matter	Below average
Background	Below average	Does not matter	Does not matter	Below average	Above average

The series of rules were applied to the data in Excel spreadsheets in the form of if/then statements with a return being the fluid type. First the species (i.e. H₂O) concentration for each sample was compared to the average for that species. The if/then statement: If (H₂O > average H₂O, if true return 1, if false return 0) was used for H₂O, H₂S, and total organics. For the ratios N₂/Ar and CO₂/CH₄ the amount was compared against 200 and 4, respectively. A series of columns in Excel was set up using the flow chart in Figure 5.6 applied to each sample to arrive at a fluid type. Nested if/then statements were used in each column as a test for fluid type. For instance, if H₂O was above average (1) and N₂/Ar was greater than 200 (1) then the fluid type returned from the testing would be plume fluids. This was done for each 20 foot interval sample in each well. The computer generated fluid log was imported into Logger program for plotting. Figures 5.7 through 5.9 present the fluid logs developed by this process for the wells. Figure 5.10 through

Figure 5.13 presents the FIS logs and fluid logs for Wells 38C-19, 51B-16, 67-17 and 84-30, respectively.

The computer generated fluid logs present a fluid type for every sample. Fluid types occur in zones over 1,000 feet thick. In addition there are zones where the fluid types change rapidly with depth. These zones would be considered mixed fluids. As with trying to separate rock units there may be some overlap as to the fluid types and some consolidating of fluid types into one type based on thickness of the unit.



LEGEND

T	TRUE	P	PLUME
F	FALSE	B	BACKGROUND
M	METEORIC	X	NO FLUID TYPE
C	CONDENSATE		

Figure 5.6. Flow chart illustrating the determination of fluid types.

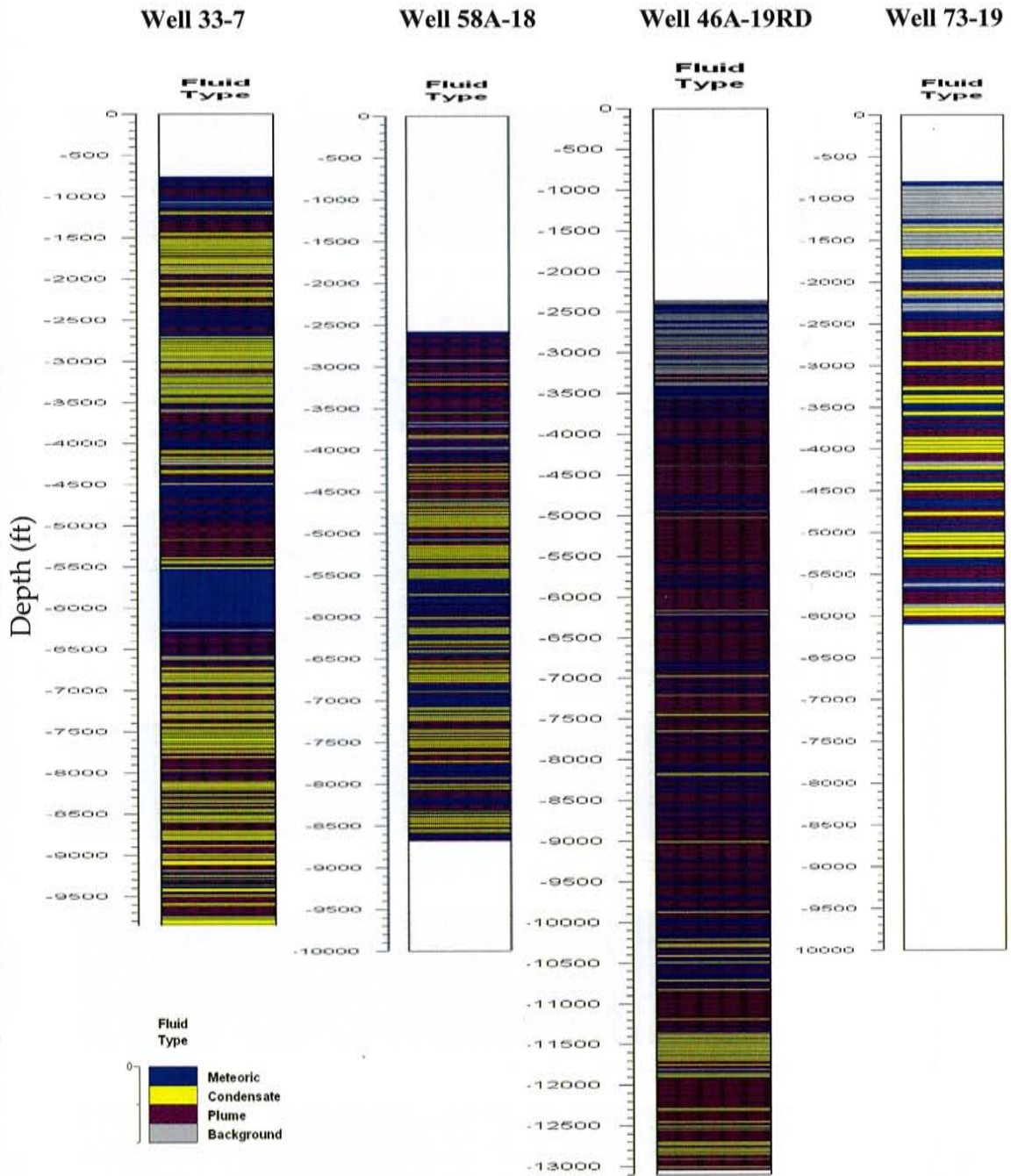


Figure 5.7. Fluid logs for Wells 33-7, 58A-18, 46A-19RD, and 73-19 that occur on the western side of the field.

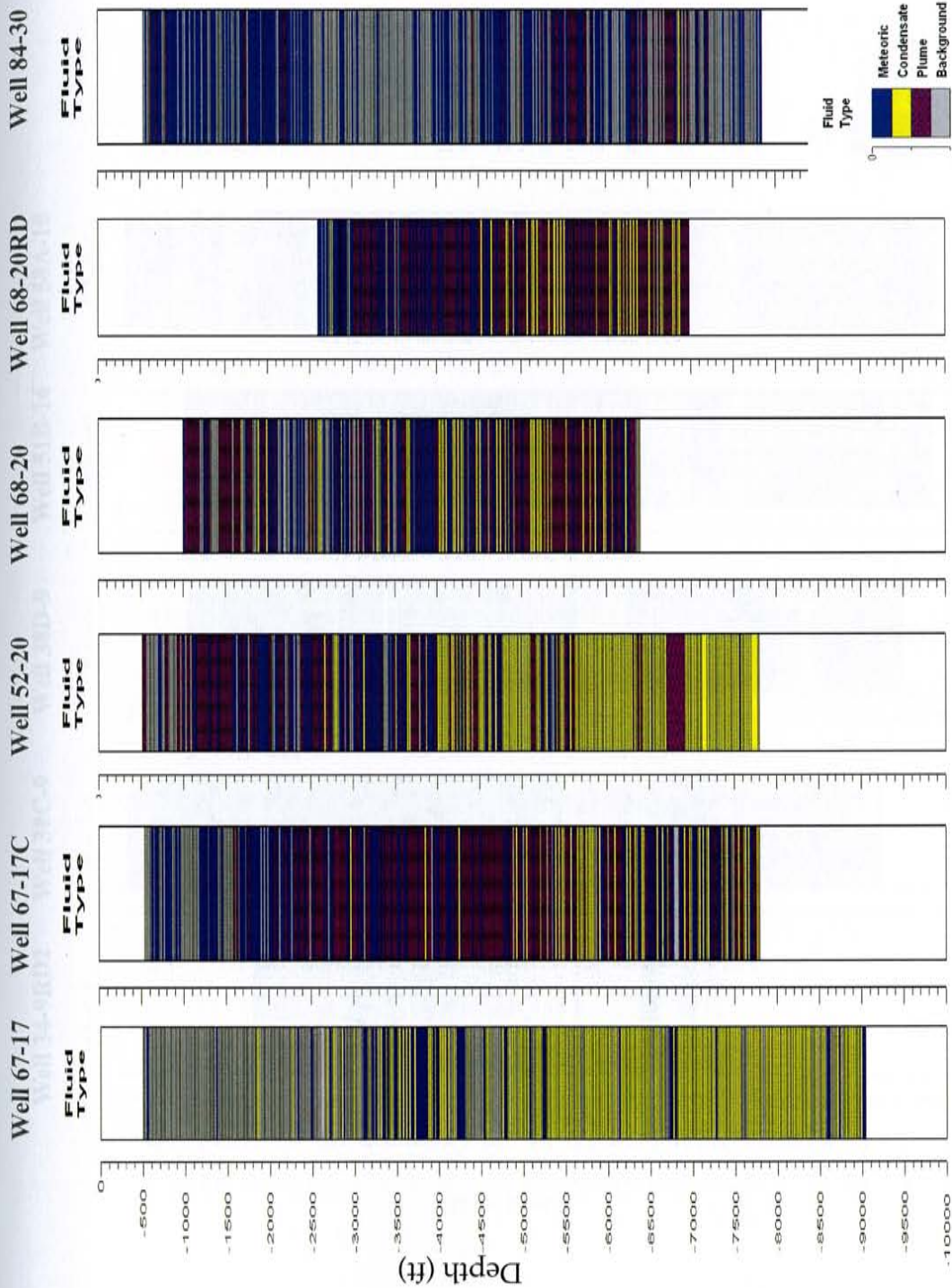


Figure 5.8. Fluid logs for Wells 67-17, 67-17C, 52-20, 68-20, 68-20RD, and 84-30 that occur on the middle southern portion of the field.

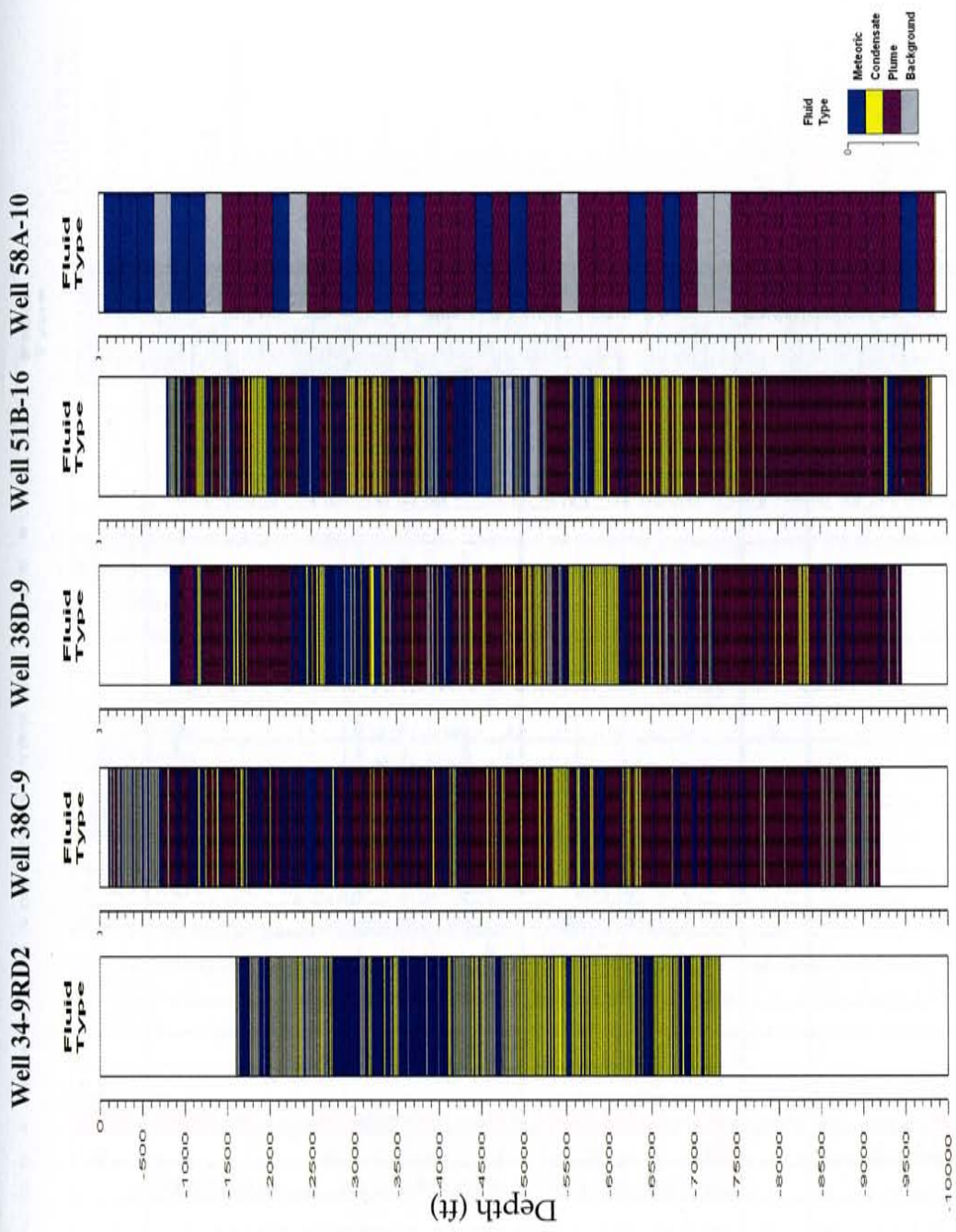


Figure 5.9. Fluid logs for Wells 34-9RD2, 38C-9, 38D-9, 51B-16 and 58A-10 located on East Flank of the Coso field.

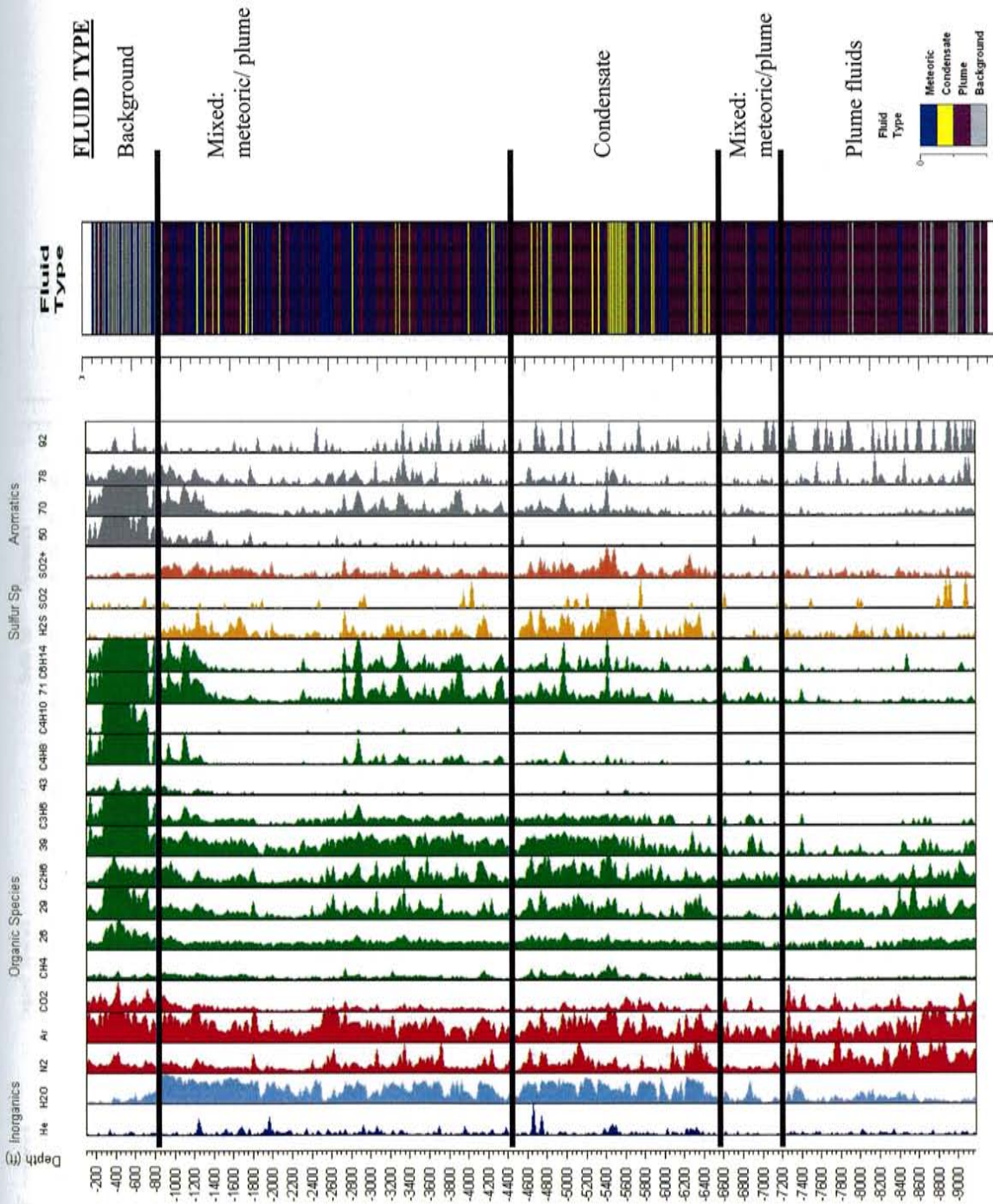
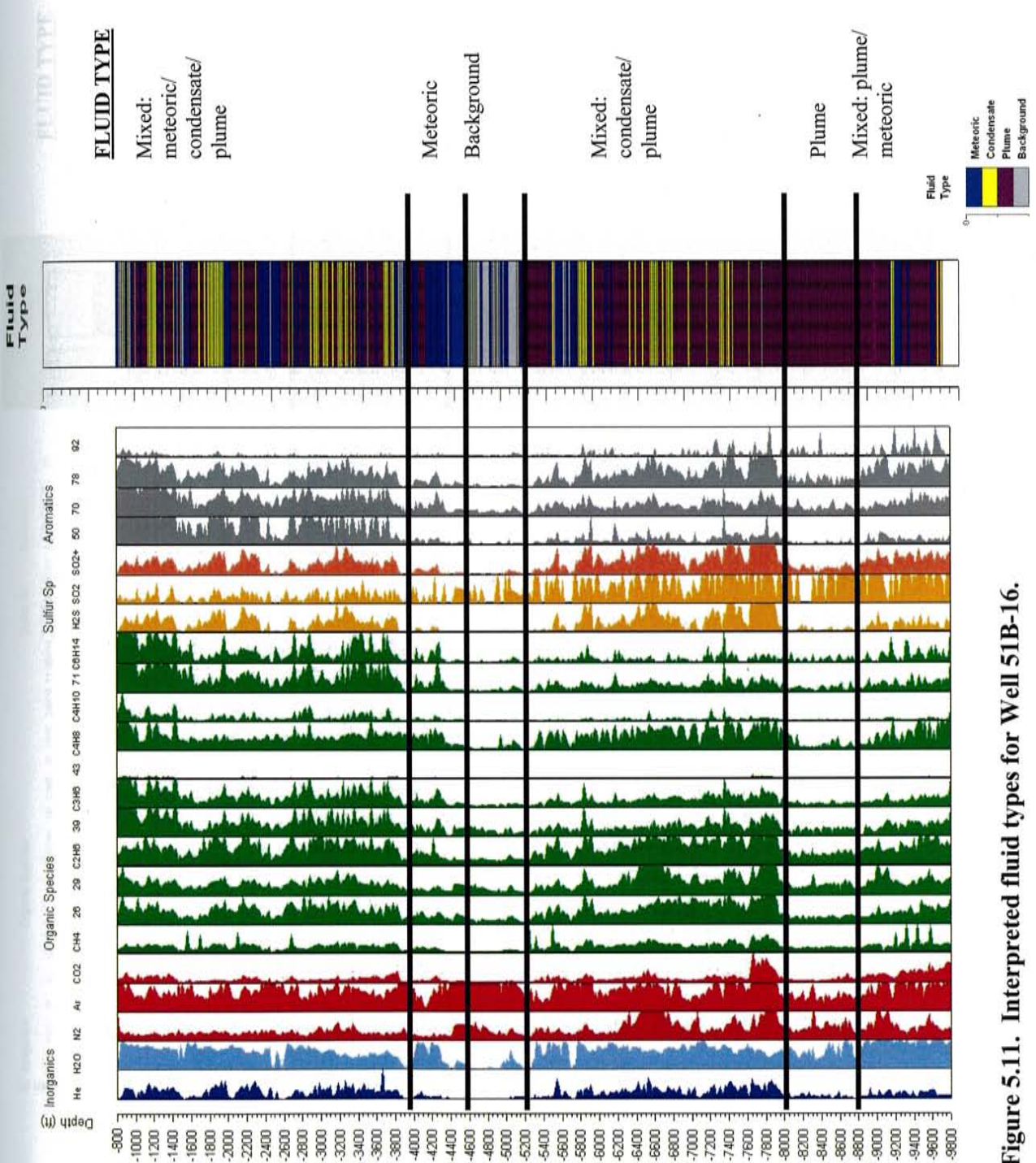


Figure 5.10. Interpreted fluid types for Well 38C-9.



FLUID TYPE

Mixed:
meteoric/
condensate/
plume

Meteoric
Background

Mixed:
condensate/
plume

Plume
Mixed: plume/
meteoric

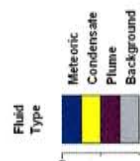


Figure 5.11. Interpreted fluid types for Well 51B-16.

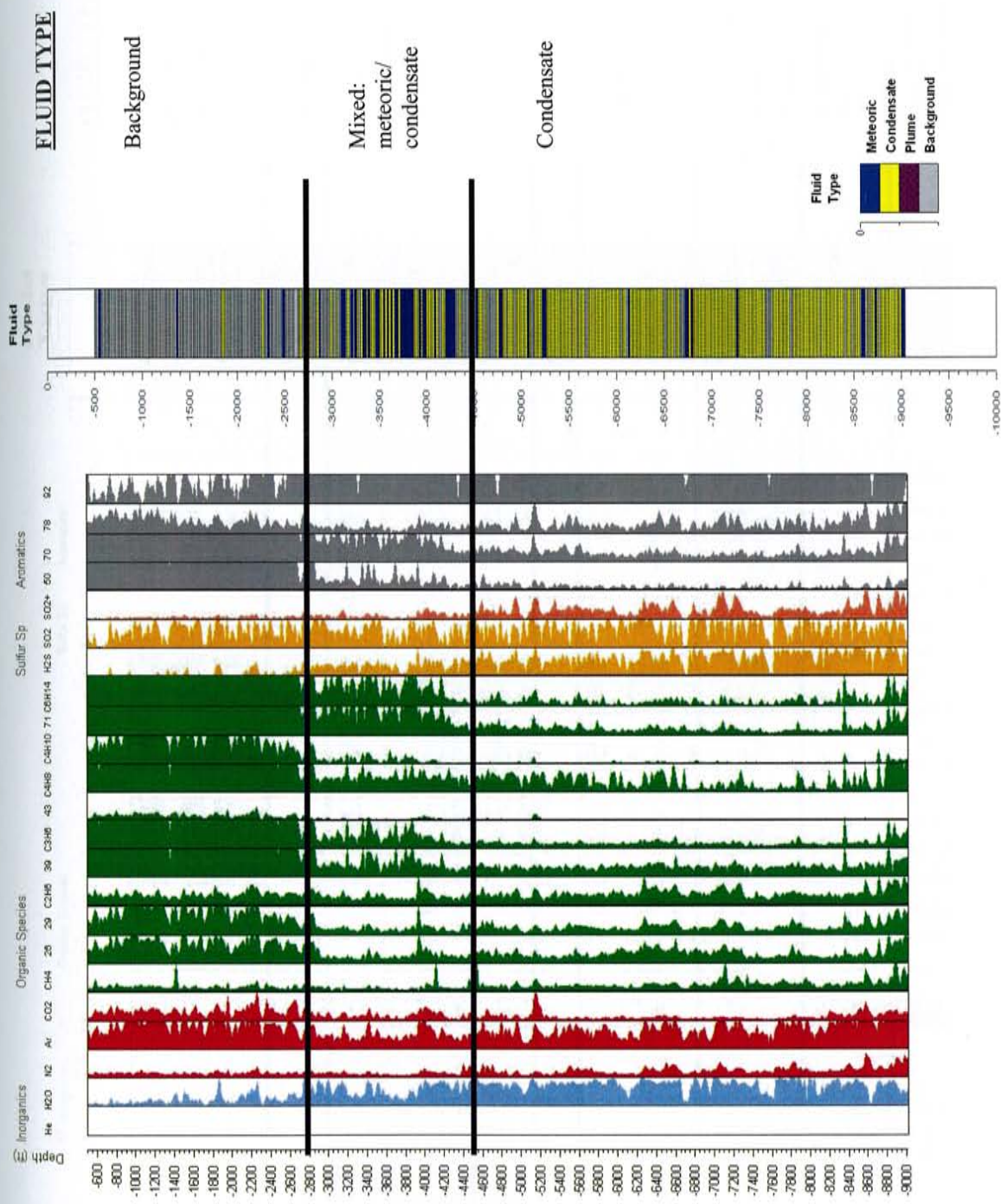


Figure 5.12. Interpreted fluid types for Well 67-17.

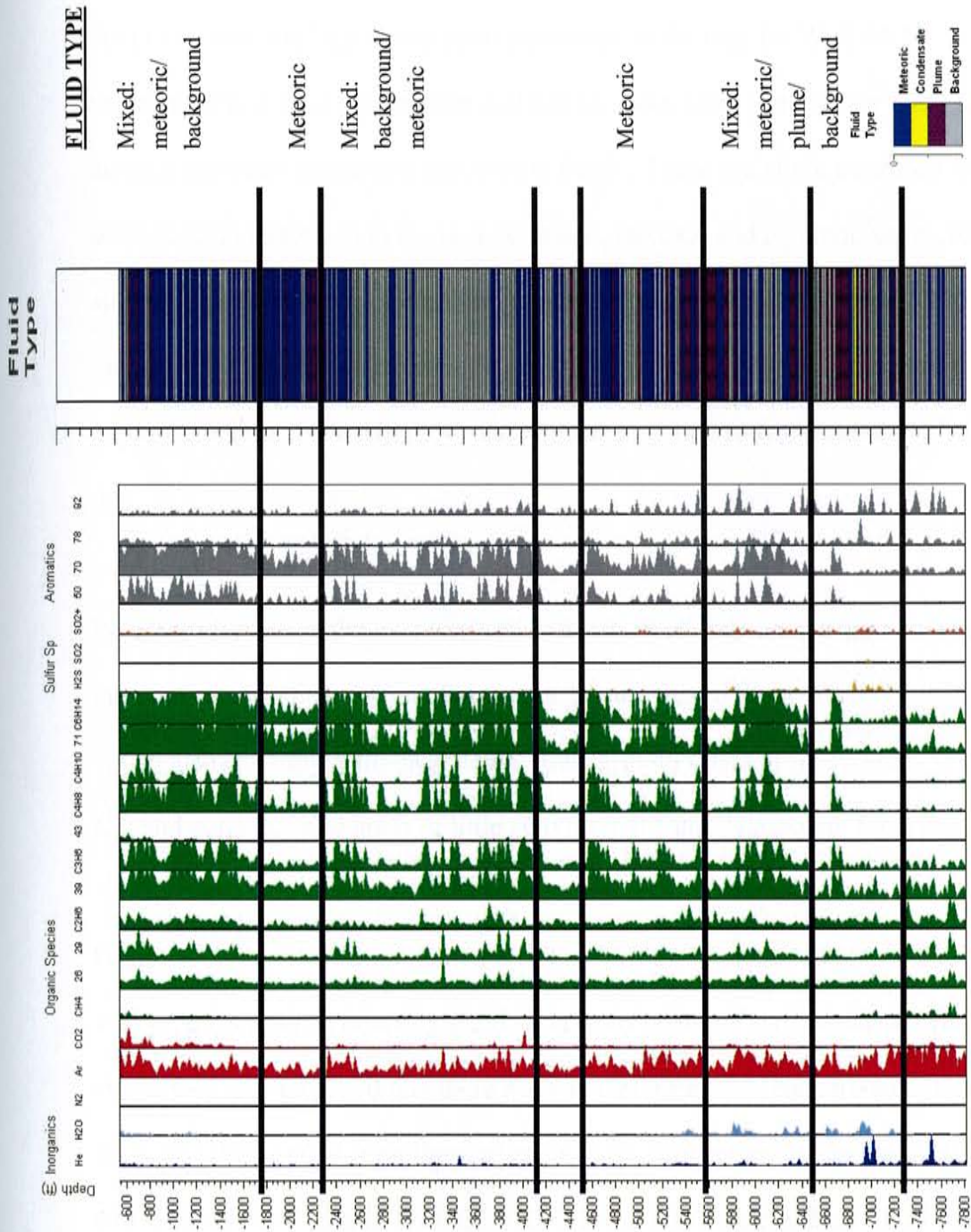


Figure 5.13. Interpreted fluid types for Well 84-30.

Well 38C-9 is located on the East Flank and is a 8 MW producer. Based on the previous discussions and breaks observed in Figures 5.1 and 5.9, Figure 5.10 presents the interpreted fluid types for this well. From the surface to approximately 7200 feet is a series of meteoric, condensate and mixed fluids. Background occurs from surface to about 800 feet; the logs in this zone are similar to the logs for Well 84-30. A mixed meteoric/plume zone occurs from 800 feet to about 4500 feet. Below 4500 feet the H₂S amount increases suggesting condensate fluids. There is a slight transition zone from 6600 to 7200 feet wherein the H₂S decreases, the CO₂ and N₂ amounts increase suggesting a mixed zone with plume fluids and meteoric fluids. Below 7200 feet, the mass spectra are interpreted as indicating plume fluids. Also note the general lack of organic compounds, and high N₂ and Ar peaks on the FIS log particularly below 7200 feet.

Figure 5.11 presents the logs for Well 51B-16. Well 51B-16 is a high enthalpy well and the fluid types indicate plume fluids at depth and mixed plume fluids throughout. Well 38C-9 also has similar fluids at depth. Background fluids occur between 4600 to 5200 feet and correspond to areas of little activity in the gas data except for argon.

Figure 5.12 presents the combined logs for Well 67-17 with interpreted fluid type. This well presents a series of background and mixed meteoric and condensate fluids. From the surface to about 2800 feet there is a zone interpreted as background. This zone is similar to Well 38C-9 from the surface to about 800 feet and occurs in Well 52-20 from 600 to about 3000 feet; in Well 67-17C to about 2000 feet; in Well 73-19 to about 2500

feet and throughout Well 84-30. There is a peak in the CO₂/CH₄ ratio and lack of water. This zone may represent a cap on the geothermal system where fluids can not move but gas (mainly CO₂) is present. The zone looks similar to Well 84-30 suggesting that this zone may represent the parent rock or background and not the geothermal system. CO₂/CH₄ ratio is high in the magmatic column to about 3000 feet and then decreases to barely there after 5500 feet. The crustal and condensate ratios below the background are high throughout the well indicating mixed fluids of condensate and meteoric which would be consistent with an injection well.

Figure 5.13 presents the combined logs for Well 84-30 the non-producer to the south of the field. The fluid log indicates that background and meteoric fluids occur throughout the majority of the well. These fluid types are consistent with a well that is non-producing and located on the margin or out of the field.

5.2. The CO₂/N₂ vs. Total Gas Diagram

The CO₂/N₂ versus Total Gas diagram was developed by Norman et al (2002) to illustrate boiling and condensation processes. Gas partition coefficients for CO₂ and N₂ are considerably different. As steam separates from liquid during boiling, gases such as H₂, N₂, and CH₄ preferentially move into the vapor phase. The more soluble gases, CO₂ and H₂S, stay partially in the liquid phase. A change in the ratio of CO₂ to N₂ would indicate that boiling had occurred. Fluids that have undergone different degrees of boiling have a negative slope on the diagram whereas the condensation trend is a positive slope.

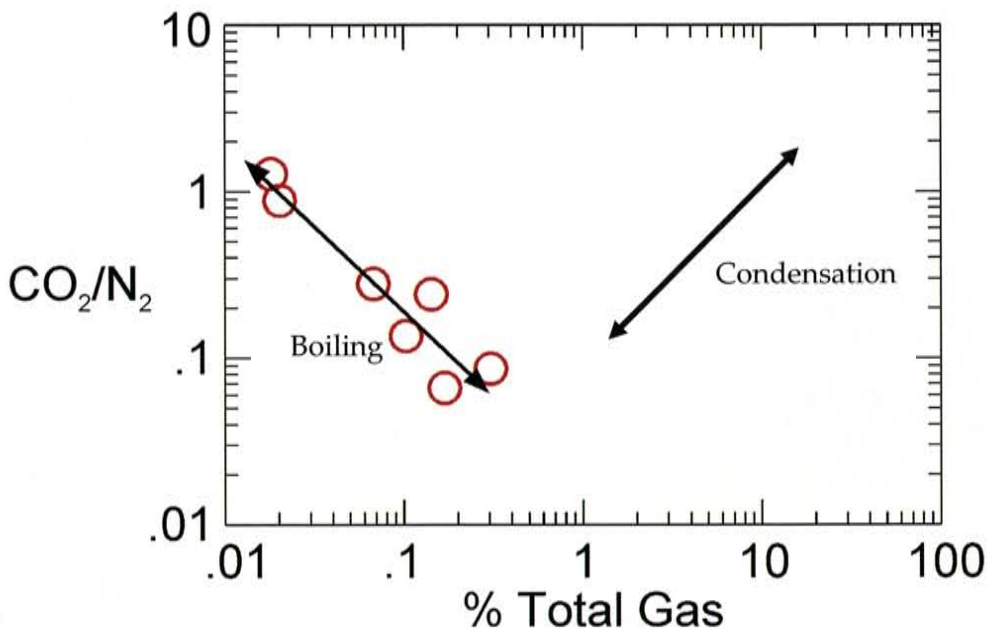
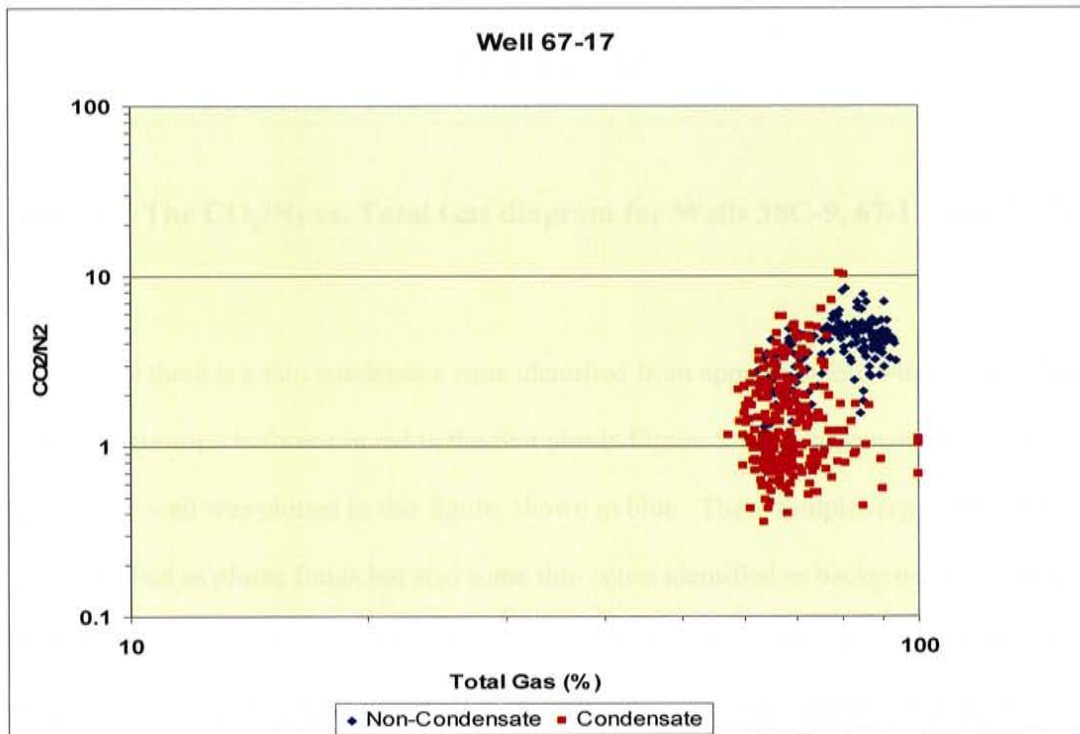
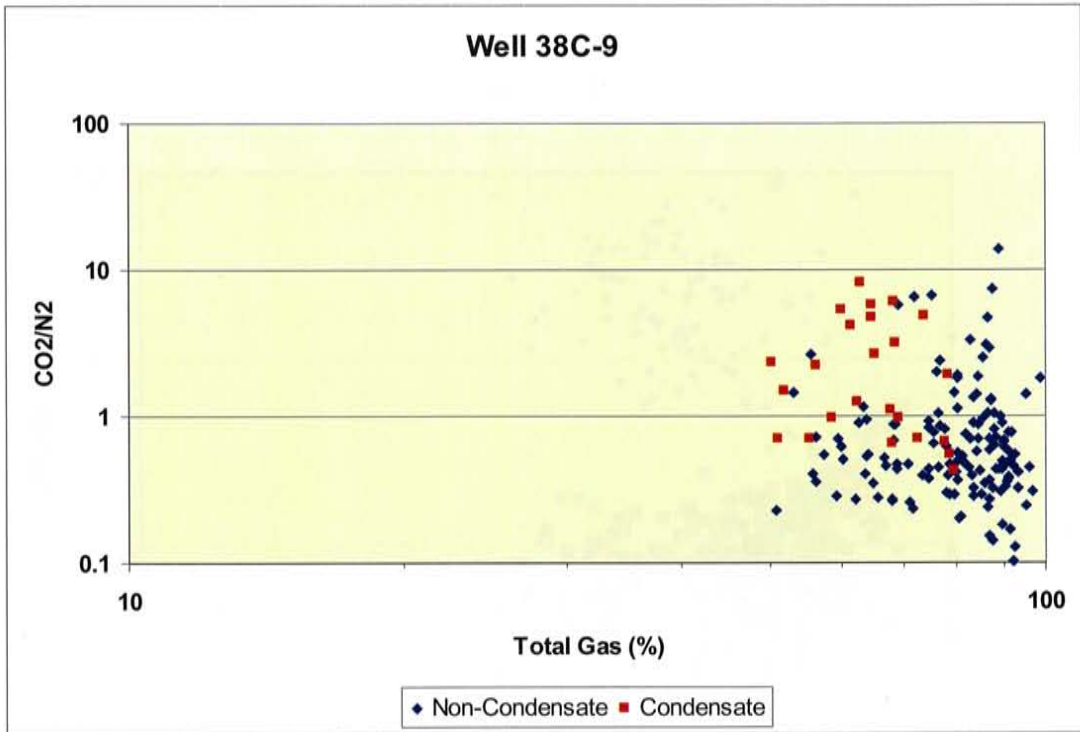


Figure 5.14. The CO_2/N_2 vs. Total Gas Diagram. Boiling trends plot with a negative slope whereas condensation trends plot with a positive slope, Norman et al (2002).

This diagram was used to determine if the condensate zones identified in the Coso Wells in Figures 5.7 through 5.9 would show a condensation trend. The zones identified as condensate were plotted in Figure 5.15 for Wells 38C-9, 67-17, and 33-7. Non-condensate zones were also plotted on the same figure to determine if these zones showed a separate population from the samples that were identified as condensate fluids.

Although FIT analysis is qualitative it is still useful to see if the condensate or boiling trend may occur in the data. Exact numbers for the % total gas and the ratio could not be obtained due to the qualitative nature of the FIT analysis particularly for water.



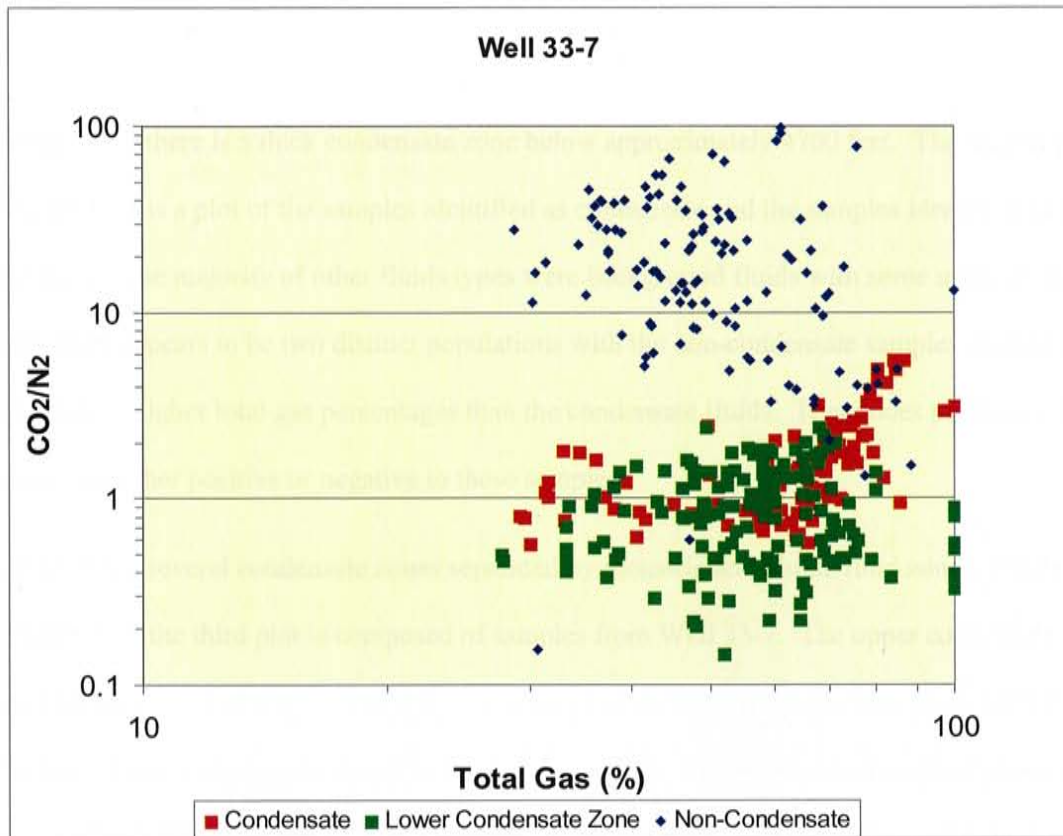


Figure 5.15. The CO₂/N₂ vs. Total Gas diagram for Wells 38C-9, 67-17, and 33-7.

In Well 38C-9 there is a thin condensate zone identified from approximately 5400 to 5800 feet. This condensate zone is shown in red in the first plot in Figure 5.15. The remainder of the samples in the well was plotted in this figure, shown in blue. These samples represent a zone mainly identified as plume fluids but also some thin zones identified as background and meteoric fluids. There appears to be two distinct populations however the condensate samples are not entirely separate from the other fluid types that were plotted. The few samples that are shown in blue near the condensate samples may represent thin condensate zones or the background fluid

within the other fluid types plotted. The background fluids tended to have high total gas concentration. There does appear to be a slight positive trend line to the condensate samples.

In Well 67-17 there is a thick condensate zone below approximately 4700 feet. The second plot in Figure 5.15 is a plot of the samples identified as condensate and the samples identified as other fluid types. The majority of other fluids types were background fluids with some meteoric zones. Again there appears to be two distinct populations with the non-condensate samples tending to have slightly higher total gas percentages than the condensate fluids. There does not appear to be a trend line either positive or negative to these samples.

Well 33-7 has several condensate zones separated by meteoric and plume fluid zones, Figure 5.7. In Figure 5.15 the third plot is composed of samples from Well 33-7. The upper condensate zone from 1500 to 3500 feet was plotted with the removal of the thick meteoric zone from 2400 to 2700 feet. These samples are shown in red on Figure 5.15. The intermediate zone of plume and meteoric fluids from 3500 to about 6700 feet were plotted in blue on the diagram and the lower condensate zone was plotted in green. The two zones identified as condensate plot within in the same area on the diagram and appear to represent one population. The zone identified as plume and meteoric fluids plot as a separate population. The condensate samples also appear to have a slight positive slope.

The CO₂/N₂ versus total gas diagram indicates that the Coso fluids appear to have distinct populations with those zones identified as condensate by the FIS method plotting in the same area on the diagram with slight positive trend. In addition, the fluids identified as background fluids appear to plot as a separate population with high total gas and that plume and meteoric fluids appear as a distinct population from the condensate samples.

5.3. Comparison to Temperature Logs

Temperature logs are a primary source of data from any well. Hotter zones are considered target areas for production. Values for two ratios, N_2/Ar , and CO_2/CH_4 , were plotted against temperature for four wells, 38C-9, 51B-16, 33-7, and 46A-19. This represents over 1,100 data points. From the literature reviewed, N_2/Ar and CO_2/CH_4 ratios should be high at higher temperature. Figure 5.16 presents the correlation of the temperature with each of the ratios.

General trends indicate that although there is not a linear correlation, the highest values for N_2/Ar and for CO_2/CH_4 occur only at hotter temperatures. In each of the graphs there is also a cluster of data along the base of graphs. Plotting the ratios with depth for the wells shows a scattering of higher values at select depths (Figure 5.17) such as in Well 38C-9 below 3,000 feet in general and in particular from about 7,000 to about 8,500 feet. Wells 51B-16 and 46A-19RD also show distinct zones of high N_2/Ar and CO_2/CH_4 , respectively. These discrete zones suggest that the high values for the ratios are based on fracture locations and that the majority of the values obtained are from the wall rock.

Wells

When the FIS and fluid source logs are plotted versus the temperature logs (Figures 5.18 through 5.20, and Appendix C) it can be seen that the wells that are interpreted to have mixed and/or plume fluids have temperatures above the production temperature of $480^{\circ}F$ ($250^{\circ}C$). Zones that have temperatures above this range also tend to have high N_2/Ar and/or CO_2/CH_4 ratios at select depths in those zones.

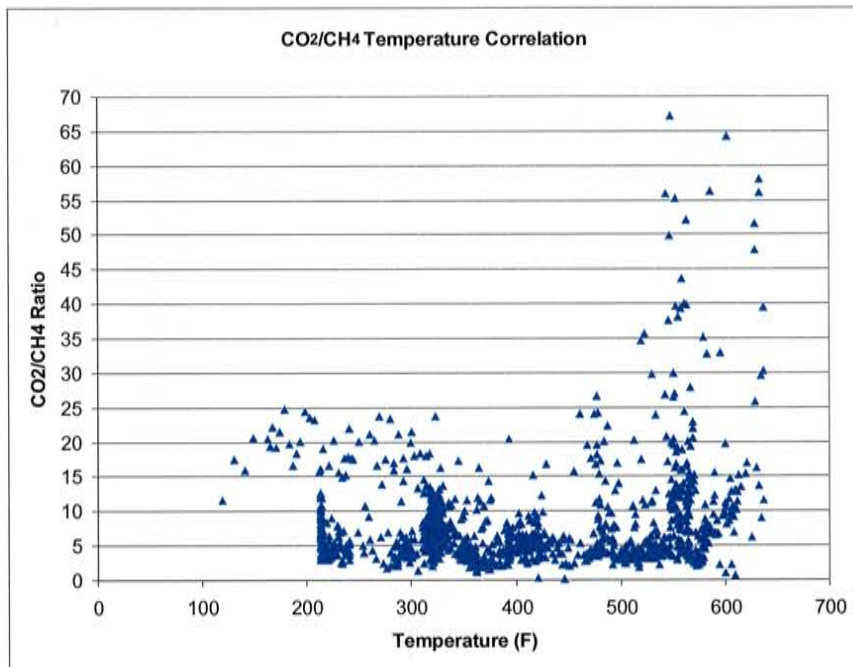
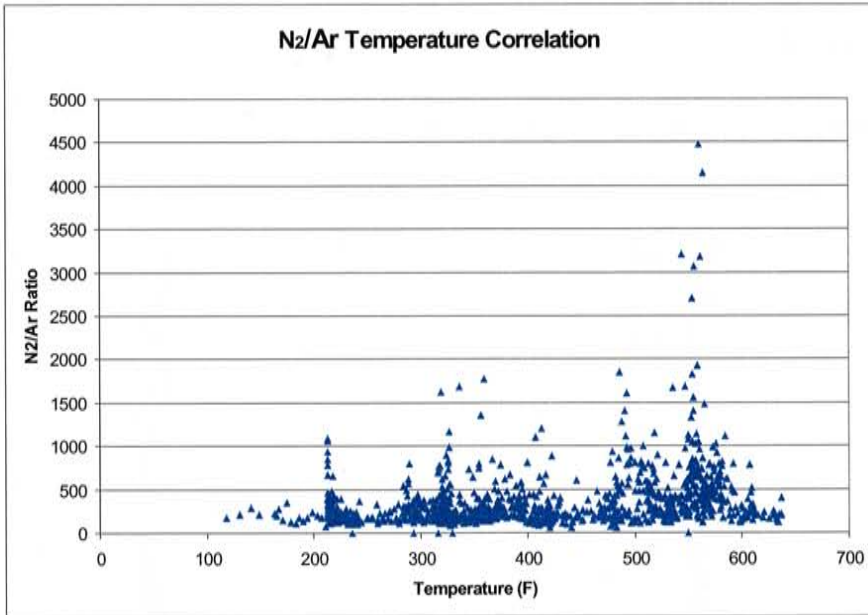
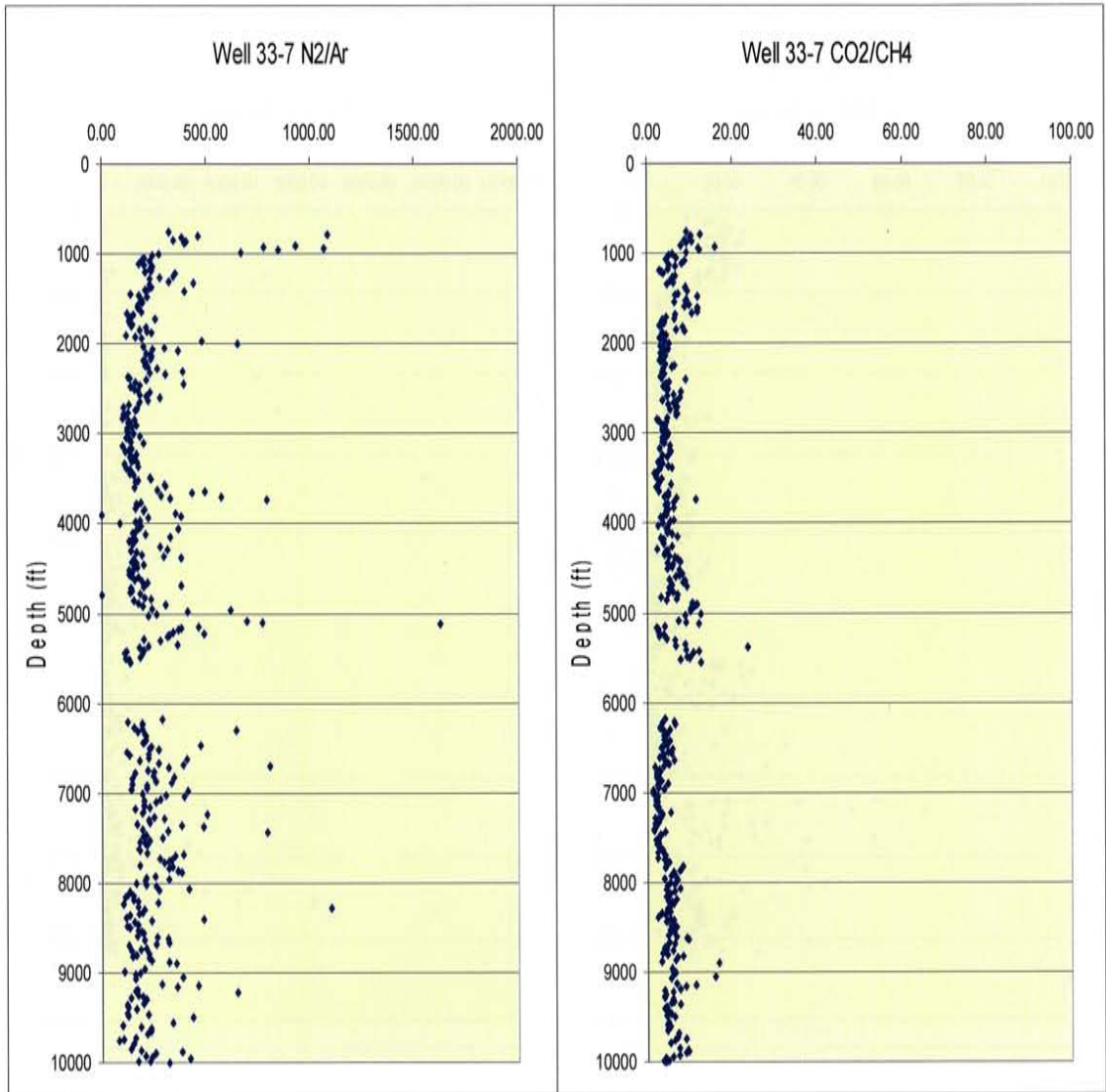
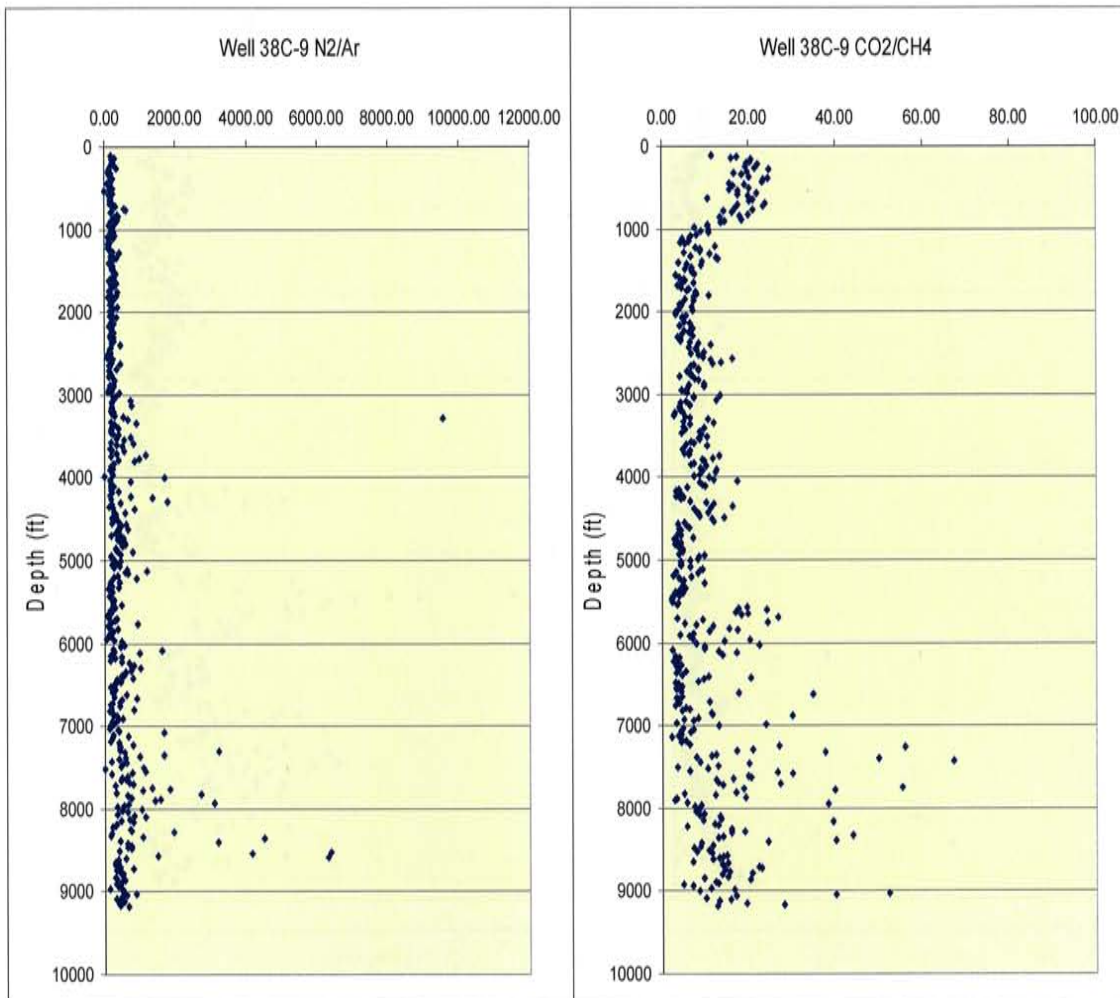
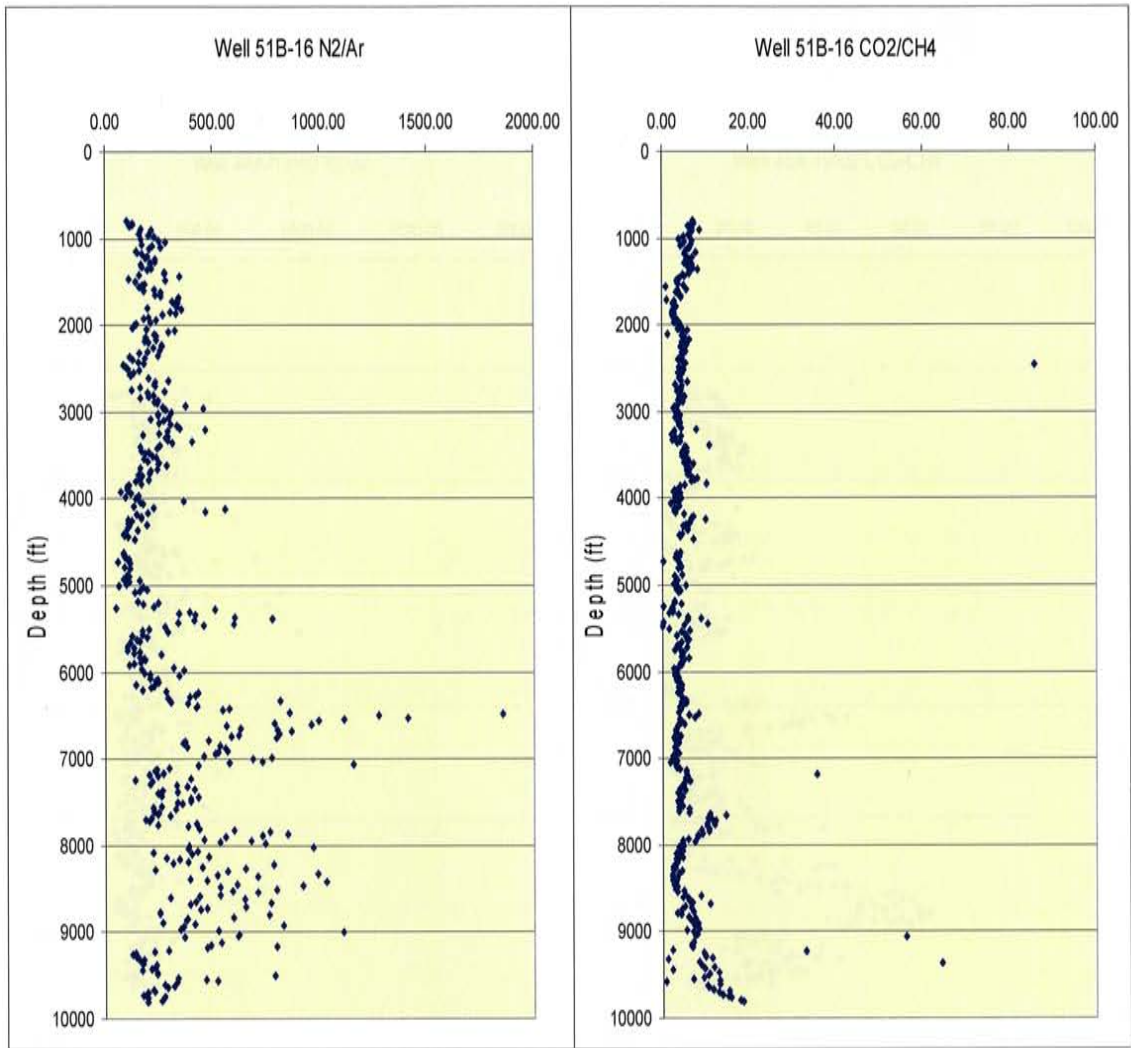


Figure 5.16. Correlation of ratios with temperature. Note for N₂/Ar and CO₂/CH₄ there are higher ratios only with higher temperatures. Low ratios exist throughout the range of temperatures.







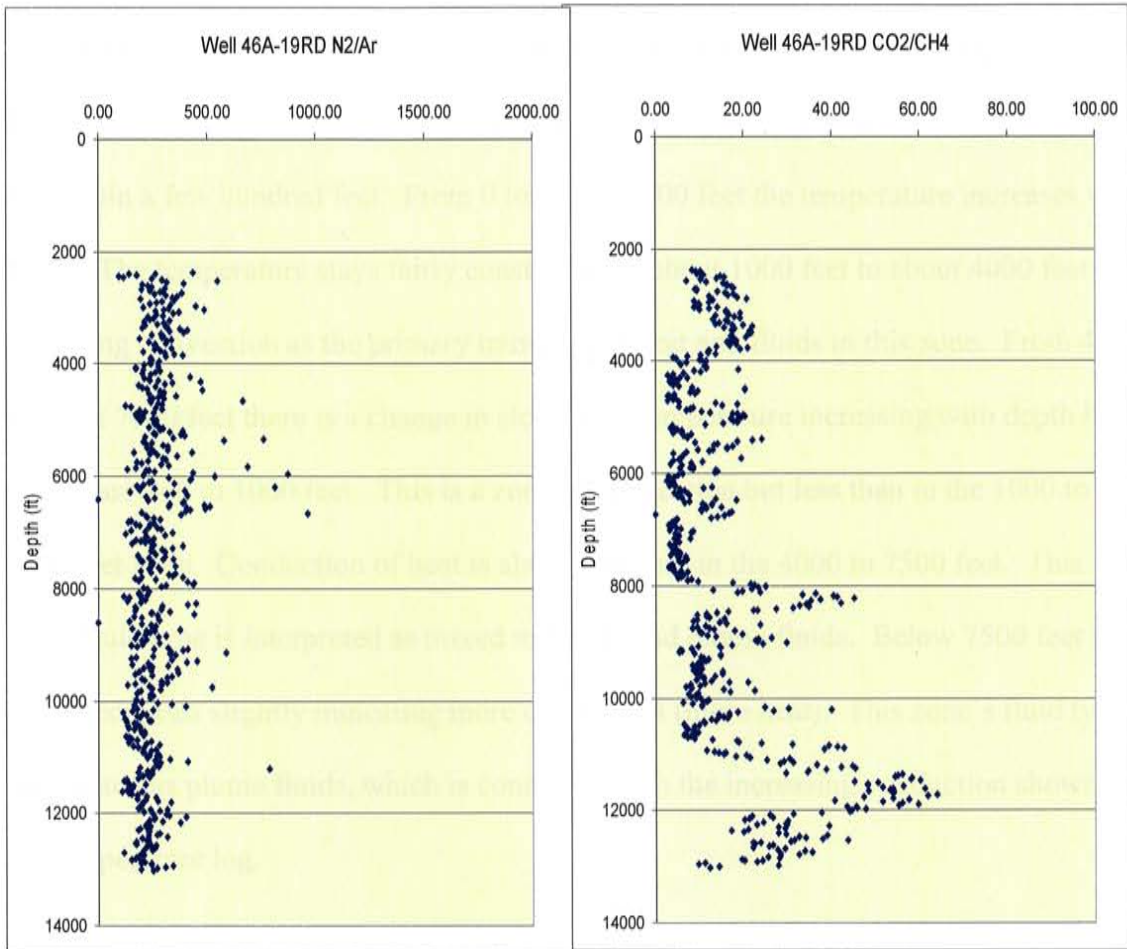


Figure 5.17. N_2/Ar and CO_2/CH_4 ratios versus depth for four wells. High values for ratios may correspond to fractures.

Interpreted fluid types generally correspond to changes in the temperature log for Well 38C-9 (Figure 5.18). The breaks interpreted for fluid types correspond to the temperature log within a few hundred feet. From 0 to about 1,000 feet the temperature increases with depth. The temperature stays fairly constant from about 1000 feet to about 4000 feet indicating convection as the primary transport of heat and fluids in this zone. From 4000 to about 7500 feet there is a change in slope with temperature increasing with depth but not as fast as 0 to 1000 feet. This is a zone of convection but less than in the 1000 to 4000 feet zone. Conduction of heat is also increasing in the 4000 to 7500 feet. This zone's fluid type is interpreted as mixed meteoric and plume fluids. Below 7500 feet the slope decreases slightly indicating more conduction (more heat). This zone's fluid type is interpreted as plume fluids, which is consistent with the increasing conduction shown on the temperature log.

The FIS logs and temperature logs for Well 51B-16 are presented in Figure 5.19. The temperature log increases with temperature as indicated by flatter slopes in those zones with plume fluids. In those zones with meteoric fluids and background the temperature has a limited increase indicating convection as oppose to conduction.

Figure 5.20 presents the temperature log and FIS logs for Well 67-17. A significant break occurs in the temperature log between 2400 to 2800 feet. Below 2800 feet, the temperatures remain relatively constant at about 350°F, with only a slight increase with

depth. At 2800 feet the FIS logs show a significant change in chemistry with increase in H₂O and decrease in organics. The fluids are interpreted to be background to 2800 feet and then a series of meteoric and condensate fluids.

Appendix C contains the temperature logs versus FIS logs for the other wells. Breaks in the temperature logs roughly correspond to changes in gas chemistries. Changes in gas chemistries will most likely be most pronounced in fracture locations. The temperature logging device may lag behind in recording these exact fracture locations and thus the breaks in temperature logs only roughly correspond to changes in gas chemistries. In addition, hotter fluids will tend to heat up the surrounding wall rock over time.

Temperature logs are typically run over several days and pumping rates in order to obtain accurate temperature profiles. The influx of hot fluids into a zone that is already at a high temperature may not show up on temperature logs as discrete increases in the log.

Wells that have been interpreted to have thick zones of plume fluids correspond to temperature logs that have indicated high well temperatures. Low temperature wells tend to have little to no plume fluid zones.

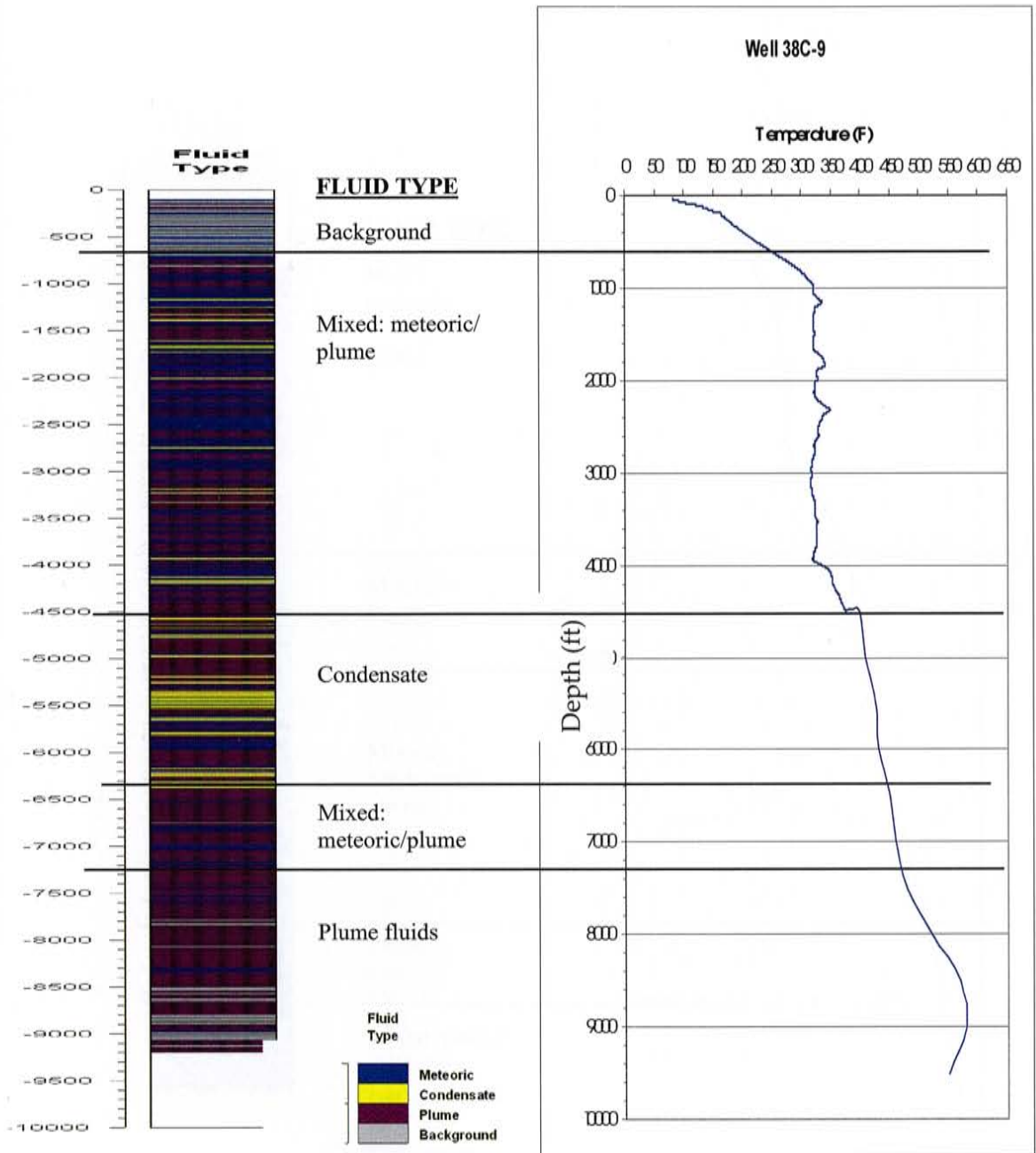


Figure 5.18. Temperature log versus FIS logs for Well 38C-9. Note correlations between changes in all the logs.

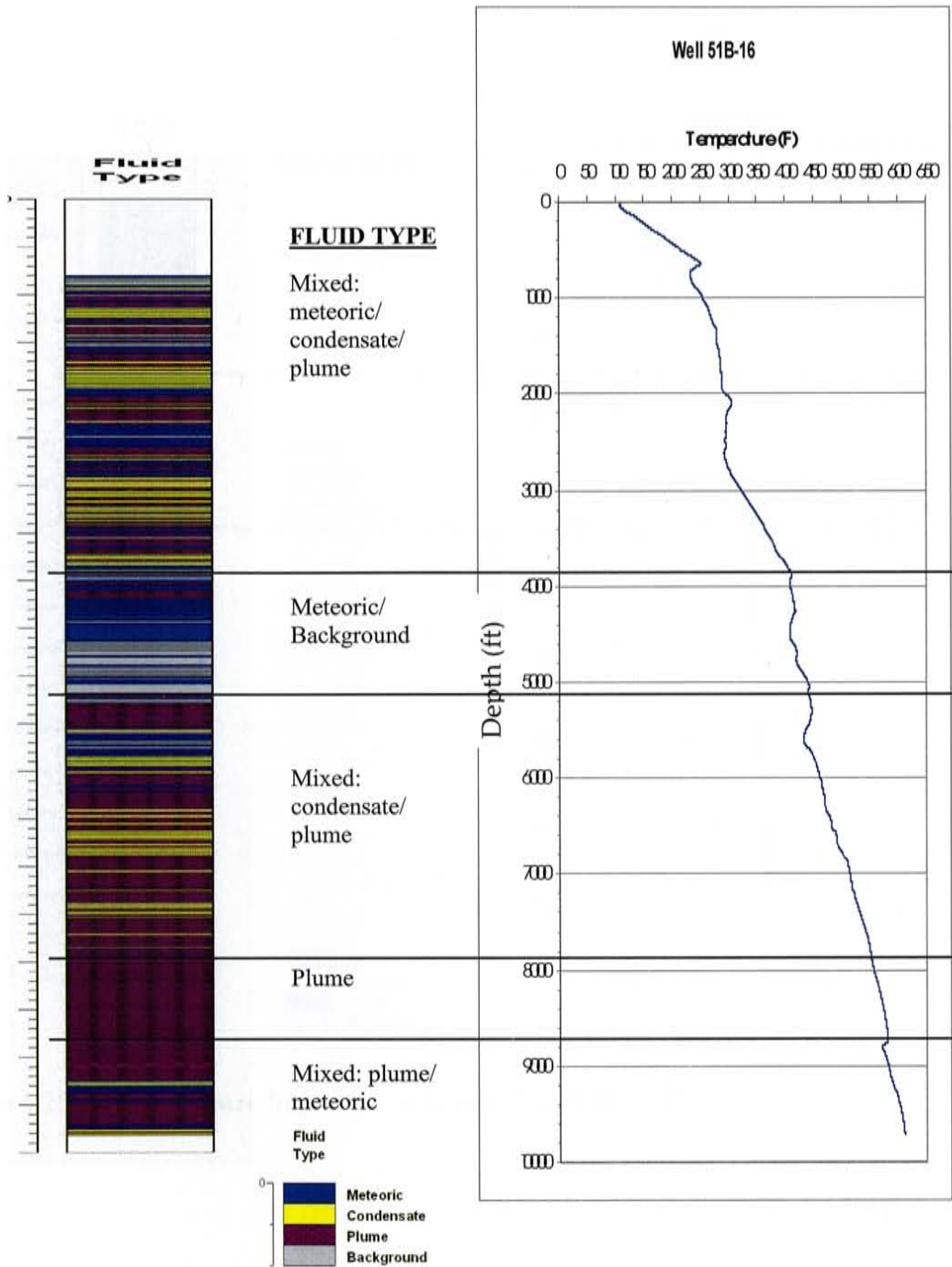


Figure 5.19. Temperature log and FIS logs for Well 51B-16.

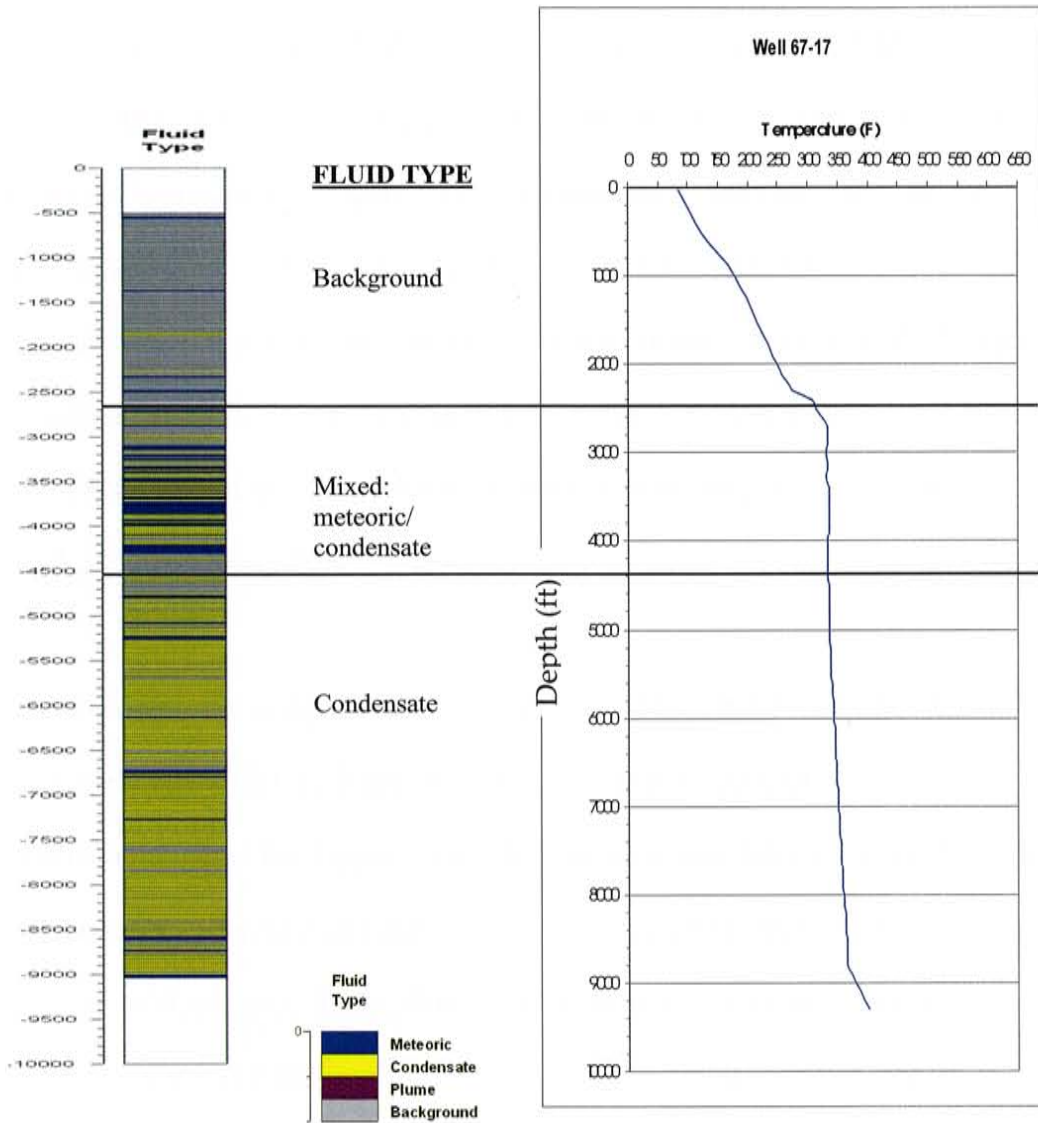


Figure 5.20. Temperature log versus FIS logs for Well 67-17.

5.4. Correlation with Rocks and Veins

Kovac et al. (2005) conducted a petrologic and geologic investigation of Well 34-9RD2. Kovac et al. (2005) produced a rock type log from observations of drill cuttings and thin sections which is presented in Figure 5.21. Dominant rock types are quartz diorite, granodiorites and granite. The major alteration mineral is calcite, followed by hematite, clay, and chlorite. If the rock types correspond to the changes observed in the FIS data, then the data are recording in part the rocks and not the fluids in the system. If the rock types do not correspond directly with the FIS data, then the data is recording mainly the effect of the fluid on the system.

Figure 5.21 presents the comparison of rock types, vein mineralogy with the fluid logs developed for Well 34-9RD2. It can be seen that there is no correlation between the rock types and the interpreted fluid types. From 4000 to 5000 feet, there are three different fluid types and six different rock types. There is no correlation between the rock types recorded and the fluid types. From 5000 to 6800 feet is a thick layer of granite with two different fluid types. The occurrences of the fluid types do not correlate with minor rock types observed in the granites. This lack of correlation indicates that FIS data is based on the geothermal fluids and not just on the rock types observed.

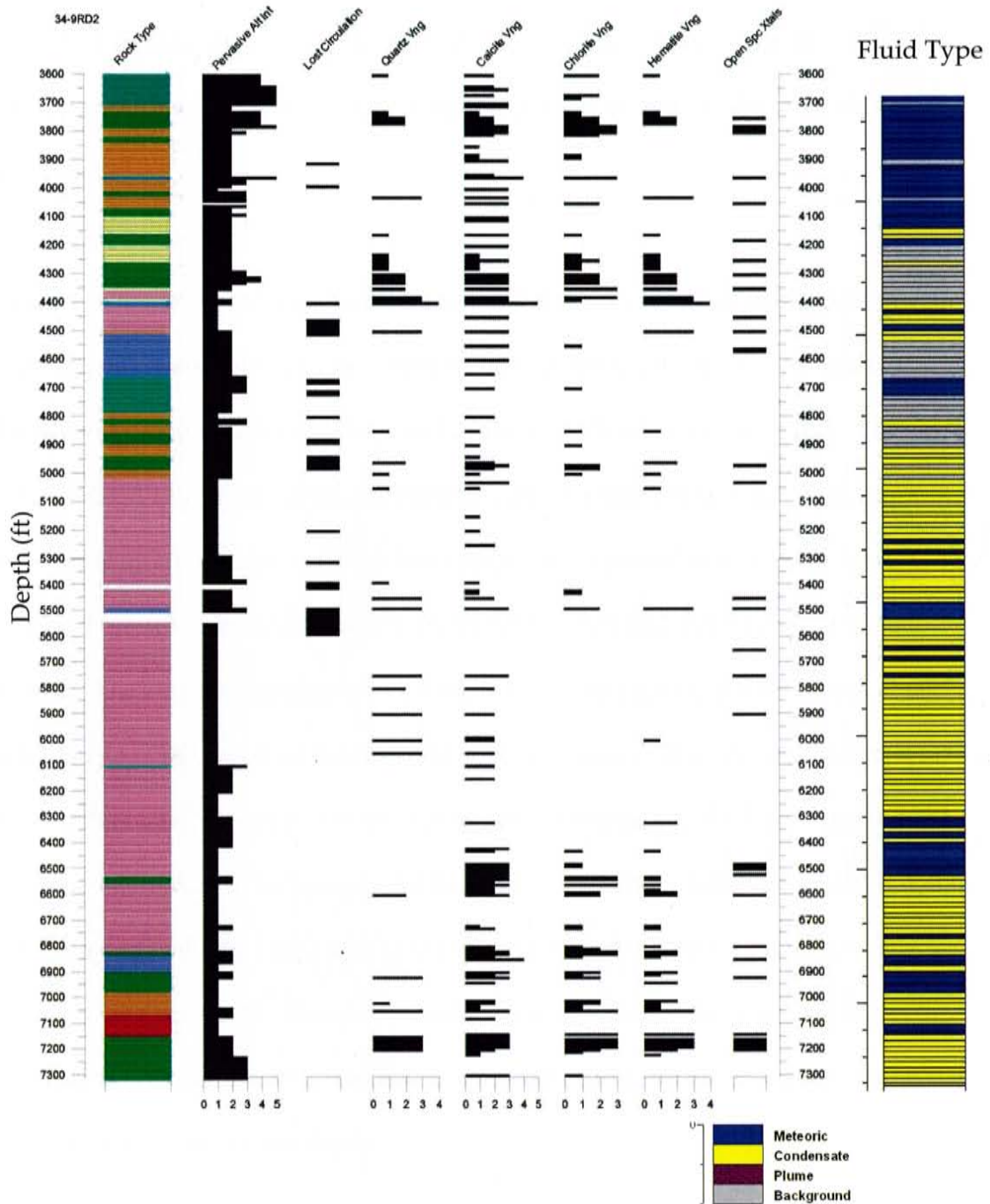


Figure 5.21. Rock types plotted with gas analyses for Well 34-9RD2. Rock types are coded as follows: greens/yellow- diorites, orange-granodiorite, pink-granite, red-microgranite, purple-metasediments, and blue-massive veining. Fluid types are: blue – meteoric, yellow – condensate, grey - background

Vein assemblages should correlate to some degree with FIS signatures if the vein minerals were deposited during the geothermal event. In addition, if peaks in the FIS data represent fractures then the vein assemblages and location of the veins should correspond.

Calcite is a major secondary mineral throughout the Coso reservoir and occurs in vein assemblages consisting of calcite, hematite, and chlorite; with calcite and quartz intergrown, which indicates boiling; and as calcite with several generations. The assemblage of calcite, hematite, and chlorite indicates recharging, cool, oxidizing waters. Hematite (Fe_2O_3) contains oxidized iron compared to reduced iron in pyrite (FeS_2). The zones interpreted as meteoric fluids correspond to zones with calcite, hematite, and chlorite. The zones interpreted as condensate fluids particularly the zone from about 5,000 feet to 6,300 feet does not have many vein minerals. The few vein minerals tend to occur at thin zones interpreted to be meteoric fluids within this thick condensate zone. The zone interpreted to be background fluid type, from about 4,200 feet to about 4,400 feet, has quartz veining along with calcite, hematite, and chlorite. Quartz typically will precipitate above 300°C . The quartz could represent older, hotter temperatures at this zone and the calcite, hematite, chlorite assemblage represents the cooler, oxidizing waters of the current system at this depth.

The correlation of vein mineralogy with fluid type is further evidence that the peaks in the FIS mass spectra represent fractures, and is recording the geothermal system and not the existing rocks.

5.5. Timing of Fluid Inclusions

The graphs presented for the differences in Wells 68-20 and 68-20RD in Section 4.4 argue that the FIS analyses of the wells at the Coso field are seeing the modern system. The increase of more than 100 percent change in the H₂O and CO₂ ratios at the break in the casing indicate that the inclusions are being replaced. The overall average concentration has changed as well as shown in Figure 4.20. Some of the change seen in the average concentrations may be due to FIT's precision but in particular the change at the break in the casing is significantly higher than the error calculated on FIT's analysis (see Table 7). In addition, FIT can process 565 samples in one batch run. The two wells, 68-20 and 68-20RD were submitted as one batch. Errors that would have been produced between batch runs did not occur with this group of data.

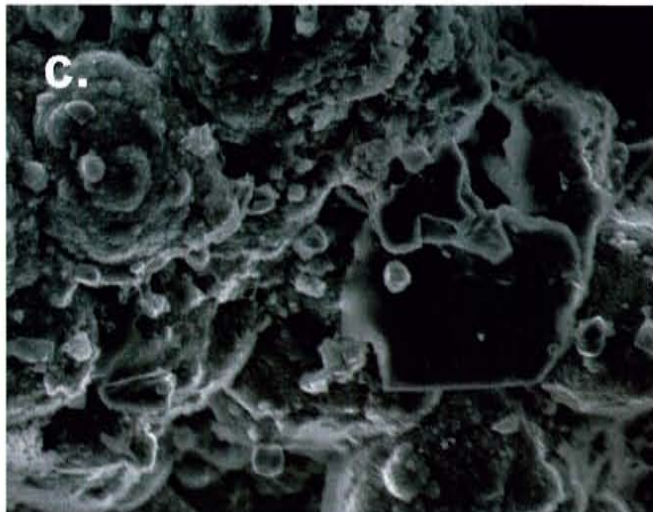
The log of Well 68-20RD in Figure 4.19 shows an increase in various chemical species peaks compared to those observed in Well 68-20. Although the concentration of various species from the geothermal system is lowered during the flashing process, the differences seen in the wells suggest that there is still some concentration of these gaseous species particularly CO₂, N₂, and CH₄. The changes in the bulk fluid inclusion chemistry from one that shows significant peaks of CO₂, N₂, and CH₄ to a more subdued log with less significant peaks of these compounds indicate that fluids within the newer well are creating new fluid inclusions that are overprinting the older fluid inclusions.

The largest changes in the ratios occur at depths of fluid injection identified by FIS analyses and petrographic study of drill cuttings that show abundant secondary minerals. The changes also drop off with depth of the well, further suggesting that the changes are a result of the injection water creating new fluid inclusions and destroying the geothermal gas fluid inclusions. The discrete peaks are assumed to represent fractures that dip, controlling the flow of injection fluid. Fractures in Coso are generally steeply dipping (Unrh and Hauksson 2006). The re-drill and the original are at most 150 feet away from each other and the steeply dipping fractures would allow the injected fluid at about 2800 feet to travel down to the 4600-foot level, where there is a change in the relative concentrations. The fractures would not have to go through the full depth but rather could intersect at various levels. Based on stress and strain rates, cold water entering the hot rocks through the existing fractures would cause thermal fracturing of the rock with reopening of old inclusions and, as the cold water equilibrates with the hot water, deposition of minerals and creation of new fluid inclusions representing the injection events.

Figure 5.22 shows growth of new minerals in Well 68-20RD. These photographs show overgrowing of existing minerals with silica and destruction of smaller minerals and growth of new minerals (Moore & Norman, 2006). McLin et al. (2006) examined cuttings from both wells and concluded that due to the size and uniform shape, silica layers formed as a precipitate and further infilling of pore spaces occurred. The silica deposition was due to the silica concentration of the injected fluid. Amorphous silica which is not observed anywhere else in the Coso system was observed in this scale indicating high fluid environment.

A geothermal system, particularly one that is being exploited, is a dynamic environment. Small-magnitude earthquakes occur frequently, resulting in fractures of various dimensions opening and closing (Feng and Lees 1998). Fluid flows either naturally or by being pumped. Pressure, temperature, and chemical changes that occur as the fluid moves through the system lead to an environment of mineral dissolution, chemical movement, and mineral deposition. These minerals would naturally trap new, modern-day fluid inclusions. Older inclusions would be destroyed as older minerals are dissolved. If the older minerals are preserved then the older inclusions would not necessarily be destroyed. Based on the order of magnitude changes in both H₂O and CO₂ concentration at the break in the casing there appears to be enough volume of new inclusions to overprint the older inclusions and produce the change seen on the FIS logs.

Our data shows that geothermal fluid inclusions assemblages can change chemical compositions in a few years and that the changes in inclusion contents are most pronounced in areas of high fluid flux. Thus, bulk fluid inclusion gas analyses of drill cuttings show chemistry of recent fluids. An implication is that all types of geothermal-system bulk-geochemical analyses will be biased toward the most recent hydrothermal event, the last changes in the system.



Well 68-20RD Silica scale

— 10 μm

SEM images show aggregates of colloidal opal A spheres.

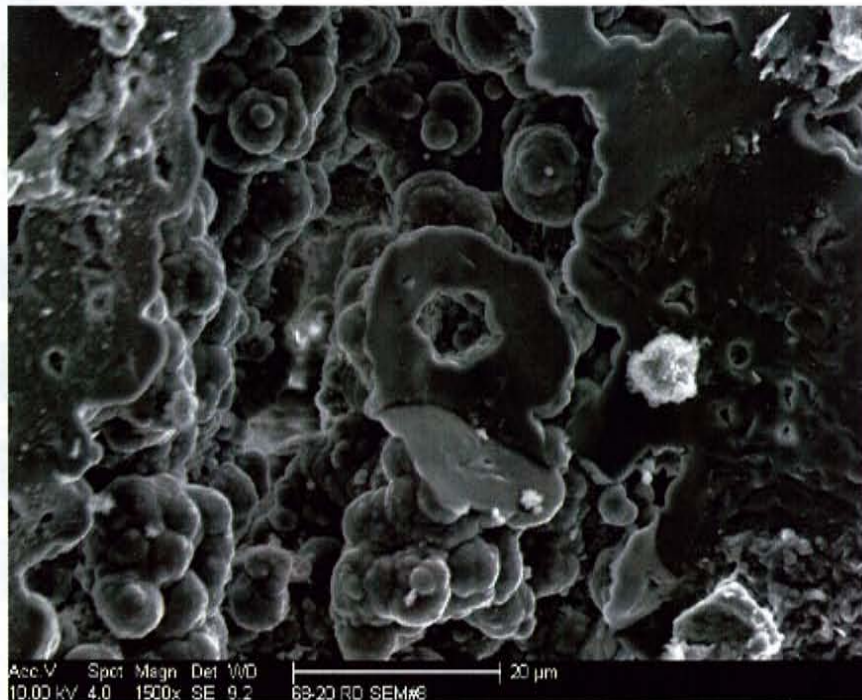


Figure 5.22. Photographs of scale in Well 68-20RD from Moore & Norman, 2006.

5.6. Fluid Models

A fluid model was developed for the Coso geothermal field using the fluid inclusion stratigraphy developed for each well. Several cross sections were prepared based on the well interpretations and compared to existing data. The legend for the all of the cross-sections is presented in Figure 5.23. The cross-sections are eastern, western, middle, southwest to northeast, and west to east (Figures 5.24 through 5.28, respectively). The locations of the cross-sections are shown with each figure.

LEGEND


	Background
	Mixed: Meteoric/Condensate/Plume
	Condensate
	Meteoric
	Mixed: Meteoric/Plume
	Mixed: Plume/Condensate
	Plume

Figure 5.23. Legend of fluid types for the cross-sections in Figures 5.24 through 5.28.

5.6.1. East Flank

Figure 5.24 presents a cross-section developed for the area of the field known as the East Flank. Four wells were studied from this area: 38C-9, 38D-9, 51B-16, and 34-9RD2.

Wells 38C-9 and 38D-9 are drilled right next to each other and both are considered moderate to large producers. Well 51B-16 has a high enthalpy but is a non-producer due to the lack of permeability. Well 34-9RD2 is currently an injection well.

It can be seen in Figure 5.24 that there is a large mixed meteoric fluid section. A background cap occurs from Wells 34-9RD2 to Wells 38C/D-9. Condensate occurs primarily in Well 34-9RD2. Below these zones are mixed plume and plume fluids. On the East Flank the plume fluids have high amounts of N₂ and CO₂ (Figure 4.12) which indicates that these fluids are possibly derived from magmatic sources. The production zone lies within the plume fluids.

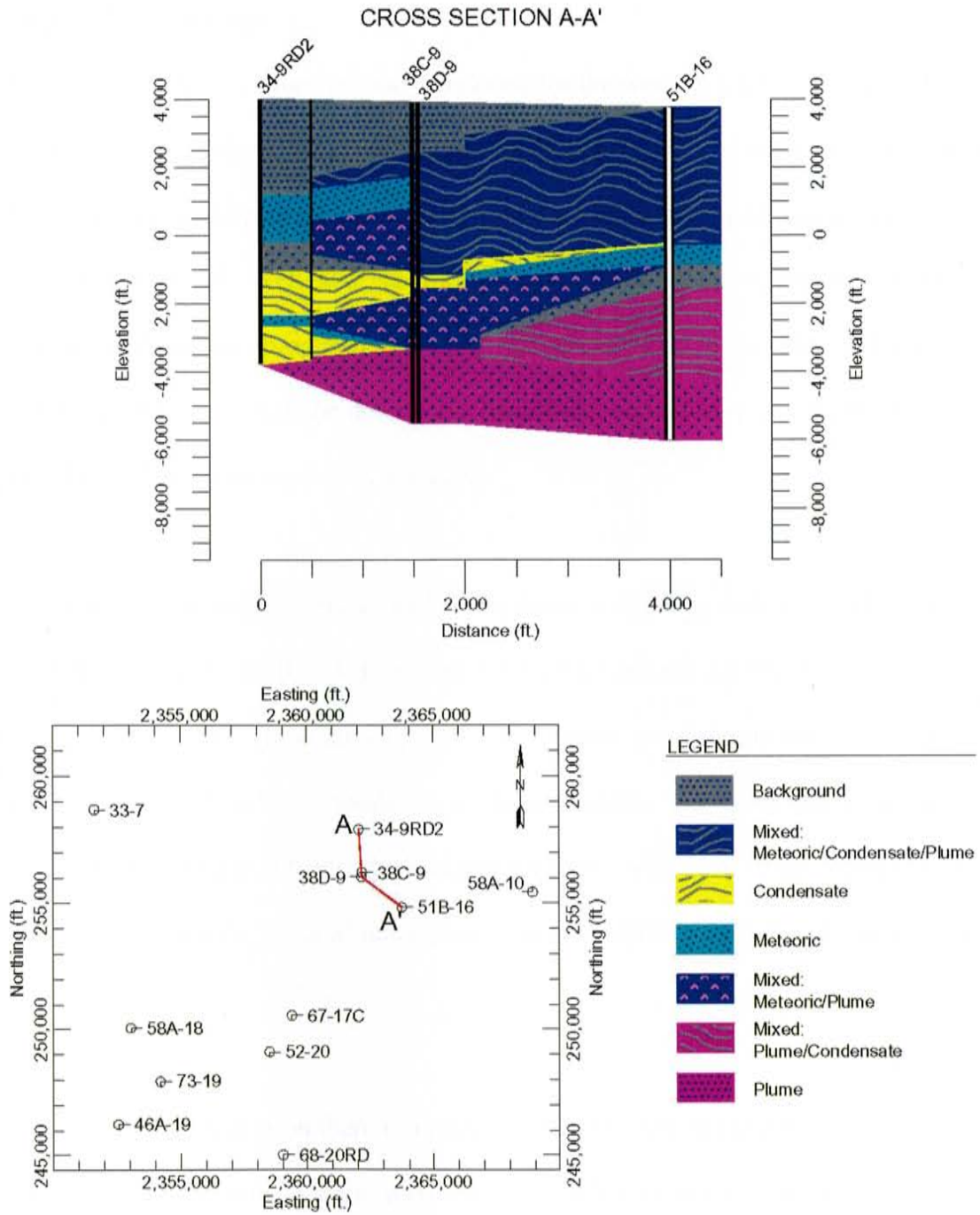


Figure 5.24. Cross-section of the East Flank with location map.

5.6.2. Western Edge

Figure 5.25 presents a cross-section developed for the western edge of the field. Four wells were placed along this cross-section: 33-7, 58A-18, 73-19, and 46A-19RD. Well 46A-19RD is the deepest interpreted well in the study, extending to approximately 9000 feet below sea level. Well 33-7 is a low enthalpy, 2-MW producer, and Well 46A-19RD is a high enthalpy non-producer. Well 58A-18 was included in the study to determine if cold water entrances could be determined from the fluid inclusion gas chemistry. Well 58A-18 is a low enthalpy, 4-MW producer.

The cross-section indicates the mixed plume fluids at depth in Well 33-7, which is a moderate producer. Well 46A-19 except for the background cap has mixed plume fluid throughout the well. These mixed plume fluids appear to move upwards to the north and Well 73-19. Well 73-19 is a moderate producer at depth. There is a zone of mixed plume fluids in this well below the background zone. Well 58A-18 has a couple of entrances of meteoric fluids which appear to be connected to the meteoric zones in Wells 33-7.

From the FIS cross-section there is a thicker zone of mixed condensate and condensate in the north. The FIS cross-section correlates well with the cross-section of homogenization temperatures and salinities shown in Figure 2.5 prepared from fluid inclusion studies conducted by Joe Moore and Dave Norman (Adams et al. 2000). The cross-section shown in Figure 2.5 indicates mixing on the north side and a plume rising from the south from near Well 73-19.

CROSS SECTION B-B'

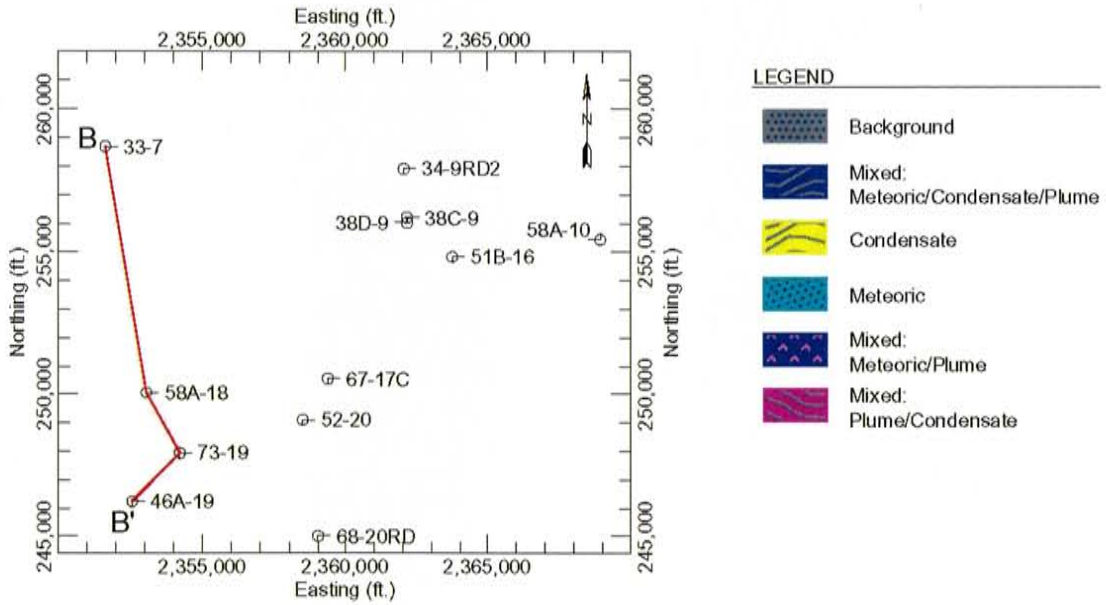
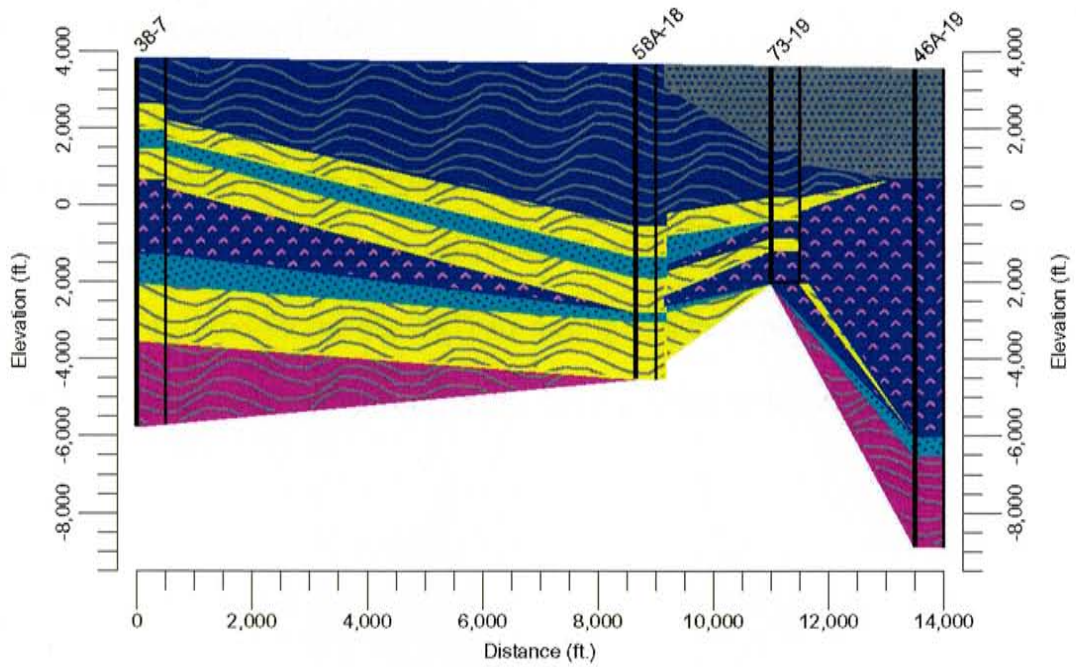


Figure 5.25. Cross-section based on FIS of the western edge of the Coso field with location map.

5.6.3. Middle of the Field

Figure 5.26 presents a cross-section for the middle of the field. Well 52-20 is a low enthalpy, 3 MW producer. The other wells in this cross-section are non-producers. The steam/condensate zone disappears to the south of the field and the background zone increases. Wells 68-20 and 68-20RD are near the southern portion of the producing field and the original well developed extensive scaling during its use as an injection well.

CROSS SECTION C-C'

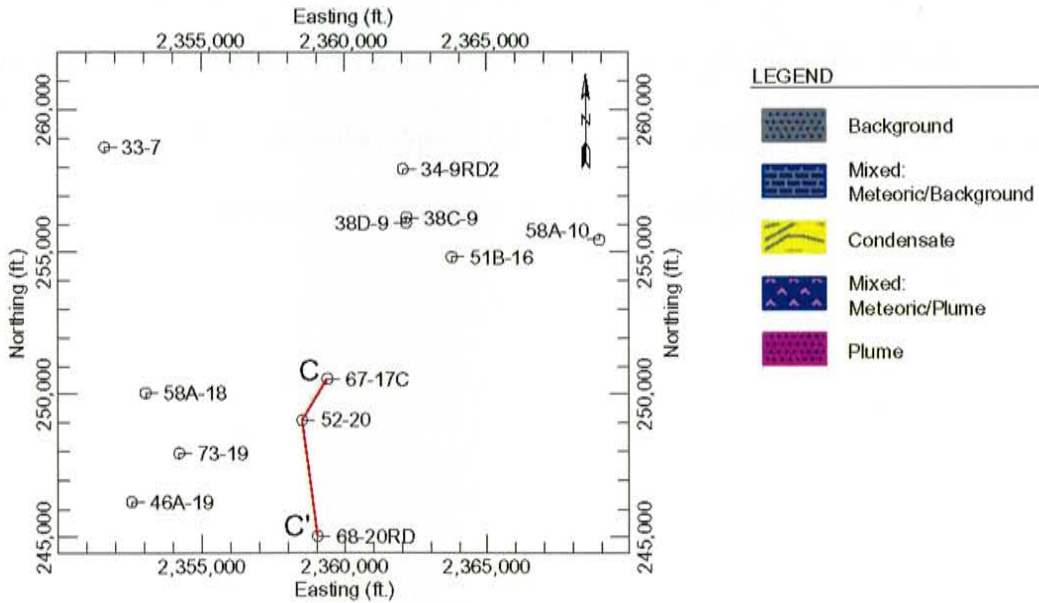
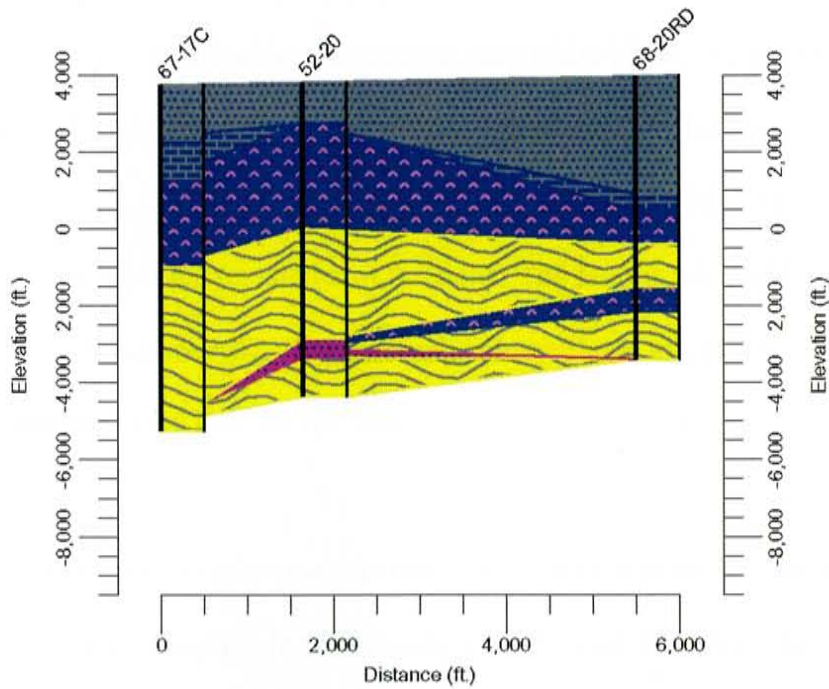


Figure 5.26. Cross section of the middle portion of the field with location map.

5.6.4. Across the Field

Figure 5.27 and 5.28 presents cross-section diagonally across the field from southwest to northeast and from west to east, respectively. Wells 38C-9, 38D-9, and 34-9RD2 are on the portion of the field known as the East Flank. A fault is thought to occur that separates the East Flank from the remainder of the field. The fault is not readily apparent in the cross-section in Figure 5.27. The rise in the plume fluids towards the East Flank and towards the west may indicate the fault.

Figure 5.28 is a west to east cross-section. Well 58A-10 is on the extreme eastern edge of the field and as shown in the cross-section, the plume fluid zone dips to approximately 12,000 feet. The domed nature of the geothermal system is evident in this cross-section with the well on the east flank having a slightly deeper plume zone. Fluids determined for Well 58A-10 are probably typical for a well located on the margins of a geothermal field with thick zones of meteoric and mixed fluids and deep plume fluids.

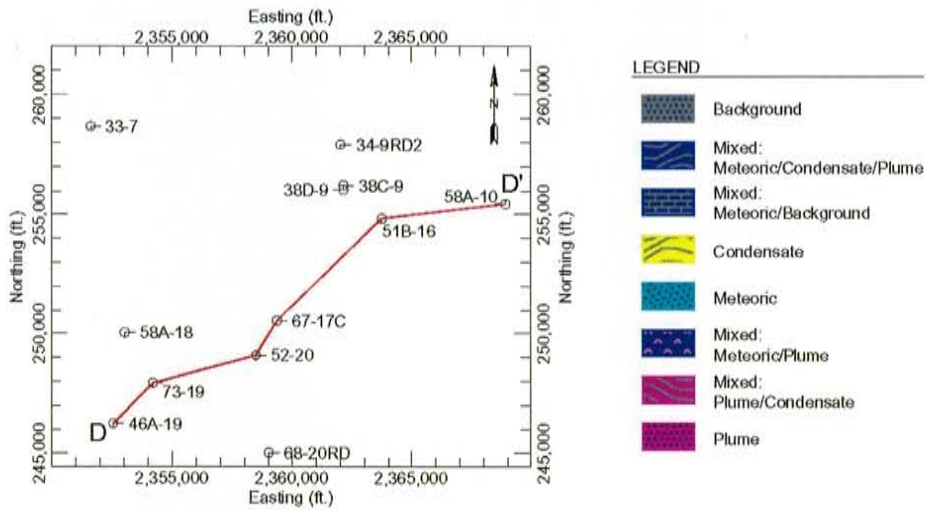
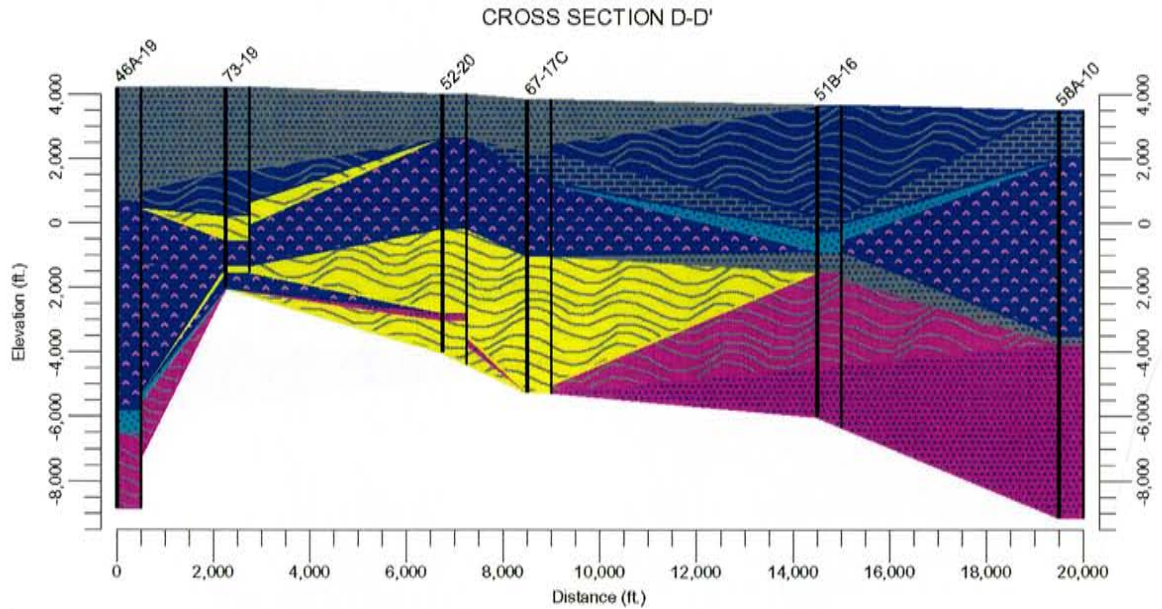


Figure 5.27. Cross-section based on FIS diagonally across the Coso field from the southwest to the northeast with location map.

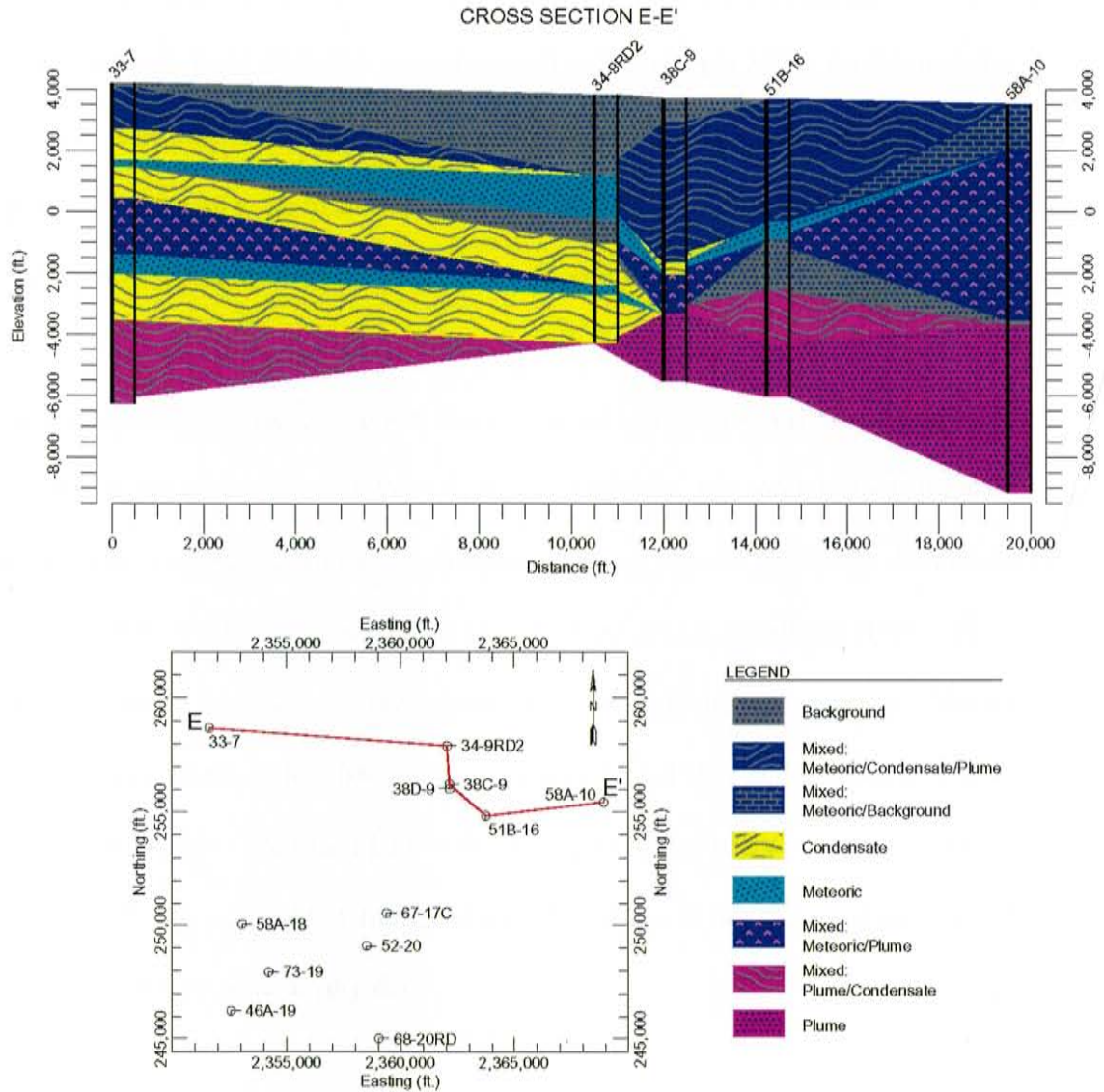


Figure 5.28. West to east cross-section based on FIS logs with location map.

5.6.5. Reservoir Model

Based on fluid cross sections a perimeter fence diagram was prepared and is presented in Figure 5.29. The fence diagram shows a rise in the plume fluids from the southwestern

section of the reservoir towards the middle and north. This rise in the deep plume fluids is evident in wells along the western edge. The increase in the background zone and lack of plume fluids in Well 68-20RD indicate a well on the margin of the geothermal field. The locations of the plume fluids are along the western edge and at the East Flank. The steep dip in the steam zone from Well 67-17 to Well 51B-16 may be indicative of a fault that apparently separates the East Flank from the rest of the field.

Several comparisons between the FIS fence diagram and the general model of a geothermal reservoir in Figure 2.2 can be made. The Coso FIS model shows three distinct zones: 1) meteoric fluids and background zone; 2) zone of mixing characterized by mixed fluids, condensate, and steam; and 3) mixed plume and plume fluid zone. These three zones correspond to the general model of a geothermal reservoir. The FIS model indicates plume fluids rising from near Well 46A-19RD and spreading up and out to the east and north. The East Flank wells appear to be a slightly different system. Marginal wells are indicated by the general model appear to not have a plume zone (Well 52-20) or the plume zone is very deep.

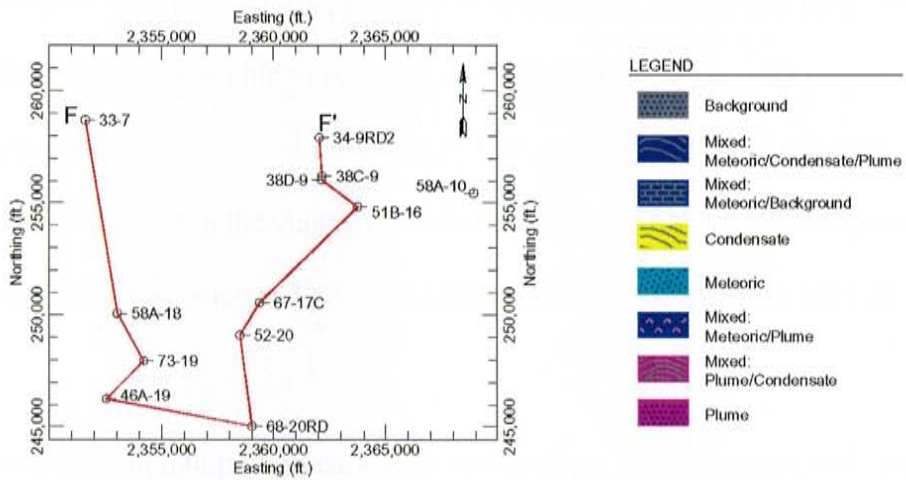
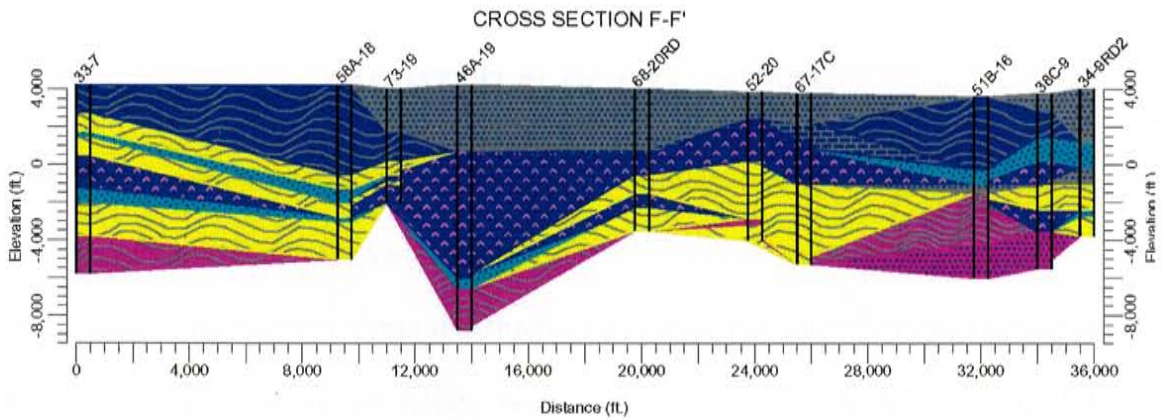


Figure 5.29. Fence Diagram of Coso Field based on FIS logs.

CHAPTER 6: CONCLUSIONS

The purpose of this research was to develop a new method of applying bulk chemical analysis of gases within fluid inclusions from well cuttings for geothermal reservoir assessment. The research shows that the fluid inclusion gas chemistry can be used in a number of different ways to assist in assessing a reservoir. The identifications of fluid types within each well is a major component of managing a geothermal field. Fluid Inclusion Stratigraphy was able to correctly identify the fluid types within each well according to company geologists, temperature logs, geology logs, and other data available. Major breaks in the chemistry were readily identifiable by a computer program using a few chemical species and ratios suggesting the ease of using the method.

Costs associated with interpreting each well are based on sampling time, FIT analysis (about \$4,000 per 565 samples), and interpretation time (a couple of days). This is much less than the \$100,000's for currently used well logging tools. One avenue still to be studied is the relationship between the FIS method and the current well logging tools such as resistivity and SP. Well logs for the Coso wells were not made available beyond the geological descriptions and temperature logs. FIS would be a low cost, useful tool to add to the well logging suite and would provide information while the well was being drilled. Successful interpretation of the Beowawe wells and Coso Well 38D-9 indicate that it is possible to make correct, useful interpretations within a few days and impact decisions about a well.

The objectives for this project have been met. A methodology for applying fluid inclusion gas analysis of drill cuttings to geothermal exploration has been developed and the FIS methodology was applied to wells while they were being drilled. Conclusions include:

- FIS can by the chemical signatures determined in the fluid inclusions arrive at the relative temperatures of the fluids. The chemical ratios used were N_2/Ar and CO_2/CH_4 ,
- Fluid types for a geothermal field can be determined based on the fluid inclusion chemistry using 23 different compounds and 2 ratios.
- A computer program created in Excel using logic statements identified in Figure 5.6 can be used to interpret the fluid types.
- Fracture patterns can be identified by FIS as peaks in chemical species plotted against depth.
- Fluid inclusion gas chemistry does not correlate to rock type but does correlate to some degree to alteration mineral assemblages.
- Fluid inclusion gas analysis of geothermal fields is mainly analyzing modern fluids. The dynamic fluid environment, as well as the high stress rates wherein fractures are continually being opened and closed also lends credence to the conclusion that the fluid inclusion gas analysis is mainly analyzing modern fluids.
- Well to well correlation shows a fluid stratigraphy that agrees with prior fluid inclusion studies and general knowledge of the field.

- The FIS method is useful while a well is being drilled to assist in well decisions.
- FIS methodology is applicable to other fields so long as a well where the geology, permeability, and fluids are known is used as background data.
- If a known well is not available, FIS may need additional study to determine the chemical signatures of fluid types however, the ratios developed here should still hold. High ratios of N_2/Ar and CO_2/CH_4 would likely indicate hotter fluids. The exact magnitude of the ratios and the relative temperatures would have to be determined.
- The FIS method will likely provide a useful, economical tool for geothermal reservoir assessment.

Additional Work to be Conducted

Additional work to be done includes the following:

- Further study on fractures and relationship to FIS peaks. The theory of Enhanced Geothermal Systems is that low permeability rocks in geothermal reservoirs can be enhanced through mechanical and/or chemical means creating higher permeability rocks thus increasing fluid flow and creating higher producing geothermal reservoirs (Tester et al, 2006). The creation of Enhanced Geothermal Systems is still in the development phase. Knowing the location of fractures, thickness of fractures, and if the fracture is located in hotter zones is important to the development of these systems. FIS may be able to identify the location of fractures to a greater degree than conventional well logging tools and thus be used to identify areas of fracture enhancement.

- Determine if there are precursors to hotter zones that can be identified using FIS before the hot zones are encountered in the well. If precursors can be identified then well decisions can be made as the well is being drilled thus saving time, money, and effort on a well.
- Further study on other geothermal fields to determine the general applicability of FIS to geothermal reservoir assessment. The applicability of FIS to other fields will help to make the method more universal. There may be different ratios and/or fluid types that will have to be identify for specific fields in order to make FIS useful for a variety of fields.

REFERENCES

- Adams, M.C., J.N. Moore, S. Bjornstad, and D.I. Norman (2000). Geologic History of the Coso Geothermal System. *Proceedings: World Geothermal Congress, Kyushu-Tohoku, Japan, 2000*, 2463-2469.
- Akasak Chitoshi, Shigetaka Nakanishi, Shigeo Tezuka, Tsuneo Ishido, and John W. Pritchett (2003). Using Self-Potential Monitoring to Help Characterize the Onikobe Geothermal Reservoir in Japan, *Proceedings: Twenty-eighth Workshop on Geothermal Reservoir Engineering*, Stanford University, Stanford, California.
- Armannsson H., G. Gislason, and T. Hauksson (1982). Magmatic Gases in Well Fluids Aid the Mapping of the Flow Pattern in a Geothermal System. *Geochimica Cosmochimica Acta*, 46: 167-178.
- Bacon, C.R., and W.A. Duffield (1980). Special Section: Geothermal Investigations in the Coso Range, California. *Journal of Geophysical Research* 85: 2379-2516
- Bacon, C.R., R. MacDonald, and R.L. Smith (1981). Pleistocene High-Silica Rhyolite of the Coso Volcanic Field, Inyo County, California. *Journal of Geophysical Research* 86: 10223-10241.
- Batini F., R. Bertani, B. Ciulli, A. Fiordelisi, and P. Valenti (2002). Geophysical Well-Logging – A Contribution to the Fractures Characterization. *Proceedings: Twenty-seventh Workshop on Geothermal Reservoir Engineering*, Stanford University, Stanford, California.
- Berard B.(2003) Personal Communication, Coso Company Geologist
- Blamey, N., and David I. Norman (2002). New Interpretations of Geothermal Fluid Inclusion Volatiles: Ar/He and N₂/Ar ratios – A Better Indicator of Magmatic Volatiles, and Equilibrium Gas Geothermometry. *Proceedings: Twenty-seventh Workshop on Geothermal Reservoir Engineering*, Stanford University, Stanford, California.
- Blewitt, G., M. Coolbaugh, W. Holt, C. Kreemer, J. Davis and R. Bennett (2002). *Transactions Geothermal Resources Council*, Vol. 26, p. 523-526.
- D'Amore, F., and A.H. Truesdell (1979). Models for Steam Chemistry at Larderello and the Geysers. *Proceedings: Fifth Workshop on Geothermal Reservoir Engineering*, Stanford University, Stanford, California
- Dilley, Lorie M., and David I. Norman (2004). Fluid Inclusion Stratigraphy: Determining Producing from Non-Producing Wells, *Geothermal Resources Council Transactions* 28: 387-391.
- Dilley, Lorie M., David I. Norman, and Brian Berard (2004). Fluid Inclusion Stratigraphy: A New Method for Geothermal Reservoir Assessment – Preliminary Results. *Proceedings of the 29th Annual Stanford Geothermal Workshop*, pp. 230-238.

- DOE 2003 Geothermal Power Plants. US DOE Energy Efficiency & Renewable Energy website. www1.eere.energy.gov/geothermal/powerplants.html
- Duffield, W.A., C.A. Bacon, and G.B. Dalrymple (1980). Late Cenozoic Volcanism, Geochronology, and Structure of the Coso Range, Inyo County, California. *Journal Geophysical Research* 85: 2379-2380.
- Dupuy, L.W. (1948). Bucket-drilling the Coso Mercury-deposit, Inyo County, California. *US Bureau of Mines Investigation* 4201.
- Ellis, A.J., and W.A. Mahon (1977). Chemistry and geothermal systems. Academic Press, New York-San Francisco-London, 392 pp.
- Fournier, R.O.(1985). The Behavior of Silica in Hydrothermal Solution, pg. 45-61. In Berger B.R. and Bethke, P.M. (eds). *Geology and Geochemistry of Epithermal Systems*. Society of Economic Geologist.
- Fournier, R.O. (1985). Carbonate Transport and Deposition in the Epithothermal Environment, pg. 62-73. In Berger B.R. and Bethke, P.M. (eds). *Geology and Geochemistry of Epithermal Systems*. Society of Economic Geologist.
- Feng, Q. and Jonathan M. Lees, (1998). Microseismicity, Stress, and fracture in the Coso geothermal field, California. *Tectonophysics* 289: 221-238.
- Garside, L.J., L.A. Shevenell, J.H. Snoe, and R.H. Hess (2002). Status of Nevada Geothermal Resource Development. *Geothermal Resource Council Transaction*. V. 19, pg. 191-200.
- Giggenbach, W.F. (1981). Geothermal Gas Equilibria. *Geochimica Cosmochimica Acta* 44: 2021-2032.
- Giggenbach, W. F. (1986). The use of Gas Chemistry in Delineating the Origin of Fluid Discharges over the Taupo Volcanic Zone: A Review. *International Volcanological Congress, Hamilton, New Zealand Proceedings Seminar 5*: 47-50.
- Giggenbach, W.F. (1997). The Origin and Evolution of Fluids in Magmatic-hydrothermal Systems. In H. L. Barnes, *Geochemistry of Hydrothermal Ore Deposits*. New York: J. Wiley and Sons, Inc., pp. 737-796.
- Graney, J.R., and S.E. Kesler (1995). Factors Affecting Gas Analysis of Inclusion Fluid by Quadrupole Mass Spectrometry. *Geochimica et Cosmochimica Acta* 59(19): 3977-3986.
- Grant, M.A., I.G. Donaldson, and P.F. Bixley (1982). *Geothermal Reservoir Engineering*. New York: Academic Press, 369 pp.
- Hall, D. (2002). Fluid Inclusion Technologies, Inc. <http://www.fittulsa.com>.
- Hall, D. (2006). Fluid Inclusion Technologies, Inc write up on process, internal memorandum.

- Henley, R.W. (1985). The Geothermal Framework for Epithermal Deposits. In B.R. Berger and P.M. Bethke (eds), *Geology and Geochemistry of Epithermal Systems: Reviews in Economic Geology*, vol. 2, Society of Economic Geologists, pp. 1-24.
- Henley, R.W., and A.J. Ellis (1983). Geothermal Systems, Ancient and Modern. *Earth Science Reviews* (19): 1-50.
- Kovac, K.M., J. Moore, J. McCulloch, and D. Ekart (2004). Geology and Mineral Paragenesis Study within the COSO-EGS Project. *Proceedings: Twenty-ninth Workshop of Geothermal Reservoir Engineering*, Stanford University, Stanford, California.
- Kovac, K.M., J. Moore, and SJ Lutz (2005). Geologic Framework of the East Flank, Coso Geothermal Field: Implications for EGS Development. *Proceedings: 30th Workshop on Geothermal Reservoir Engineering*, Stanford University, Stanford, California.
- Kurilovitch, Lynne, Dave Norman, Matt Heizler, Joe Moore, and Jess McCulloch (2003). ⁴⁰Ar/³⁹Ar Thermal History of the Coso Geothermal Field. *Proceedings: Twenty-eighth Workshop on Geothermal Reservoir Engineering*, Stanford University, Stanford, California.
- Landis, G.P., and A.H. Hofstra (1991). Fluid Inclusion Gas Chemistry as a Potential Minerals Exploration Tool: Case Studies from Creede, CO, Jerritt Canyon, NV, Coeur d'Alene District, ID and MT, Southern Alaska Mesothermal Veins, and Mid-continent MVT's. *Journal of Geochemical Exploration* 42: 25-59. Amsterdam: Elsevier Science Publishers B.V.
- Layman, E.B. (1984). A simple basin and range fault model for the Beowawe geothermal system, Nevada. *Trans. Geothermal Resources Council*, Vol. 8, pp. 451-456.
- Lutz, S.J., J.N. Moore, M.C. Adams, and D.I. Norman (1999). Tracing Fluid Sources in the Coso Geothermal System Using Fluid-inclusion Gas Chemistry. *Proceedings: Twenty-fourth Workshop of Geothermal Reservoir Engineering*, Stanford University, Stanford, California.
- Moore, Joseph N., Alan J. Anderson, Michael C. Adams, Roger D. Aines, David I Norman, and Mark A. Walters (1998). The Fluid Inclusion and Mineralogic Record of the Transition from Liquid- To Vapor-Dominated Conditions in The Geysers Geothermal System, California. *Proceedings: Twenty-third Workshop of Geothermal Reservoir Engineering*, Stanford University, Stanford, California.
- Moore, Joseph N., David I. Norman, and B. Mack Kennedy (2001). Fluid Inclusion Gas Compositions from an Active Magmatic-Hydrothermal System: A Case Study of The Geysers Geothermal Field, USA. *Chemical Geology* 173(1-3): 3-30.
- Morin, R.H., S.H. Hickman, C.A. Barton, A.M. Shapiro, W.R. Benoit, and J.H. Sass (1998). Hydrologic Properties of the Dixie Valley, Nevada Geothermal Reservoir from Well-Test Analyses. *Proceedings: Twenty-third Workshop on Geothermal Reservoir Engineering*, Stanford University, Stanford, California.

- Nielson, Dennis L., Joseph N. Moore, and Matthew T. Heizler (1999). Lower Limits of Hydrothermal Circulation in the Tiwi Geothermal Field, Luzon. *Proceedings: Twenty-seventh Workshop on Geothermal Reservoir Engineering*, Stanford University, Stanford, California.
- Norman, D.I., and J.A. Musgrave. (1995). N₂-Ar-He Compositions in Fluid Inclusions: Indicators of Fluid Source. *Geochimica et Cosmochimica Acta* 58(3): 1119-1131.
- Norman, D.I., and F.J. Sawkins (1987). Analysis of Volatiles in Fluid Inclusions by Mass Spectrometry. *Chemical Geology* 61: 1-10.
- Norman, D.I., Joseph N. Moore, Lorie M. Dilley, and Brian Berard (2004). Geothermal Fluid Propene and Propane: Indicators of Fluid Source: *Twenty-Ninth Workshop on Geothermal Reservoir Engineering*, Stanford University, Stanford, California, Jan. 26-28, 2004.
- Norman, D.I., Lorie M. Dilley and Jess McCulloch (2005). Displaying and Interpreting Fluid Inclusion Stratigraphy Analyses on Mud Log Graphs: *Thirtieth Workshop on Geothermal Reservoir Engineering*, Stanford University, Stanford, California, January 30-February 2, 2005.
- Norman, D.I., J.N. Moore, and J. Musgrave. (1997). Gaseous Species as Tracers in Geothermal System. *Proceedings: Twenty-second Workshop of Geothermal Reservoir Engineering*, Stanford University, Stanford, California.
- Norman, D. I., J.N. Moore, B. Yonaka, and J. Musgrave. (1996). Gaseous Species in Fluid Inclusions: A Tracer of Fluids and an Indicator of Fluid Processes. *Proceedings: Twenty-first Workshop of Geothermal Reservoir Engineering*, Stanford University, Stanford, California.
- Norman, D.I., Nigel Blamey, and Joseph N. Moore (2002). Interpreting Geothermal Processes and Fluid Sources from Fluid Inclusion Organic Compounds and CO₂/N₂ Ratios. *Proceedings: Twenty-seventh Workshop on Geothermal Reservoir Engineering*, Stanford University, Stanford, California.
- Ohmoto H. (1968). *The Bluebell Mine, British Columbia, Canada: Chemistry of the Hydrothermal Fluids (Gases and Salts in Fluid Inclusions)*. PhD. Dissertation, Princeton University.
- Roberts, Jeffery J., Brian P. Bonner, and Paul W. Kasameyer (2001). Electrical Resistivity Measurements of Intact and Fractured Geothermal Reservoir Rocks. *Proceedings: Twenty-sixth Workshop on Geothermal Reservoir Engineering*, Stanford University, Stanford, California.
- Ross, C.P., and R.G. Yates (1943). The Coso Quicksilver District, Inyo County, California. *U.S. Geological Survey Bulletin* 936-Q, 395-416.
- Tester, Jefferson W., (2006) Chairman of Interdisciplinary Panel, *The Future of Geothermal Energy, Impact of Enhanced Geothermal Systems (EGS) on the*

United States in the 21st Century. Department of Energy, Geothermal Program,
Renewable Energy and Power Department.

Unruh, J. and E. Hauksson (2006). Active Faulting in the Coso Geothermal Field,
Eastern California. *Geothermal Resources Council Transactions* 30.

White, D.E. (1968). Hydrology, Activity and Heat Flow of the Steamboat Springs
Thermal System, Washoe County, Nevada. *Geological Survey Professional Paper*
548-C.

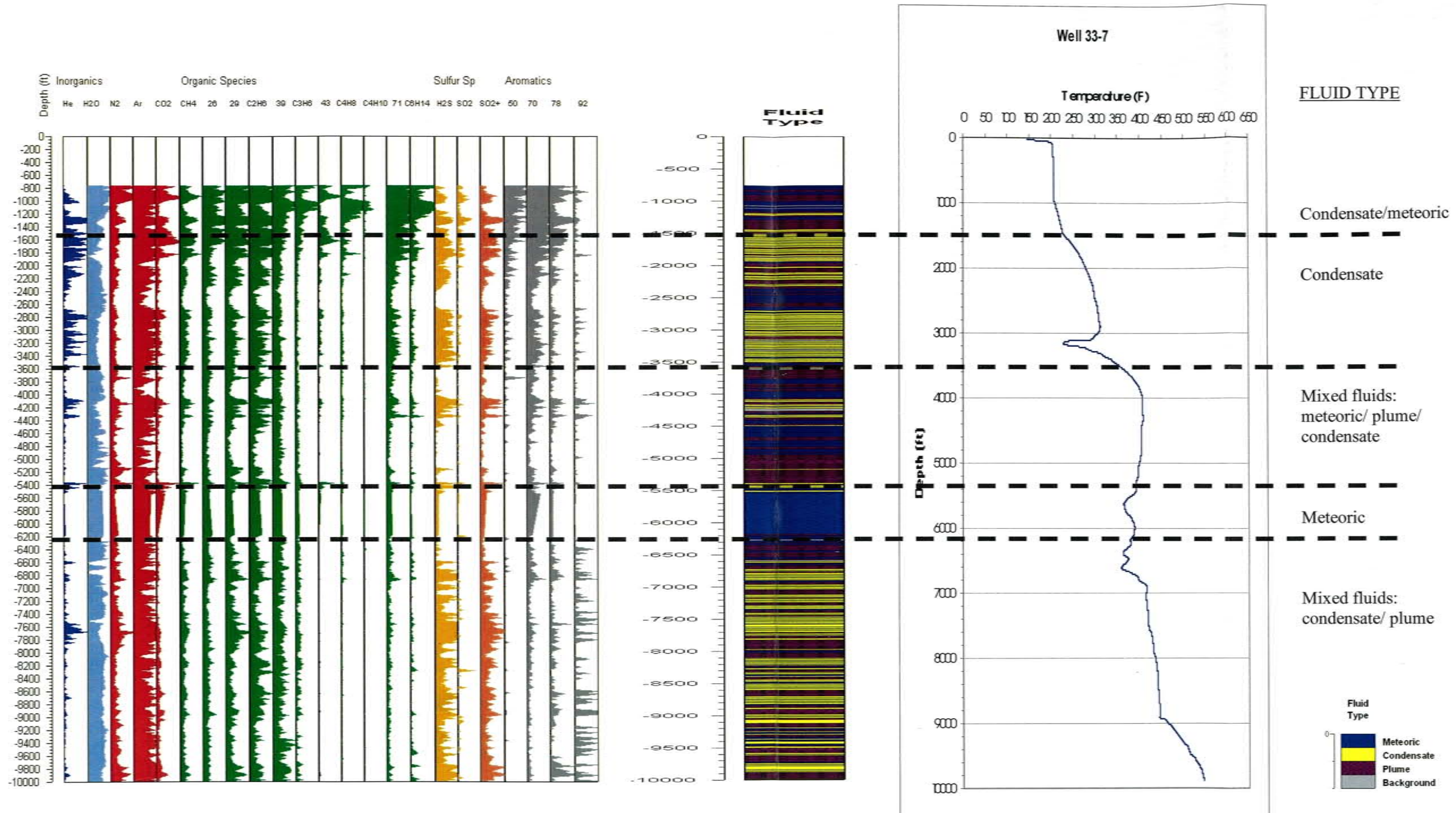
White, D.E., L.J.P. Muffler, and A.H. Truesdell (1971). Vapor-dominated Hydrothermal
Systems Compared with Hot-water Systems. *Economic Geology* 66: 75-97.

Wohlez K., Heiken G. (1992) *Volcanology and Geothermal Energy*, University of
California Press, Berkeley, CA

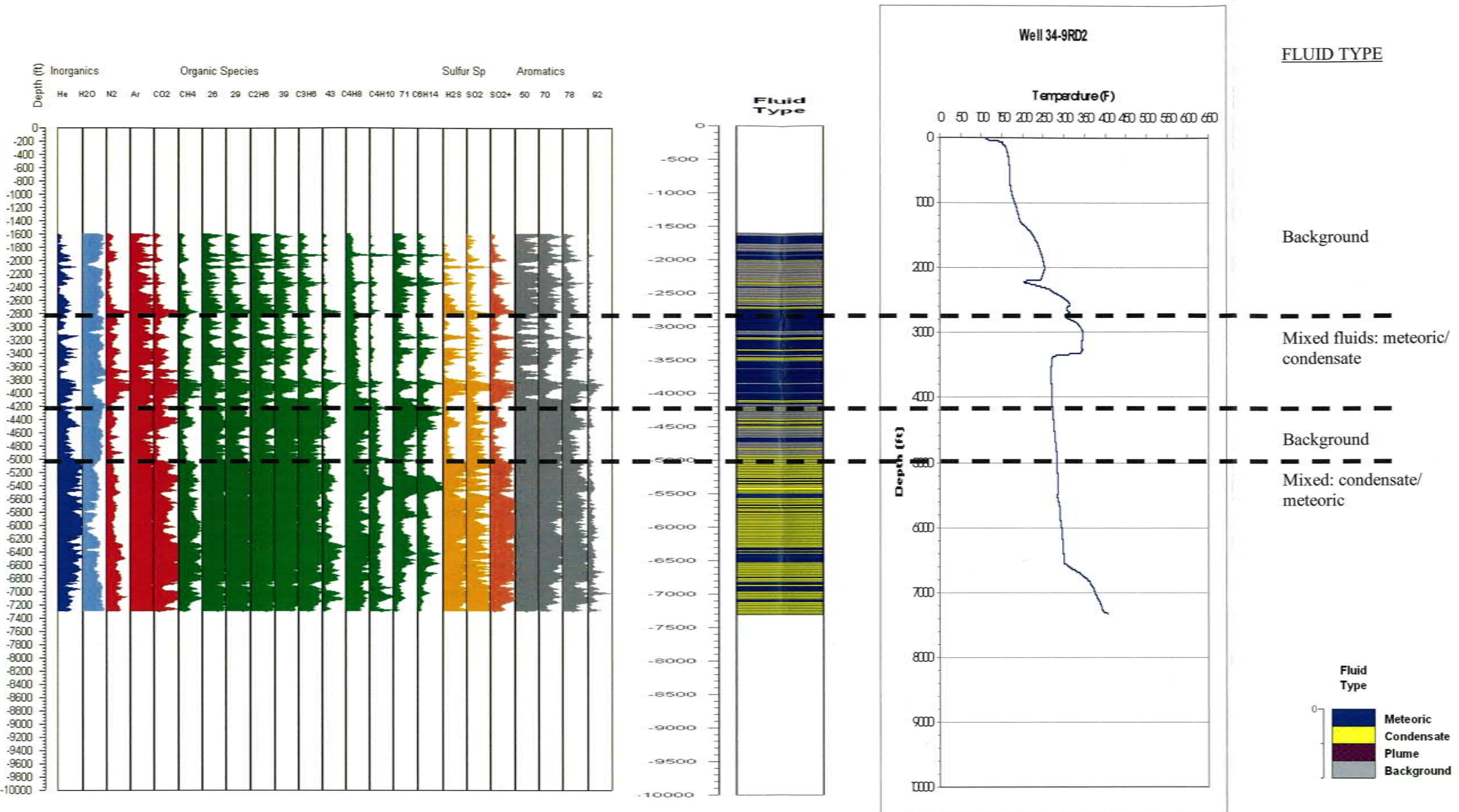
APPENDIX A: FIT DATA SET FOR ENTIRE PROJECT (CD)

APPENDIX B: EXCEL LOGGER FILES AND LOGGER FILE (CD)

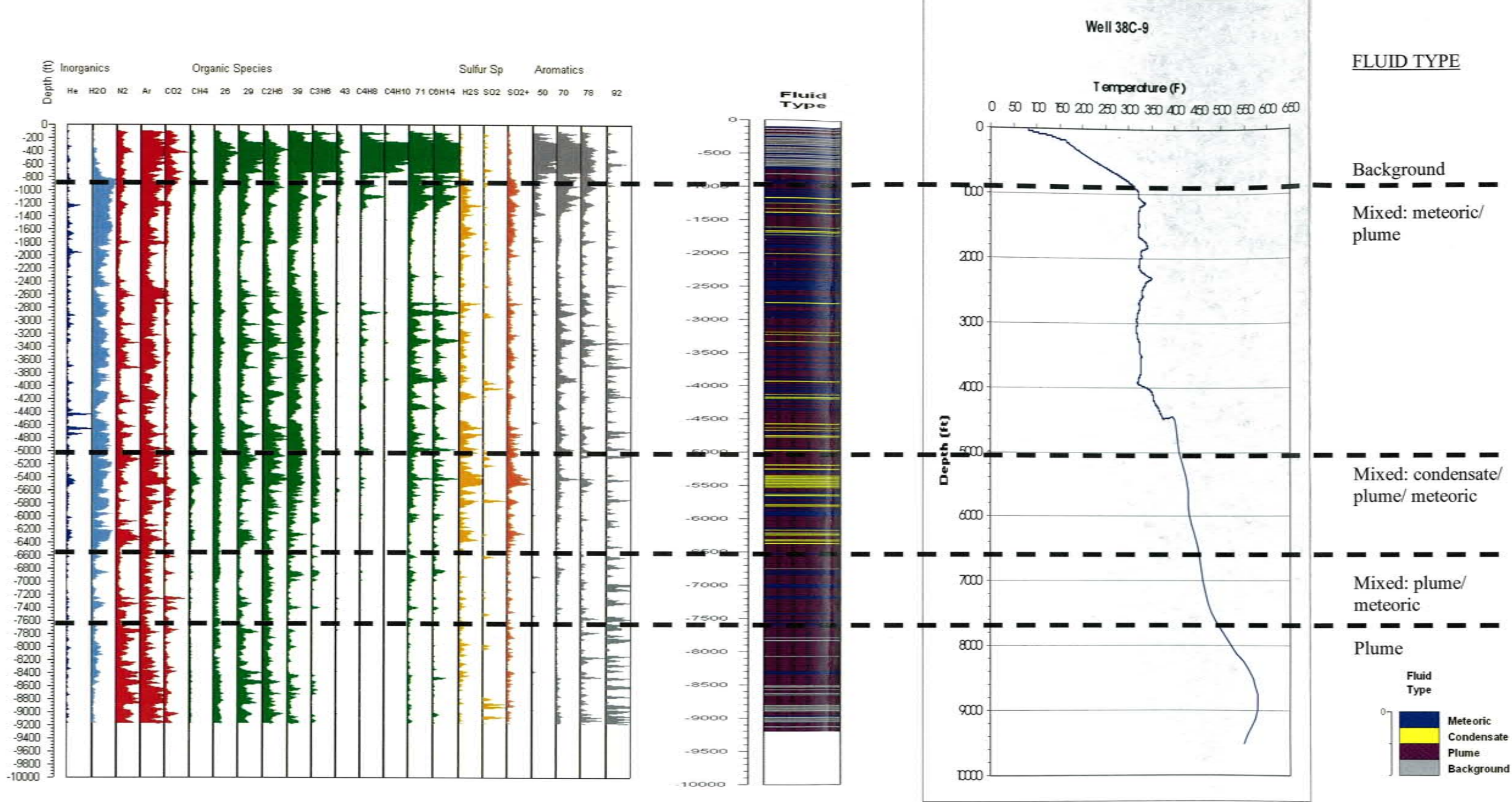
APPENDIX C: FIS LOGS FOR THE COSO WELLS



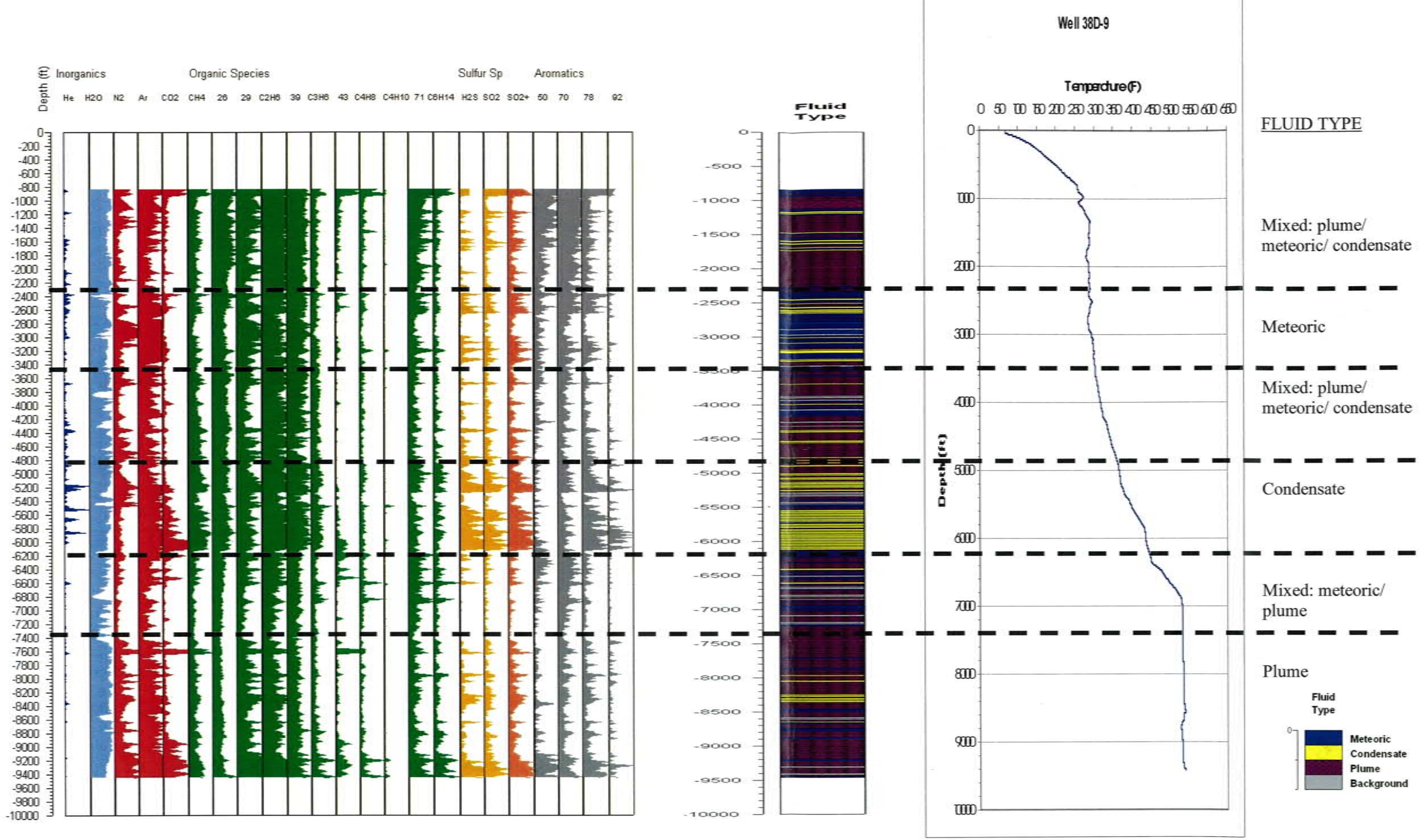
Well 33-7 located on the northwest side of the field is a low temperature, 3 MW producer. The gas chemistries indicate mixed fluids of meteoric and condensate. After about 6300 feet is mixed fluid zone with mixture of condensate and possible plume fluids. The CO₂/CH₄ magmatic ratio is high at this depth and the N₂/Ar ratio is low. The zone below 6300 feet is different from the first zone above 2400 feet in the lack of heavy organics and aromatics. The lack of heavy organics particularly mass spectrum 43 indicates hotter fluids. Note the distinct peaks across many of the mass spectra indicating a fracture.



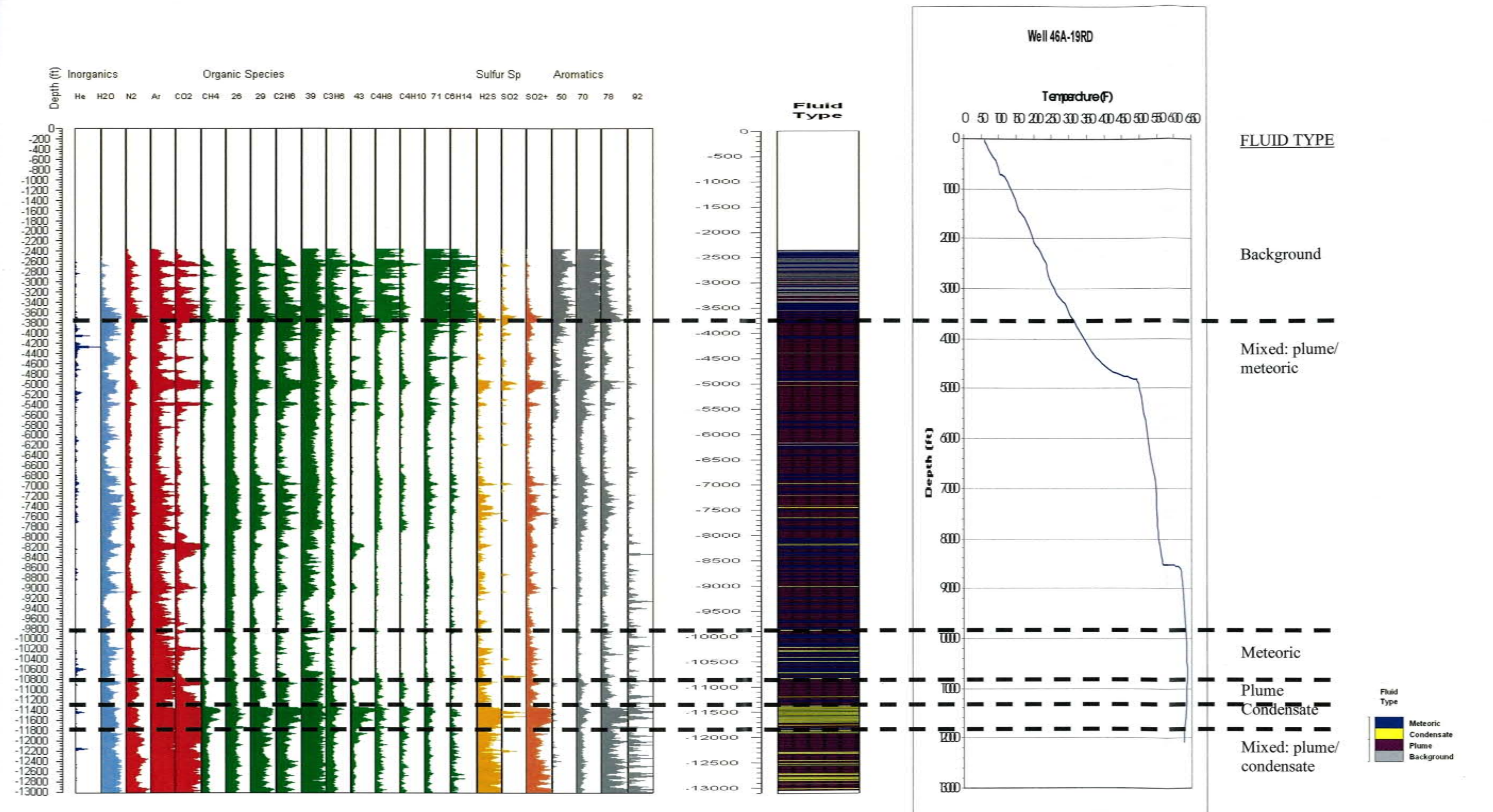
Well 34-9RD2 is an injection well and the gas chemistries indicate a mixed fluid of meteoric and condensate throughout the well. There are high CO₂, high organics, and high H₂S signatures suggesting injection fluids. This well does not show plume fluids. The temperature log indicates temperatures less than 350⁰F. Dashed lines indicate zones where chemistries are slightly different and these zones roughly correspond to changes in the temperature log.



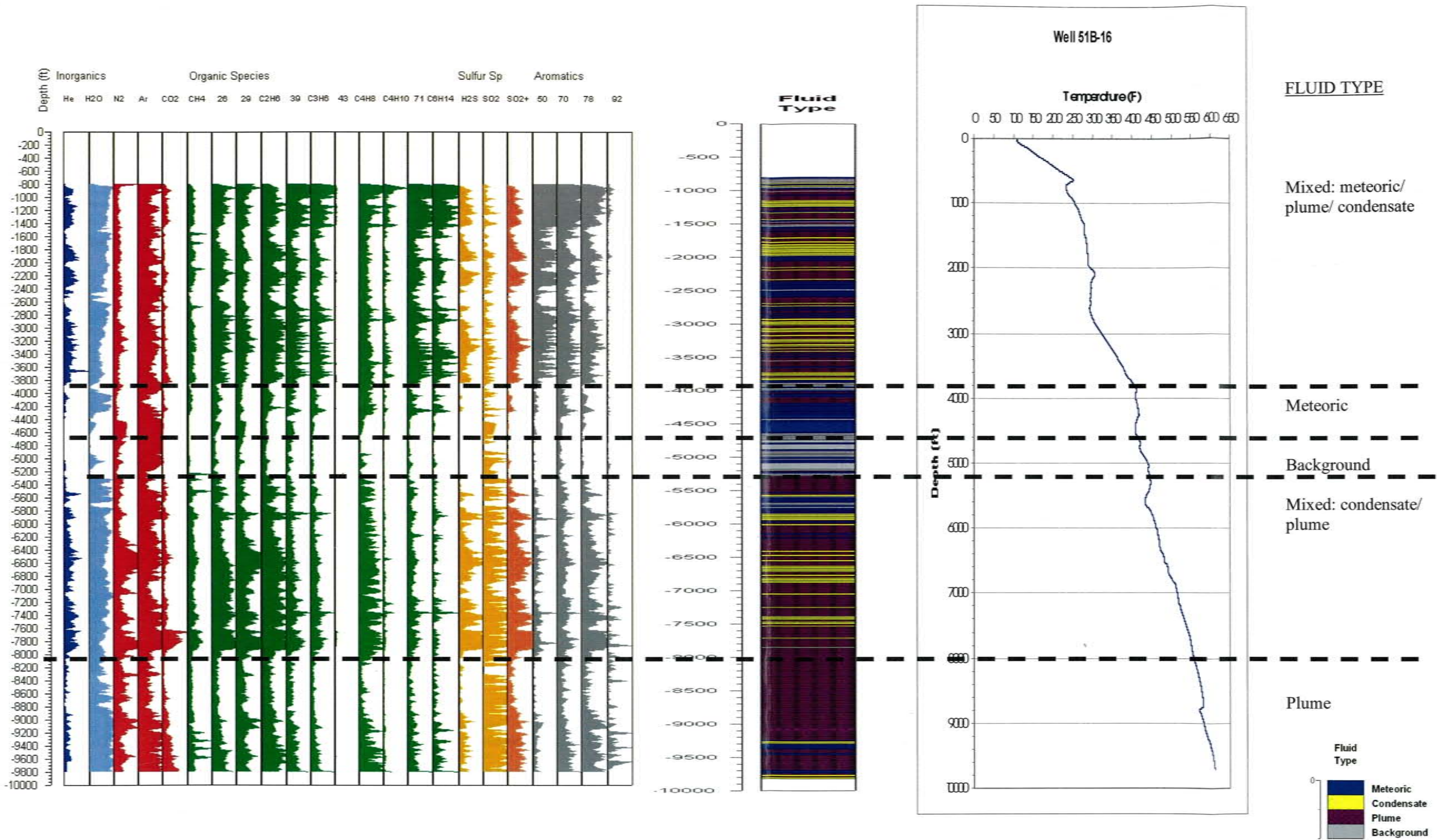
Well 38C-9 is an 8 MW producer located on the East Flank. This well is a good example of the different types of fluids. The background zone is from the top of the well to about 800 feet. This is followed by a meteoric fluid zone which is indicated by the H₂O, crustal ratios are high and some condensate. Below about 2400 feet the magmatic ratios increase, the organics decrease and H₂O decreases suggesting hotter fluids hence this section is most likely a mixed fluid zone with steam-heated fluids mixed with meteoric fluids. A zone of condensate with higher condensate ratios follows from about 4400 to 6400 feet. A change occurs at 6400 feet. The condensate ratios decrease, the magmatic ratios start to increase, the gas/water ratio increases, and the H₂O signature decreases as well. There is a slight transition zone from 6400 to 7600 feet and then plume fluids are encountered. This is the production zone for this well.



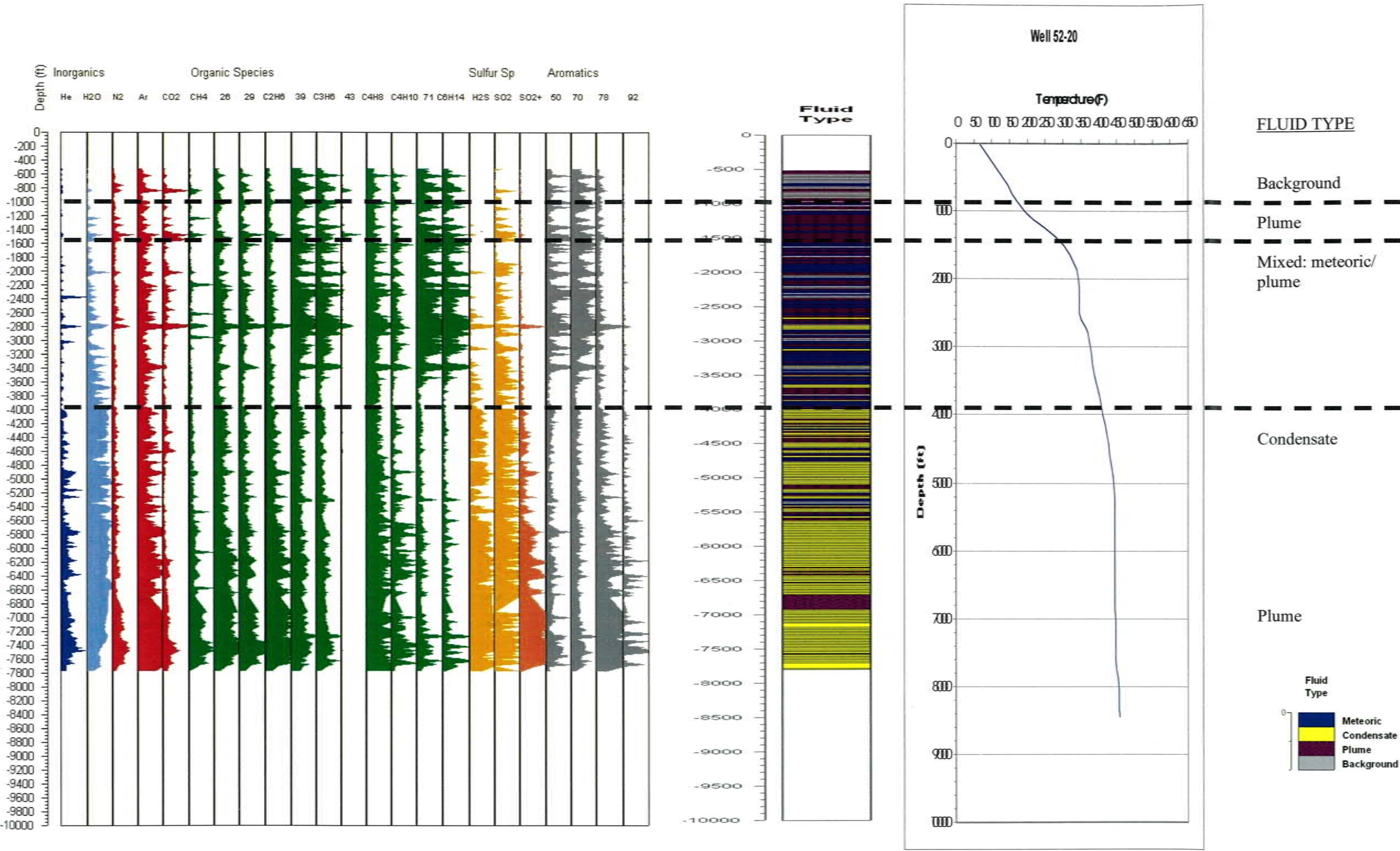
Well 38D-9 is a 7 MW producer located on the East Flank near Well 38C-9. This well was sampled while drilling. The first set of samples from 840 feet to 6100 feet was analyzed as drilling continued. Due to encountering the condensate zone from 4800 to 6100 feet it was concluded that the well was similar to Well 38C-9 and there was a high probability that it would produce. Plume fluids were encountered below 7200 feet and the signature is similar to Well 38C-9 below 7200 feet.



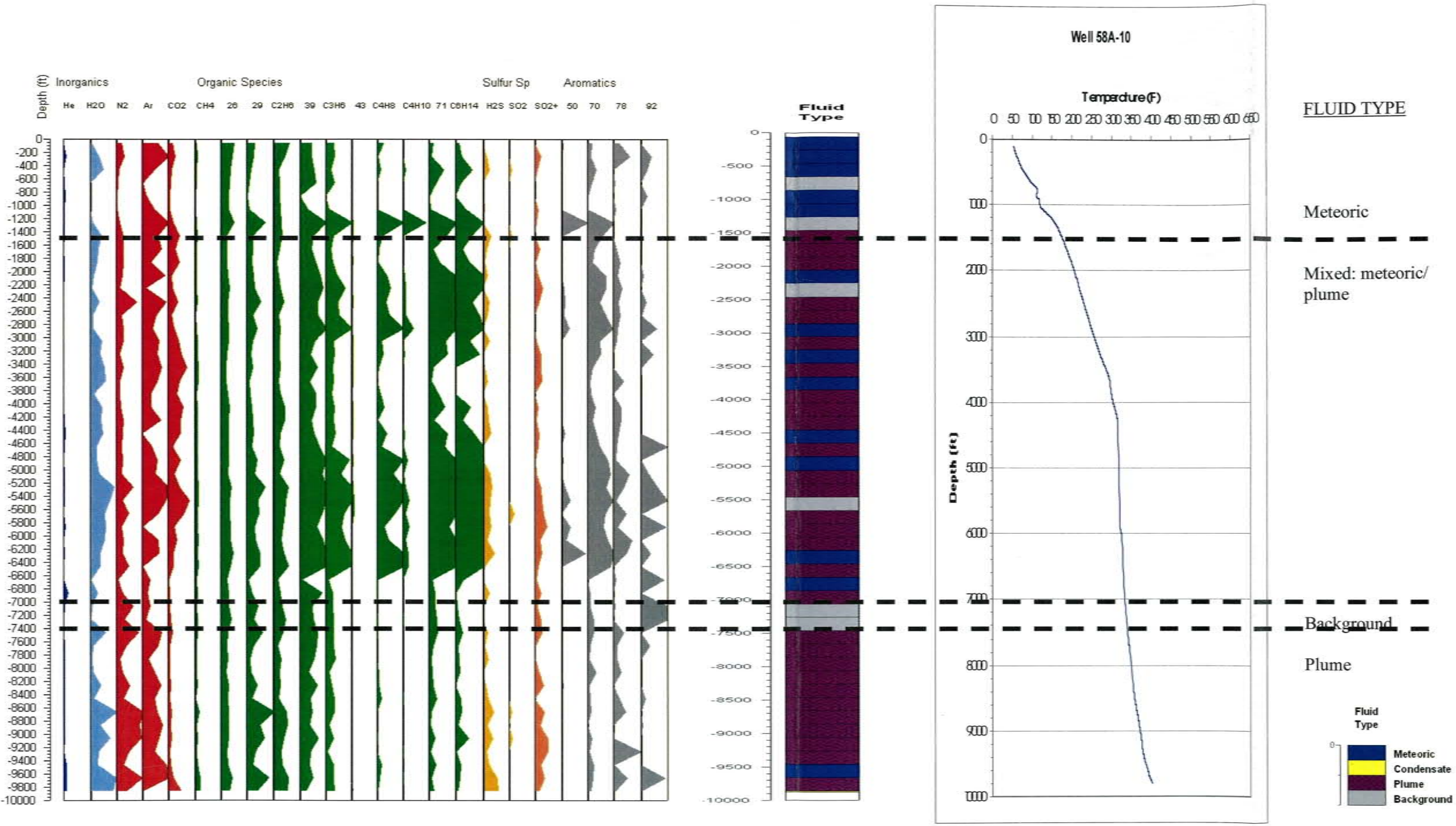
Well 46A-19RD is the deepest and hottest well in the field. It is a non-producer due to lack of permeability. To a depth of about 3700 feet is interpreted as background fluid signature. Below this zone, the H₂O increases but still is not a strong signature, the organics decrease slightly and the condensate ratios increase. This zone was interpreted as mixed fluids of meteoric and plume fluids. Below 10,100 feet the zone was interpreted as meteoric, plume and condensate zones.



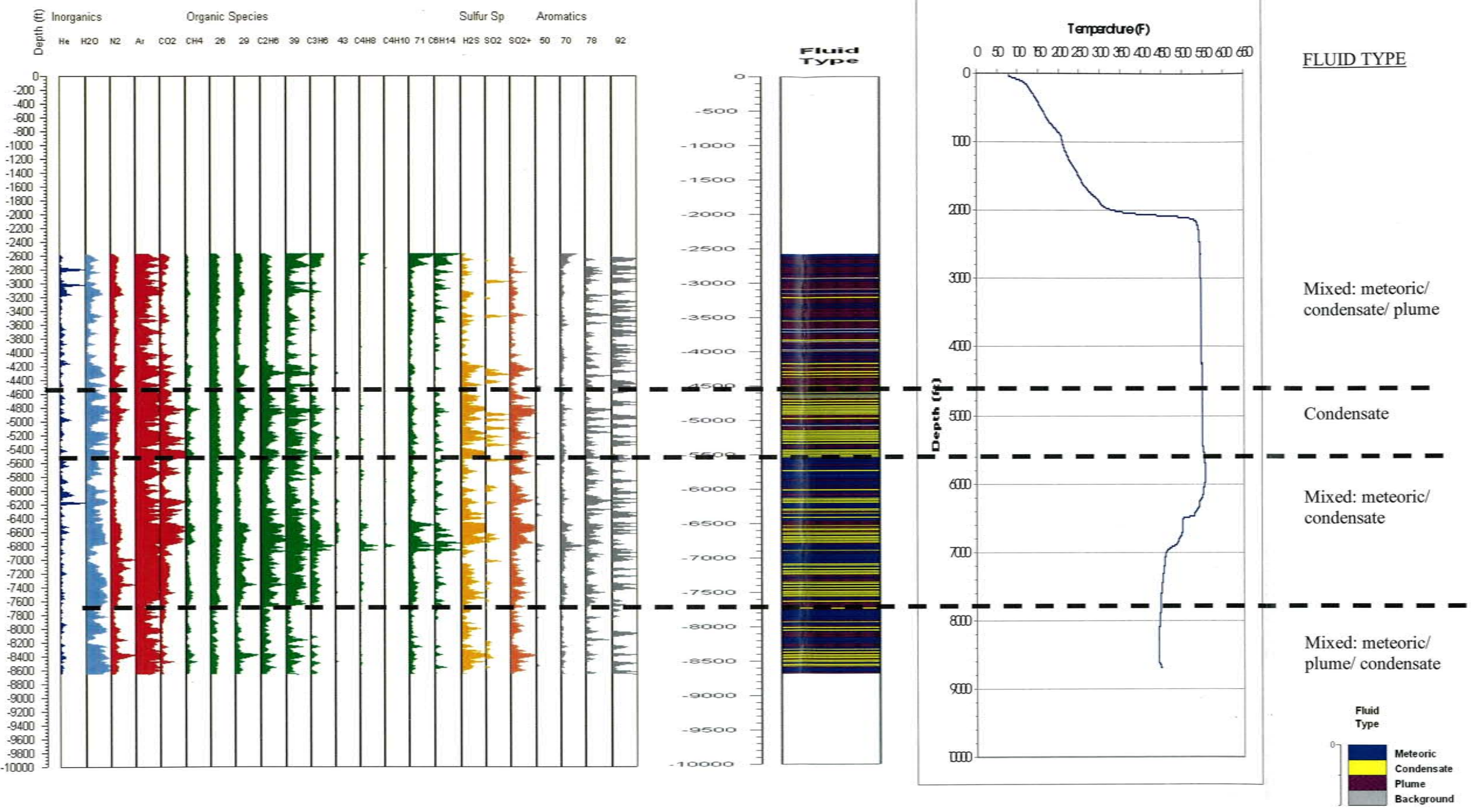
Well 51B-16 is a non-producer on the East Flank despite the high temperatures. The FIS signature is interpreted as mixed meteoric and condensate fluids to about 8000 feet. After 8000 feet, the zone is interpreted as plume fluids due to the presence of high magmatic ratios and low condensate ratios. Note the zone from 4600 to 5200 feet where there is only a few mass spectra that has a signature. Occasional zones occur in the wells where there is little to no FIS signature possibly indicating zones of low permeability.



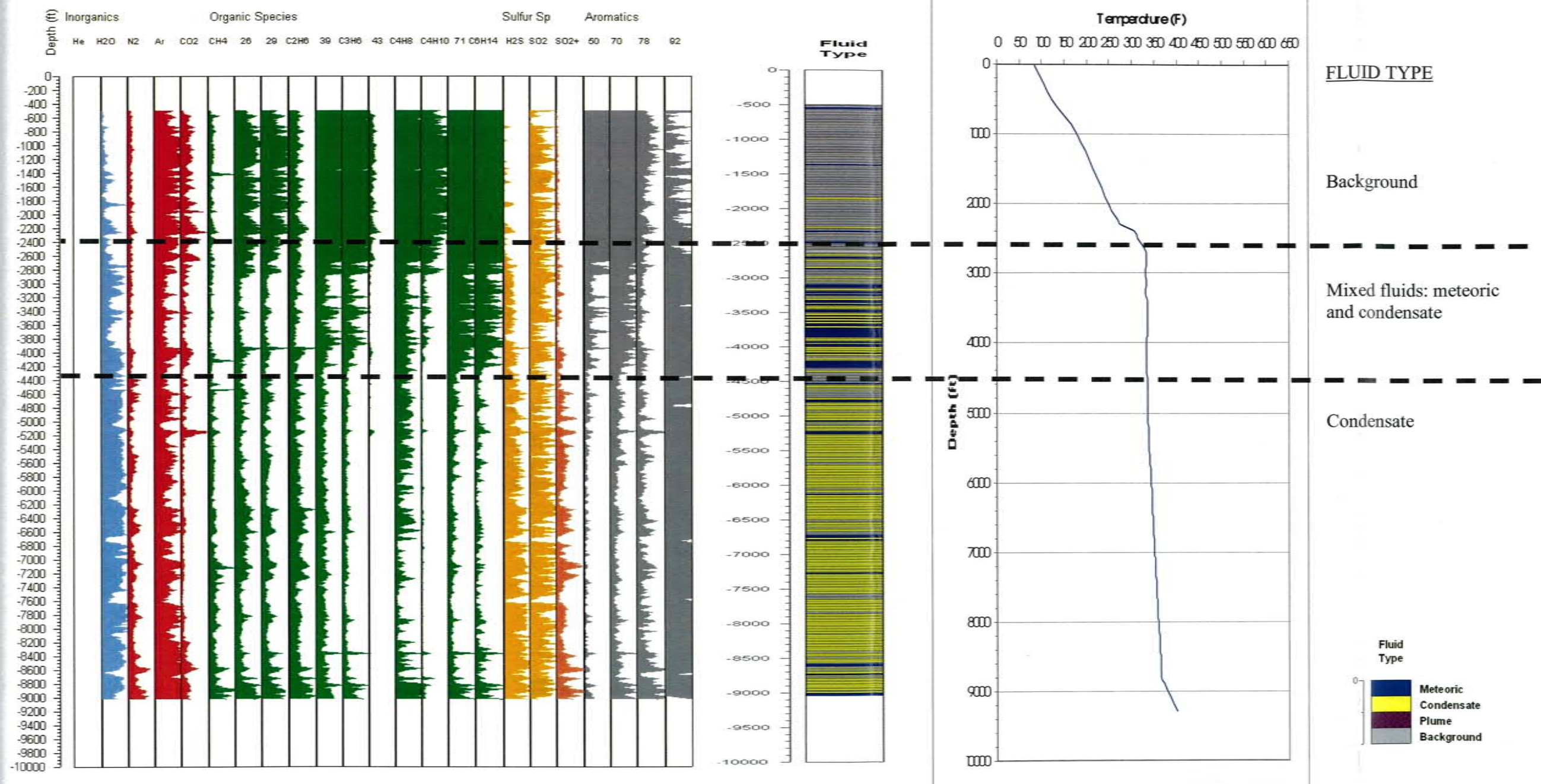
Well 52-20 is a low temperature, 3-MW producer. The well until about 4000 feet is a series of meteoric, plume, and condensate zone. The production is most likely from the deeper condensate zone.



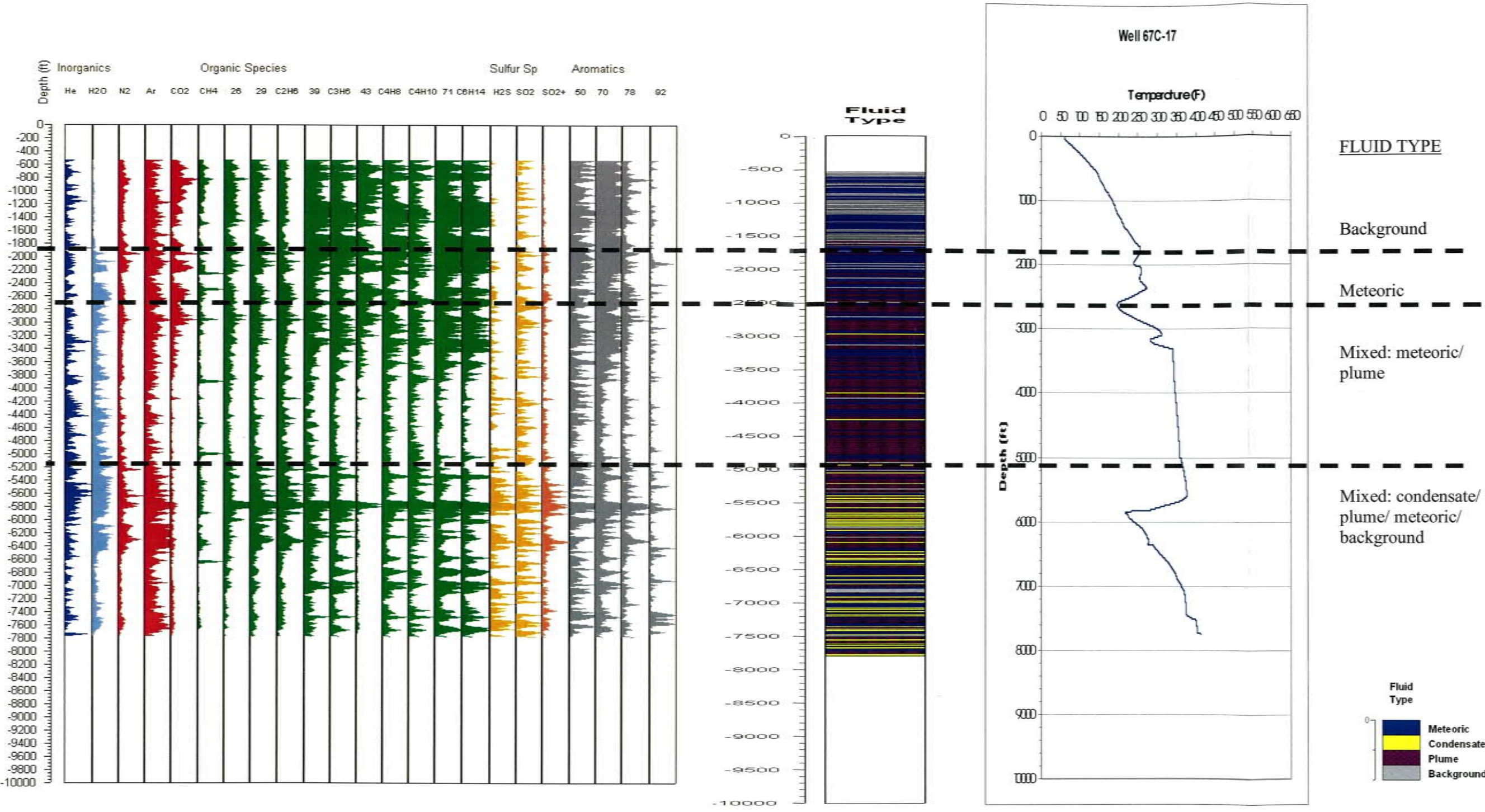
Well 58A-10 is on the eastern margin of the field and is a non-producer. It was sampled during drilling at 50-foot intervals. The FIS signatures indicate a well with mixed fluids of meteoric plume fluids with plume fluids encountered below about 7400 feet.



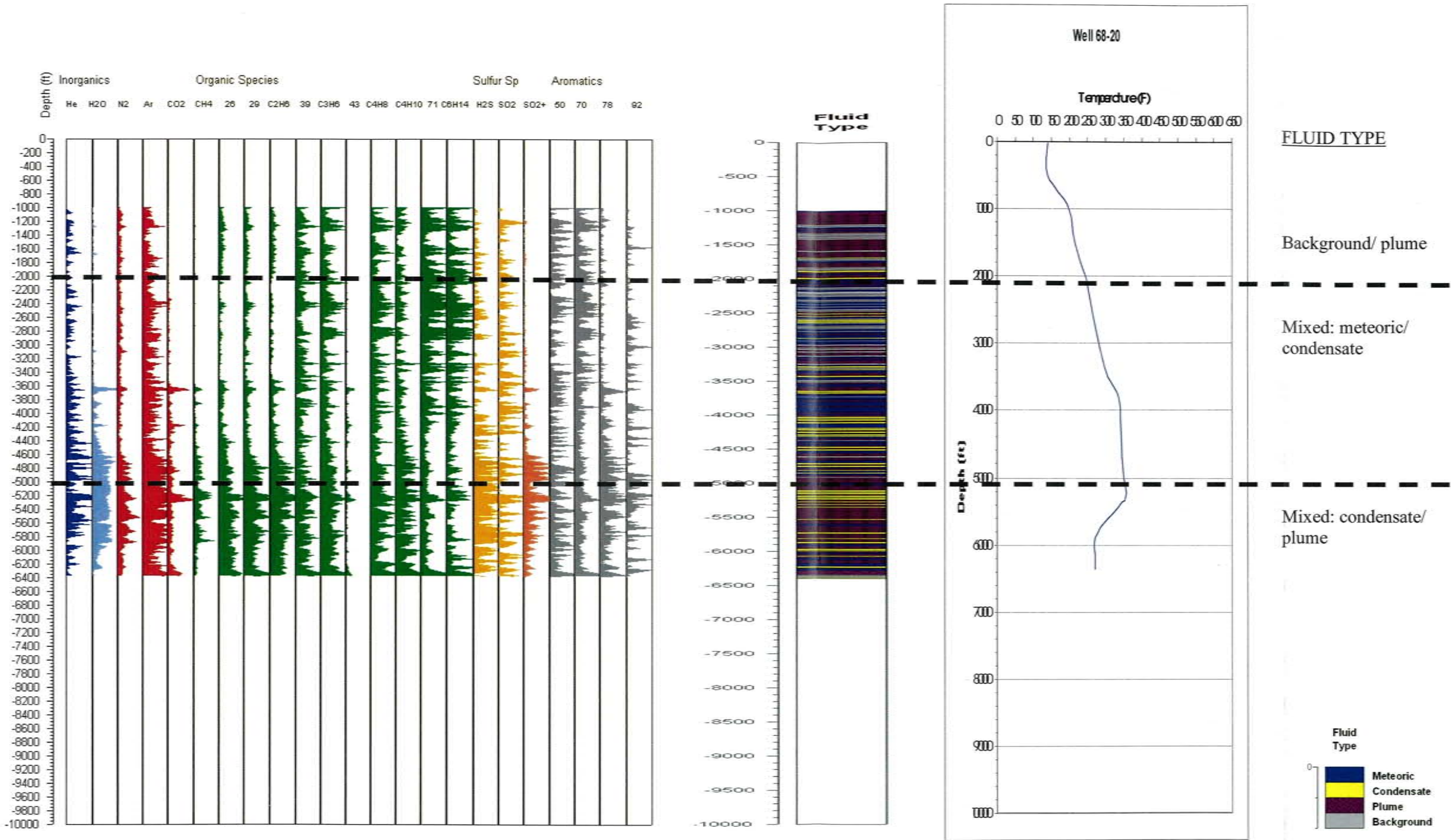
Well 58A-18 is a 4 MW producer located on the western side of the field. The well FIS signature indicates a well condensate fluids mixed with some meteoric fluids from 4500 to depth of the well. This well is known to have cold water entrances throughout the well. The change in the FIS signatures at about 4500 feet is also suggested on the temperature log.



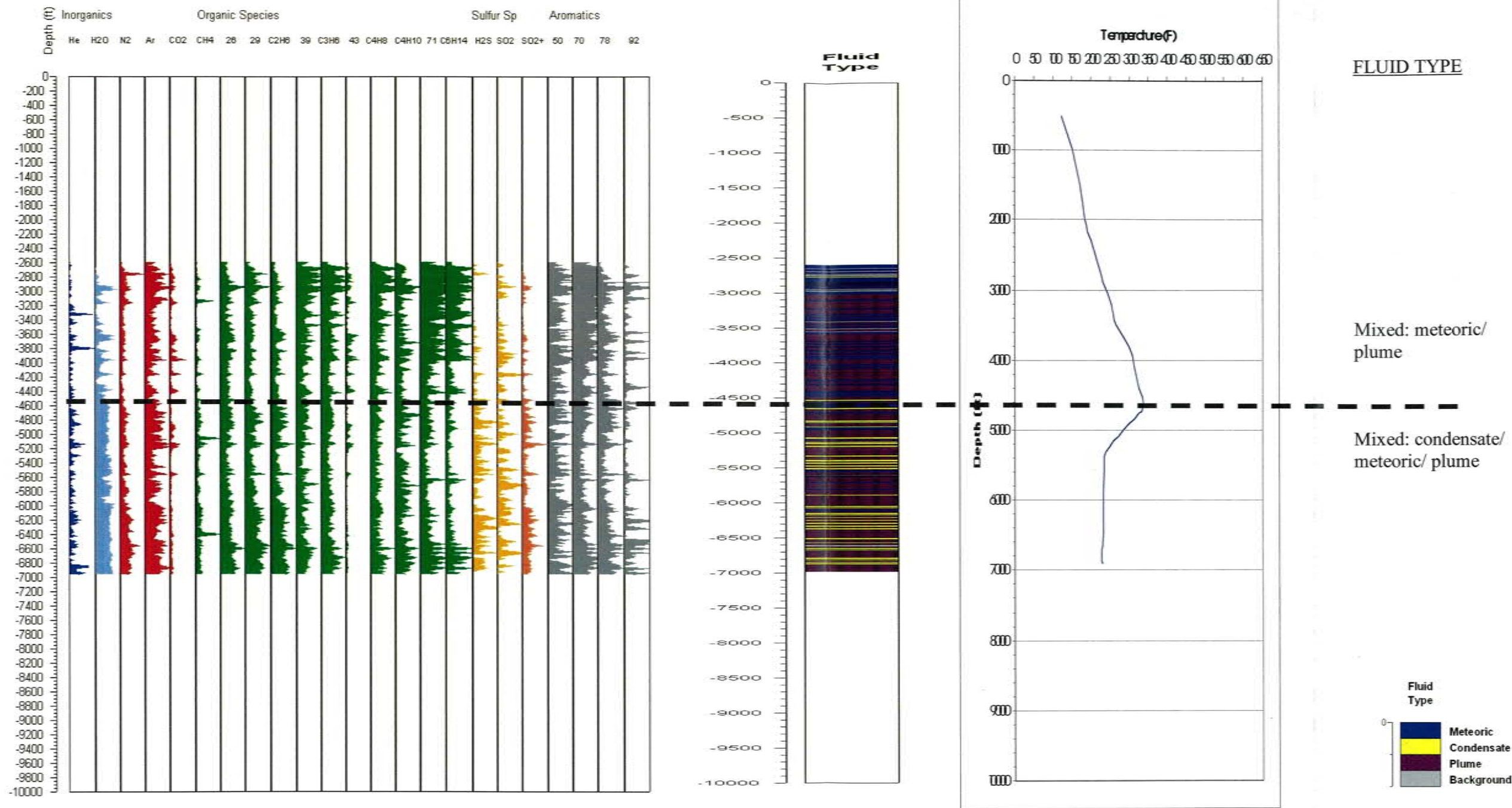
Well 67-17 is a low temperature, non-producer. This well is an injection well. The FIS signature indicates background to about 2500 feet followed by condensate and mixed fluids of meteoric and condensate fluids. Note the “magmatic” ratios decreases after 2500 feet and disappears almost completely once the well has “heated” up.



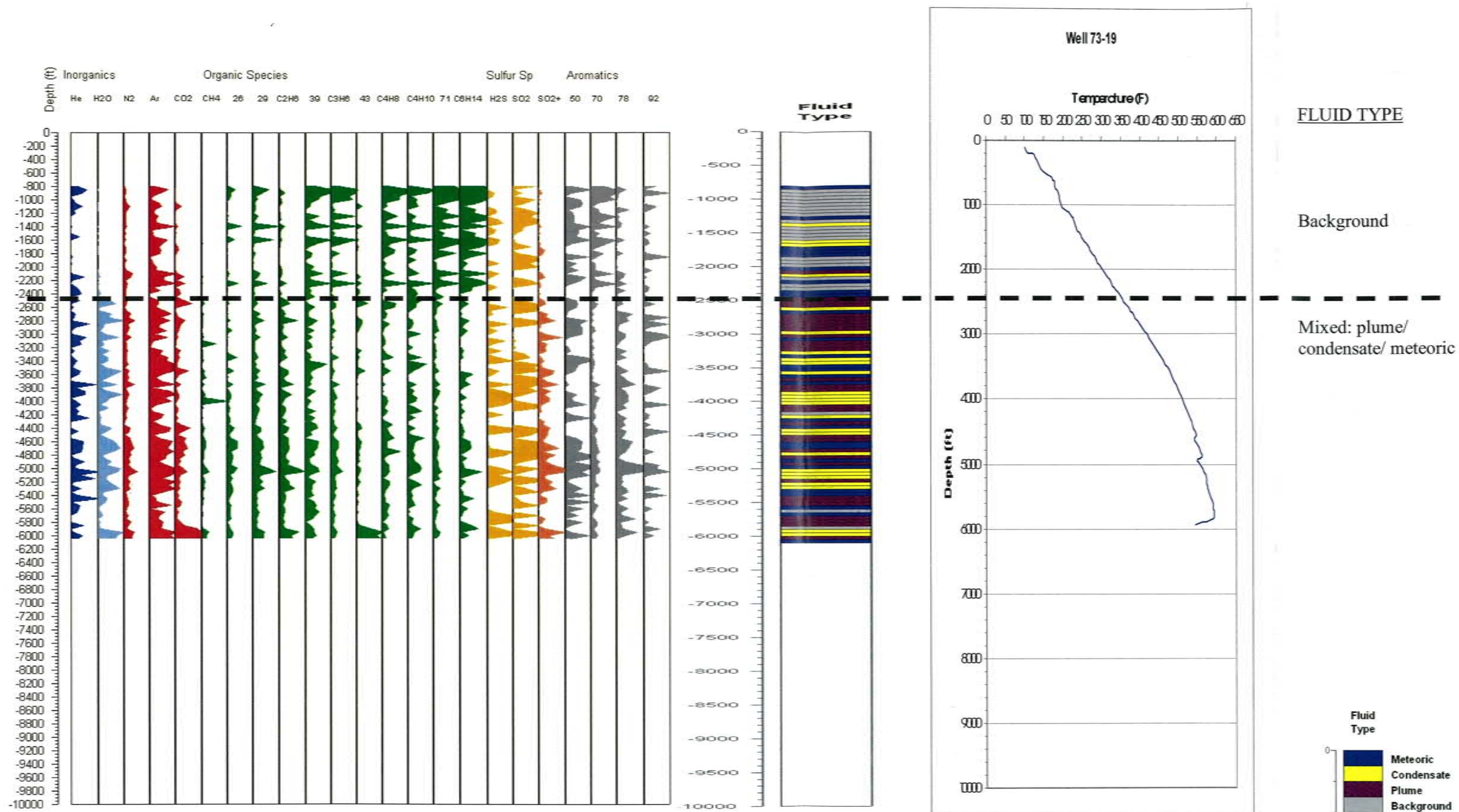
Well 67-17C is a low temperature well drilled near Well 67-17. This well has several influxes of cooler waters indicated on the temperature log. Note the large peak at 5800 feet corresponds to the point on the temperature log when the temperatures begin to increase after decreasing. This depth also corresponds to an increase in the CO₂/CH₄ ratio and FIS signature indicating condensate.



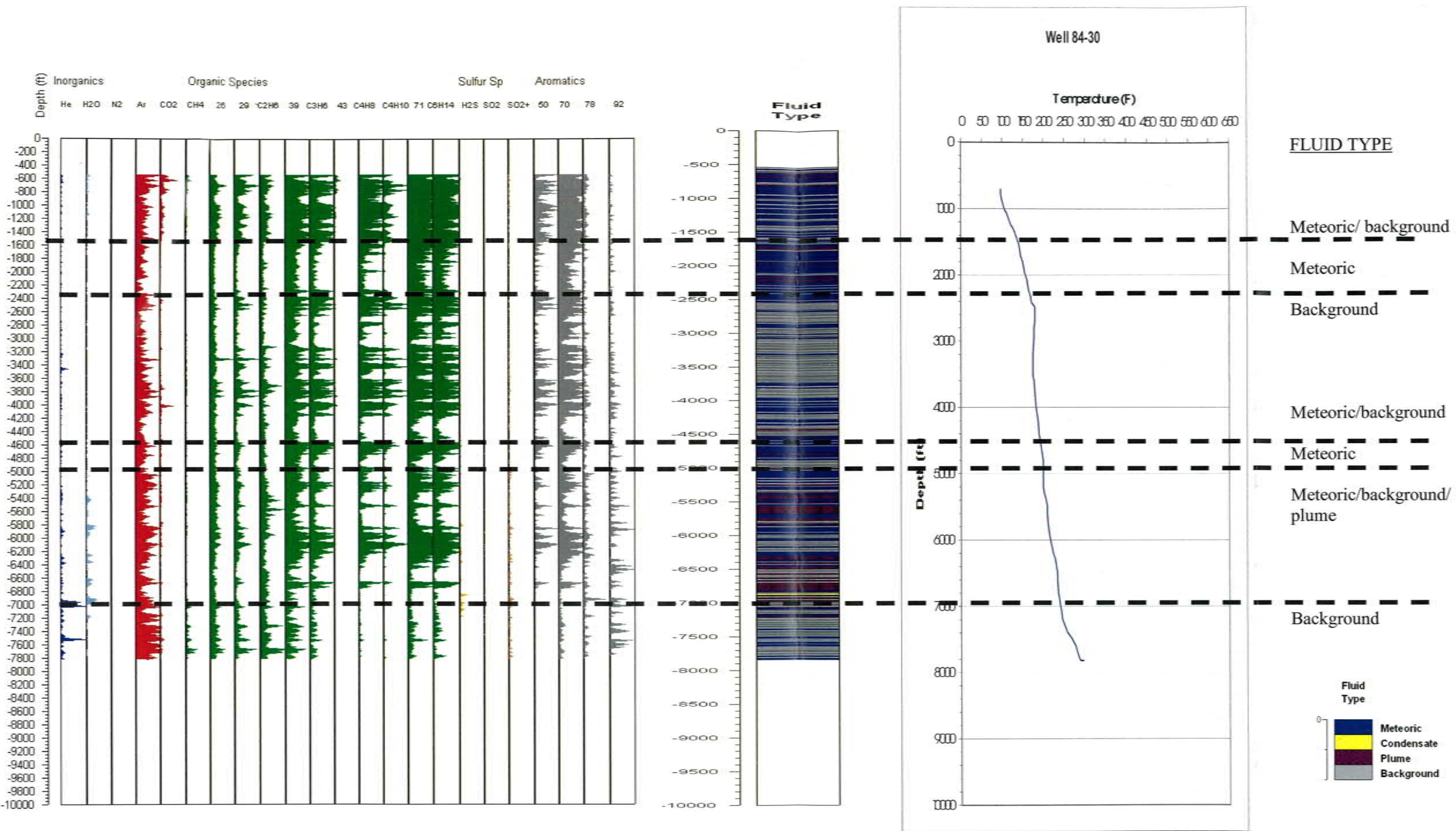
Well 68-20 is a low temperature, non-producer used as an injection well. The upper portion, above 5000 feet is a mix of background, meteoric, and condensate. Mixed condensate and plume fluids occur at depth.



Well 68-20RD is a redrill after 7 years of Well 68-20. They deviate by only at most 150 feet. The overall signature suggests similar fluids as Well 68-20: mixed meteoric/ plume/ and condensate fluids. The FIS signature is different in details with Well 68-20 suggesting changes occurred within the 7 year time span between the original well being drilled and the redrill.



Well 73-19 is a high temperature, 3 MW producer on the western side of the field. This well was sampled at 50 foot intervals. The upper zone to about 2500 feet is interpreted as background. Below 2500 feet is a zone interpreted as mixed plume/condensate/ meteoric fluids.



Well 84-30 is located to the south of the field and is a non-producer. The FIS signature is indicative of rocks that have not experienced the recent geothermal event to the same extent as the other wells. This FIS signature is seen in other wells usually near the top of the wells.